Bioamine receptors of the fruit fly *Drosophila melanogaster* as targets for insecticides

Dissertation
zur Erlangung des Doktorgrades
des Fachbereiches Biologie
der Christian-Albrechts-Universität zu Kiel
Mathematisch-Naturwissenschaftliche Fakultät
Zoologisches Institut

Vorgelegt von Samar Ezzat Ghazy El-Kholy
Tanta, Ägypten

Kiel, 2010

Erstgutachter: Prof.Dr. Thomas Röder

Zweitgutachter: Dr. Holger Heine

Termin der Disputation: 24.8.2010

Zum Druck genehmigt

Table of contents

List of Abbreviations

Amp	ampicillin
bp	base pair
Ca2+	calcium ion
cAMP	cyclic AMP
cDNA	complimentary DNA
CNS	central nervous system
DA	dopamine
DMEM	Dulbecco's modified Eagle medium
DMSO	dimethylsulfoxide
DNA	deoxyribonucleotideic acid
dNTPs	deoxyribonucleotide
ds RNA	douple stranded RNA
E.coli	*Escherichia coli*
EDTA	ethylenediamine tetra acetic acid
EL	extracellular loop of G protein coupled receptors
EtBr	ethiduim bromide
F1	first generation
FBS	fetal bovine serum
Fig.	figure
g	gram
GDP	guanosine diphosphate
GFP	green flourescence protein
GTP	guanosine triphosphate
h	hour
HEK cells	human embryonic kidney cells
Hsp70	heat shock promotor
IgG	immunoglobulin G

kb	kilobase pairs
L	liter
L3	third stage larvae
LB	Luria Broth medium
L-DOPA	dihydroxyphenylalanine
MCS	multicloning site of a plasmid vector
min	minute
µM	micromolar
ml	milliliter
NCBI	national center for Biotechnology information
ng	nanogram
OA	octopamine
PBS	phosphate buffered saline
PCR	polymerease chain reaction
PNP	p-Nitrophenyl phosphate
RNAi	RNA-interference
rpm	rounds per minute
RT-PCR	revese transcription PCR
SEAP	secreted alkaline phosphatase
sec	second
TA	tyramine
Taq	*Thermus aquaticus*
TARs	tyramine receptors

1. Introduction

The discovery of molecular targets for the development of new insecticides is critical for successful control of a variety of insect pests. The extensive databases for genome sequences of insects, microorganisms and viruses provide valuable information for identification of new targets. Cell-surface proteins, including biogenic amine receptors, are prime targets for insecticides.

Biogenic amines are important messenger substances and regulators of cell functions. Both vertebrates and invertebrates have several biogenic amines, including dopamine, serotonin, histamine, and acetylcholine, which exist in both major metazoan groups, namely protostomes and deuterostomes. In contrast, noradrenaline and adrenaline occur only in vertebrates (Blenau and Baumann, 2001), whereas their presumed invertebrate counterparts, octopamine (OA) and tyramine (TA), are restricted to invertebrates (Roeder, 1999).

All the catecholamines (so named because they share the catechol moiety) are derived from a common precursor, the amino acid tyrosine. Octopamine and tyramine are monoamines synthesized from tyrosine. OA is the end product in the synthesis pathway, TA acts as precursor for OA synthesis. TA is the direct decarboxylation product of tyrosine. This reaction is catalyzed with the tyrosine decarboxylase. OA is produced from TA through the action of tyrosine-ß-hydroxylase.

Biosynthesis of dopamine (DA) also starts from tyrosine, which is converted to dihydroxyphenyl- alanine (L-DOPA) by the enzyme tyrosine hydroxylase. Downstream, the enzyme dopa decarboxylase catalyzes the conversion of L-DOPA to dopamine. Release of these biogenic amines is similar as for most neurotransmitters, they are transported from the cytoplasm to specialized storage vesicles. Upon the arrival of an action potential, the influx of calcium ions leads to the fusion of vesicles with the neuronal membrane and then vesicles discharge their content into the synaptic cleft. Under normal conditions, specialized transporter molecules in the nerve terminals recycle neurotransmitter compounds that have been released into the synaptic cleft by pumping them back into the nerve terminal. This action is highly effective and compound specific. Interference with reuptake has significant effects. Cocaine for example interacts with insect octopamine reuptake, thus inducing hyperactivity of the treated insects (Scavone *et al.*, 1994). In vertebrates, cocaine interacts with reuptake for dopamine and serotonin, inducing all the known psychotropic effects of this compound.

The following figure summarizes the biosynthesis of tyramine, octopamine and dopamine.

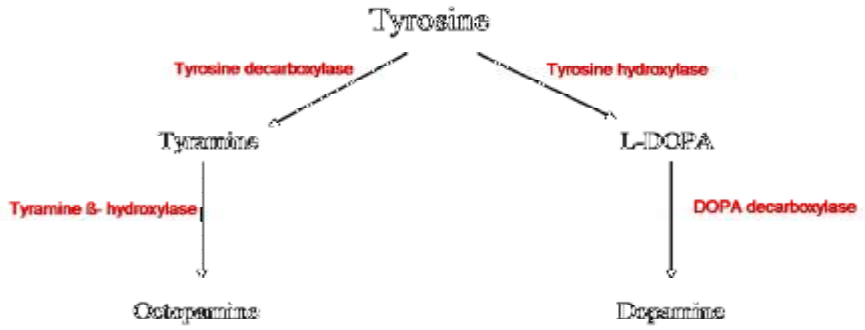

Figure 1: Synthesis of TA, OA and DA.
The amino acid tyrosine is the starting point for the synthesis of these compounds. TA is the direct decarboxylation product of tyrosine. This achieved through the tyrosine decarboxylase. OA is produced from TA through the tyrosine-*ß*-hydroxylase. Biosynthesis of dopamine starts from tyrosine which converts to dihydroxyphenylalanine (L-DOPA) by the enzyme tyrosine hydroxylase. Dopa decarboxylase then catalyzes the conversion of L-DOPA to dopamine.

In insects, biogenic amines act as neurotransmitters, neuromodulators and neurohormones. Biogenic amines control endocrine and exocrine secretion, the contraction of muscles, and the activity of neurons and in addition they are involved in learning and the formation of memory (Schwaerzel *et al.*, 2003; Riemensperger *et al.*, 2005; Unoki *et al.*, 2005).

Biogenic amines mediate these cellular and physiological effects by binding to specific membrane protein that belong to the superfamily of G-protein coupled receptors (Fig.2). It is a family that comprises diverse molecules as neurotransmitter receptors, rhodopsin, olfactory receptors and cytokine receptors and it includes attractive targets for insecticides.

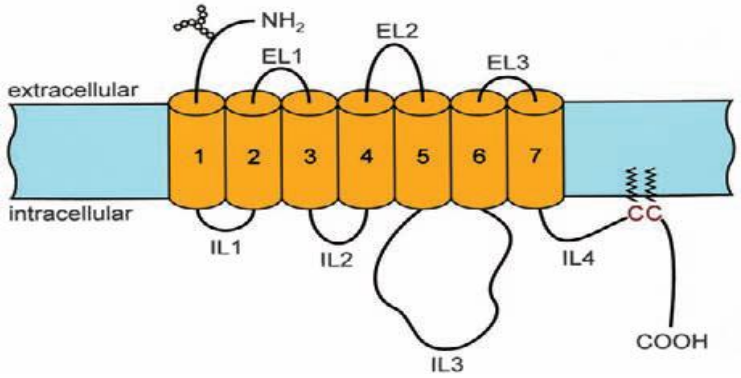

Figure 2: G-protein coupled receptors
The polypeptide spans the membrane seven times. The transmembrane regions (TM 1–7) are depicted as cylinders. The N-terminus (NH2) is located extracellularly and often contains glycosylated residues (o). The C-terminus (COOH) is located intracellularly. The membrane-spanning regions are linked by three extracellular loops (EL1–EL3) that alternate with three intracellular loops (IL1–IL3). Post-translational palmitoylation of cysteine residues (C) in the cytoplasmic tail creates a fourth intracellular loop (IL4) (Blenau and Baumann, 2001).

G-protein coupled receptors or 7TM receptors comprise a large protein family of transmembrane receptors that sense molecules outside the cell and activate inside signal transduction pathways and subsequent cell responses. The N-terminus is located extracellularly, whereas the C-terminus is located intracellularly. The N-terminus is the target of a common posttranslational glycosylation. The membrane-spanning regions are linked by three extracellular loops (EL) that alternate with three intracellular loops (IL). Cysteine residues in the C-terminus of the polypeptides are the target of posttranslational palmitoylation. This modification creates a fourth intracellular loop (Horstmeyer *et al.*, 1996). A receptor is activated after binding of the specific biogenic amine in a binding pocket formed by the TM regions in the plane of the membrane. Individual residues in TM3, TM5, and TM6 were shown to participate in ligand binding. For positively charged ligands such as biogenic amines, negatively charged counter ions inside and close to the binding pocket have been identified as crucial for receptor activation. Once the ligand is bound, the receptor changes its conformation. This structural alteration usually mechanically activates the intracellular trimeric GTP-binding proteins (G proteins) which exchange its bound GDP for a GTP. The G-protein's α subunit, together with the bound GTP, can then dissociate from the ß and γ subunits to further affect intracellular signaling proteins or target functional proteins directly depending on the α subunit type (G_s, G_i or G_q). There are two major signal pathways involving the G protein coupled receptors: the cAMP signal pathway and the phosphatidyl-inositol signal pathway (Hille, 1994; Clapham and Neer, 1997).

In the cAMP signaling pathway, GPCR activation leads to subsequent change of intracellular messenger concentrations (Fig.3). A change in the intracellular concentration of cAMP and/or Ca^{2+} is most likely to take place. As a result of GPCR activation, cAMP can change in two directions: cAMP levels are either elevated or decreased. The cellular response depends on the specificity of interaction between the receptor and the G protein (Gudermann *et al.*, 1996; Gudermann *et al.*, 1997a; Gudermann *et al.*, 1997b). When the receptor binds to a Gs-type protein, the activated Gαs subunit will interact with adenylyl cyclase (AC) in the plasma membrane. This leads to an increase of cyclase activity and production of cAMP from ATP with the help of cofactor Mg^{2+} or Mn^{2+}. The rise in cAMP will then activate cAMP-dependent protein kinase (protein kinase A, PKA). Phosphorylation of serine and/or threonine residues by PKA modifies the properties of various substrate molecules including cytosolic proteins, ligand-gated and voltage dependent ion channels, as well as transcription factors, such as CREB, CREM, and ATF-1 (De Cesare *et al.*, 1999). Several biogenic amine receptors are also known to inhibit adenylyl cyclase activity. This effect is mediated by interaction of the

receptor with inhibitory G proteins (Gi). Interaction of adenylyl cyclase with activated Gαi subunits most likely competes with binding of activated Gαs subunits and thereby interferes with cyclase activation.

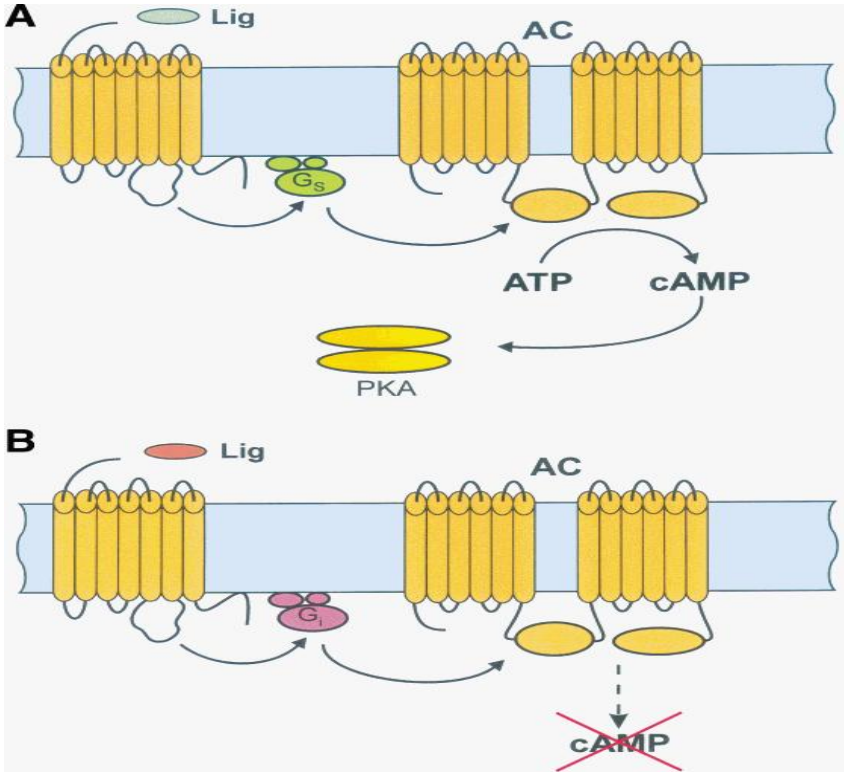

Figure 3: Biogenic amine receptors coupled to intracellular cAMP signaling pathways
A: Biogenic amine receptors are activated by binding of agonists (ligand, Lig). The ligand bound receptor then activates a stimulatory G protein (Gs), which leads to an increase in the enzymatic activity of adenylyl cyclase (AC). Adenylyl cyclase catalyzes the conversion of ATP to cAMP. As the intracellular concentration of cAMP increases, cAMP-dependent protein kinase (PKA) is activated and phosphorylates different target proteins on serine and threonine residues. B: Several biogenic amine receptors are known to inhibit AC activity via inhibitory G proteins (Gi).

Another pathway that is activated by several biogenic amine receptors results in an increase of Ca^{2+}. In this case, the amine-activated receptor binds to G proteins of the Gq/o family (Gudermann *et al.*, 1996; Gudermann *et al.*, 1997a; Gudermann *et al.*, 1997b). The activated Gαq/o subunits bind to and stimulate phospholipase C (PLC) activity (Rhee and Bae, 1997). The enzyme hydrolyzes phosphatidylinositol 4,5-biphosphate into two second messengers, IP_3 and DAG (Fig. 4). The IP_3 freely diffuses and binds to specific IP_3 receptors on the membrane of intracellular Ca^{2+} stores (endoplasmic reticulum and metochondria). These receptors are second messenger-gated Ca^{2+} channels. Therefore, after binding of IP_3, the channel pore is opened and Ca^{2+} is released into the cytoplasm. Ca^{2+} ions play a pivotal role in the regulation of many cellular functions by directly controlling enzymatic or ion channel activities. Furthermore, Ca^{2+} can also bind to members of the large family of Ca^{2+} - binding

proteins (calmodulin, calbindin, calretinin, etc.) that modulate the activation properties of many effector proteins by protein-protein interaction. Since PLC not only generates IP_3 but also DAG, receptor coupling to Gq/o proteins might activate a second signaling pathway in addition to Ca^{2+} release. DAG remains associated with the membrane, where it activates protein kinase C (PKC). PKC enzymatic activity requires the presence of DAG and Ca^{2+} as well as association of the kinase with the membrane. Similar to PKA, PKC phosphorylates a variety of proteins on serine and threonine residues, which alters the functional properties of these proteins, changing their catalytic activities leading to cellular responses.

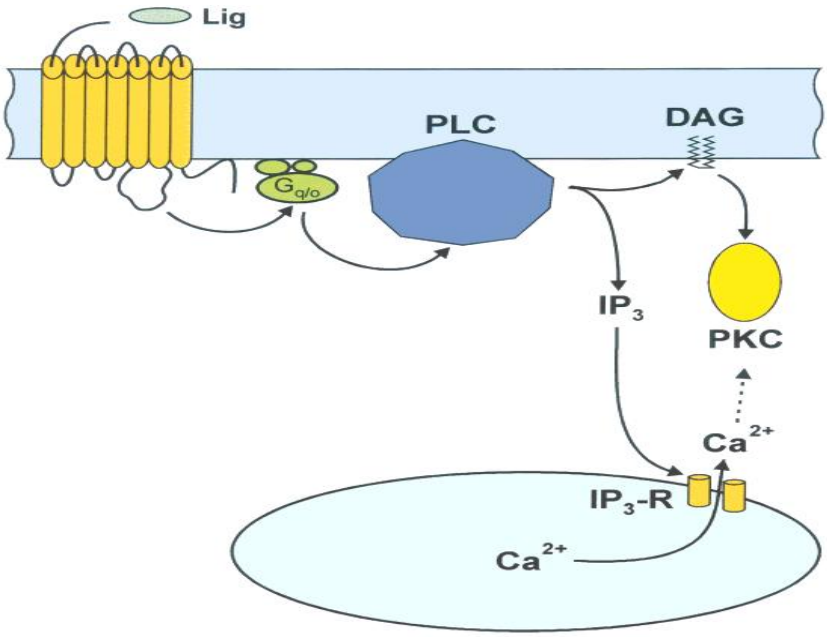

Figure 4: Biogenic amine receptors coupled to intracellular IP3/DAG signaling pathways.
Agonist (ligand, Lig)-bound biogenic amine receptors activate G proteins of the Gq/o family (Gq/o) that regulate the enzymatic activity of phospholipase C (PLC). This enzyme hydrolyzes phosphatidylinositol 4,5-bisphosphate into inositol 1,4,5-trisphosphate (IP_3) and diacylglycerol (DAG). Binding of IP_3 to specific receptors (IP3- R) that form ion channels in the membrane of the endoplasmic reticulum (ER) causes release of Ca2+ into the cytoplasm. Both the increase in intracellular Ca^{2+} and the membrane bound DAG activate protein kinase C (PKC) that phosphorylates different target proteins.

Biogenic amines have many functions controlling all phases of the life cycle of an insect. They are important chemical messengers during embryonic and larval development and they participate in the synaptic organization of the brain in the adult. As neuroactive substances they act on sensory receptors, inter- and motor neurons, and muscles and other peripheral organs such as fat body, salivary glands, corpora allata and corpora cardiaca, oviduct, etc. (Rachinsky, 1994; Park and Keeley, 1998; Walz *et al.*, 2006; Rauschenbach *et al.*, 2007).

Biogenic amines can initiate or modulate different types of behaviour and they are involved in learning and the formation of memory in insects. The effects of biogenic amines in the insect central nervous system are studied with many techniques including cell cultures, microinjections of amines and receptor ligands, and behavioural assays. Often the physiological responses to biogenic amines last for many minutes, which suggest that they may be act as neuromodulators. Biogenic amines modulate neuronal activity and the efficacy of synaptic transmission in all parts of the nervous system. The huge projection fields of many aminergic neurons support the idea of parallel modulation of entire neuronal circuits by just a few aminergic cells. In addition to synaptic neurotransmission, some aminergic neurons release the amine into the heamolymph (Hauser *et al.*, 2006). The substances are transported throughout the body and may thus have hormonal functions in specific target tissues.

1.1. Octopamine and tyramine

Octopamine has been identified almost 60 years ago in the salivary glands of *Octopus* (Erspamer, 1952). Starting from this, it has been identified in countless invertebrates, in the central nervous system, but also in peripheral organs (Roeder, 1999). The physiological role of octopamine at different levels of the organism is not completely documented. As a stress hormone in the periphery and in the central nervous system OA prepares the animal for energy-demanding behaviors such as aggression and stress resistance (Mercer and Menzel, 1982; Adamo *et al.*, 1995; Scholz *et al.*, 2000; Stevenson *et al.*, 2000; Schwaerzel *et al.*, 2003; Schroll *et al.*, 2006; Vergoz *et al.*, 2007; Hoyer *et al.*, 2008). This monoamine stimulates glycogenolysis, modifies muscle contraction, supports long-term flight, and regulates "arousal" in the central nervous system (Brembs *et al.*, 2007). Injection of OA can elicit flight motor behaviour in locusts. It is assumed that in insects OA has functions similar to those of the adrenergic system in vertebrates (Roeder, 1999). OA can modulate sensory receptors and receptor organs in insects. In many cases the sensitivities of the receptors are enhanced. The octopaminergic neurons are known to innervate most of the larval muscles (Monastirioti *et al.*, 1995). The amplitude of neuromuscular junction potential is increased by applying octopamine in a dose- dependent manner (10^{-7} to 10^{-5} M) up to 115% compared with the control (Nagaya *et al.*, 2002). Different functions of octopamine and tyramine at the sensory periphery are not very well understood, because the two amines often differ only in the degree of modulation. The increased sensitivity of sensory receptors due to the action of OA can modify behaviour and is part of the "fight or flight" function. Studies on the *Drosophila* tyramine receptor mutant ***hono*** suggest that TA can also modulate the sensitivity of olfactory

receptor cells, thus modulating behavioural responses to olfactory repellents (Kutsukake *et al.*, 2000). The modulation of interneurons or effector neurons by biogenic amines is another level of modifying signal processing. OA usually enhances the sensitivity or activity of single neurons. This effect, which can be measured at both the behavioural and the single cell level, is dependent on the state of the insect. OA can induce a state of "arousal" in inactive animals and has only minor effects on very active animals. We have only very limited information regarding non-neuronal tissue expression of TA/OA receptors. Muscular systems (Monastirioti *et al.*, 1995) including ovaries (Lee *et al.*, 2003) as well as malpighian tubules are among them (Blumenthal, 2003). But the full picture of the TARs/OARs expression pattern in neuronal and non-neuronal tissues does not exist until now.

1.2. Pharmacology of octopamine and tyramine receptors

A wealth of information is available for the OARs, for which hundreds of different compounds display high-affinity properties. Most OARs ligands are agonists and very few are antagonists. The attention of pharmacologists was directed to OAR pharmacology after it became apparent that these receptors are preferentially present in invertebrates, therefore serving as ideal targets for specific insecticides. The imbalance between agonists and antagonists may reflect the observation that octopaminergic insecticides are always OAR agonists and never antagonists.

On the basis of OA structure, substances such as synephrine were characterized by their higher affinity. The first agonists with high insecticidal potential were the formamidines, with chlordimeform as the prototype. Subsequently, additional compounds such as the phenyliminoimidazolidines or aminooxazoline derivatives were developed. They displayed extremely high affinities for OARs (Long and Murdock, 1983; Nathanson, 1985; Roeder and Nathanson, 1993; Roeder *et al.*, 1998). Some of these substances display a high insecticidal potency, but only "old" octopaminergic insecticides such as amitraz or chlordimeform were used for this purpose. A characteristic feature of these octopaminergic insecticides is the way insects react if they are exposed to them. Usually, at rather low doses, the compounds induce hyperactivity, which is often followed by the famous leaf walk-off syndrome. Insects feeding on leaves are usually too "nervous" to stay where they are; they stop feeding and finally walk off the leaves, presumably induced by a higher motor activity. At higher concentrations, this hyperactivity can induce tremors that lead to death but knowledge regarding the actions of octopaminergic antagonists is limited (Roeder, 2005).

Only one antagonist, epinastine, combines high affinity with high specificity and has a relatively broad pharmacological spectrum in vertebrates. In insects, it has a narrow pharmacological profile, which allows for specific blockades of octopaminergic neurotransmission. This makes it an ideal tool for the dissection of octopaminergic neurotransmission *in vivo* (Roeder *et al.*, 1998), a feature that was used to elucidate some aspects of octopaminergic neurotransmission (Pophof, 2002).

Similarities between the octopaminergic/tyraminergic and the adrenergic system are not only in the structure of the transmitters/hormones themselves but also in the structural and pharmacological features. Although OARs/TARs and adrenergic receptors are homologous but their pharmacological characteristics are different, giving enough room for the development of specific insecticides (Roeder, 2005). *Drosophila Oamb* represents the neural type OAR, is ubiquitously expressed throughout the animal and may be responsible for most if not all actions of OA. In addition, *Drosophila Oamb* is thought to be the target for octopaminergic insecticides (Roeder, 1999, 2005).

For insect OARs, only the activation of cAMP synthesis and the elevation of Ca^{2+} concentrations are known, presumably via activation of Gs and Gq. Insect TARs are coupled to the activation of the Gi protein, inducing the inhibition of the adenylate cyclase. The emerging picture of OA and TA signaling is rather simple. OA is stimulatory, whereas TA is inhibitory. This means that octopaminergic agonists and tyraminergic antagonists have synergistic activities, an aspect that may be relevant to the development of new strategies for pest control (Roeder, 2005).

Numerous pharmacological studies have been performed in locusts in order to classify octopamine receptor classes. According to their pharmacological properties and intracellular signaling pathways, four different classes were identified: OCT-1, OCT- 2A, OCT-2B, and OCT-3 (Evans and Robb, 1993; Roeder, 1999). Activation of OCT-1 receptors induces an increase in $[Ca^{2+}]i$, whereas activation of OCT-2A, OCT-2B, or OCT-3 receptors stimulates adenylyl cyclase and leads to increases in [cAMP]i. In comparison to the locust, only a few studies were performed in *Drosophila* and the honeybee to determine the pharmacological properties of octopamine receptors (Dudai and Zvi, 1984; Degen *et al.*, 2000).

In *Drosophila* head homogenates, octopamine is a potent stimulator of adenylyl cyclase activity (Uzzan and Dudai, 1982). Interestingly, simultaneous application of both tyramine and octopamine reduces the effect of octopamine. This observation suggests that tyramine activates specific tyramine receptors that inhibit adenylyl cyclase and thereby reduce the stimulatory effect of octopamine (Uzzan and Dudai, 1982). In membrane homogenates of

honeybee brains, octopamine also stimulates cAMP production (Blenau and Baumann, 2001). In addition, injections of octopamine into the antennal lobe of the honeybee, evoke a rapid and transient activation of PKA (Hildebrandt and Muller, 1995). The effects of tyramine were also tested on membrane preparations from honeybee brain. When tyramine is applied at high concentrations, it activates adenylyl cyclase (EC50 of ~2.2 mM) but at low concentrations (0.1–1 mM) it attenuates forskolin-stimulated cAMP production (Blenau *et al.*, 2000).

The *Bombyx mori* OA receptor isolated from the nervous tissue of *Bombyx* larvae which is nearly identical to OA receptors isolated from *Periplaneta americana*, *Apis mellifera* and *Drosophila melanogaster Oamb*, was expressed in HEK-293 cells. OA treatment at concentrations 1mM led to an increase in intracellular cAMP concentrations. The OA receptor agonist demethylchlordimeform also elevated cAMP levels to the same maximal level (approximately 5-fold greater than basal levels) as that induced by OA. By contrast, the biogenic amines TA and DA and demethylchlordimeform lacked effect. The OA-stimulated increase in cAMP levels was suppressed by antagonists; the rank order of antagonist activity was chlorpromazine > mianserin > yohimbine (Ohta, 2009).

1.3. Dopamine in invertebrates

In both vertebrates and invertebrates, the biogenic amine dopamine is implicated in many functions including locomotion, cognition, and development (Civelli, 1993; Civelli *et al.*, 1993). In vertebrates, dopamine binds to two subfamilies of dopamine receptors: D1- and D2-like receptors (Kebabian and Calne, 1979). These receptors belong to the family of GPCRs and possess different pharmacological and biochemical properties. In humans, D1- and D5-receptors constitute the D1-subfamily and activate adenylyl cyclase, whereas members of the D2-subfamily, i.e., the D2-, D3-, and D4-receptors, either inhibit adenylyl cyclase or couple to different intracellular second messenger systems (Jackson and Westlind-Danielsson, 1994; Missale *et al.*, 1998; Vallone *et al.*, 2000). Three different *Drosophila* dopamine receptors are known: *DopR1* or *DmDop1*, also known as *dDA1* (Gotzes *et al.*, 1994; Sugamori *et al.*, 1995); *DAMB* or *DopR2* (Feng *et al.*, 1996; Han *et al.*, 1996)and *D2*-like receptors, also called *D2R* (Hearn *et al.*, 2002).

In *Drosophila*, high DA concentrations coincide with larval and pupal molts. Reduced levels of DA during larval stages lead to developmental retardation and decreased fertility in adults. DA expression in non-neuronal tissue, namely the tracheal system, was reported before (Hsouna *et al.*, 2007). But the informations regarding DA and DA receptors physiology and localization in larvae and adult flies are far from being complete.

In mammals, dopamine modulates movement, motivation and cognition. Abnormal functional states of the DA system in humans is though to underlie the behavioural abnormalities of Parkinson's disease, Attention Deficit Hyperactivity disorder (ADHD), schizophrenia and addiction.

Parkinson's disease (PD) is a degenerative disorder of the central nervous system due to the loss of some dopaminergic neurons that often impairs the sufferer's motor skills, speech, and other functions. Parkinson's disease belongs to a group of conditions called movement disorders. It is characterized by muscle rigidity, tremor, a slowing of physical movement and a loss of physical movement in extreme cases (Lang and Lozano, 1998a, b; Jankovic, 2008). Although the identification of genes that are responsible for heritable forms of PD has the potential to provide insight into the mechanisms of PD, and the interplay between genetics and environment in this disorder, little about the biological functions of the genes have been identified and how their mutational alteration results in neuronal death. One promising approach to this problem involves the use of classical genetic analysis in the fruit fly, *Drosophila melanogaster*. *Drosophila* has a complex nervous system that consists of ~100,000 neurons, and includes a subset of ~200 neurons that contain the neurotransmitter DA. Although the anatomy of the fly brain and the distribution of DA neurons in the central nervous system of *Drosophila* differ from that of vertebrate brains, many fundamental cellular and molecular biological features of neuronal development and function are conserved between vertebrates and invertebrates. This conservation makes *Drosophila* a powerful system for basic studies of neuronal development and function and, more recently, studies of neuronal dysfunction. Furthermore, the completion of both human and *Drosophila* genome-sequencing projects has also revealed that a large fraction of human genes, including many involved in disease, have highly conserved counterparts in *Drosophila*. In particular, the *Drosophila* genome encodes homologs of five out of the six PD-related genes that have been identified. The important advantage of using *Drosophila* as a model for human disease to understand is the ability to conduct genome-wide genetic screens for mutations in other genes that modulate the phenotype associated with a disease model and identify genetic pathways that cause the disease, as well as those that can influence it.

Humans dopaminergic system has also been implicated in the control of the reward mechanisms and in the psychomotor effects generated by drugs of abuse, including opiates, cocaine, amphetamine and alcohol (Wise and Bozarth, 1987; Koob, 1992). Cocaine and amphetamine increase DA levels in the synaptic cleft by blocking the activity of the DA transporter (DAT), and by reversing DA transport via DAT thus elevate mood and cause

pleasure (Wise and Bozarth, 1987). However, opiates have an inhibitory effect on DA release in a variety of brain areas including the striatum, frontal cortex, mediobasal hypothalamus and amygdala (Wise, 1996). Mutant strains have different responses to the effect of alcohol on locomotion. Behaviors are remarkably similar to those described for mammals. Thus *Drosophila* also has been proposed as a model organism for studying the genetics of addiction and understanding the biochemical regulator of drugs sensitization.

Few approaches also use Drosophila as a model of studying Attention Deficit Hyperactivity disorder or ADHD (De Luca *et al.*, 2002).

Thus generations of genetically modified *Drosophila* for different components of the dopaminergic pathways constitutes a powerful tool for studying the in vivo roles of these proteins.

1.4. The role of OA and DA in learning and memory

Biogenic amines are involved in different forms of learning and memory formation in *Drosophila* and honey bees. Research on the neuronal and molecular bases of learning and memory since many years ago in insects has focused on the mushroom bodies and antennal lobes of the brain. These two structures are involved primarily in processing olfactory stimuli. Experimental evidence suggests that DA signals the presence of reinforcers and modulates intrinsic mushroom body neurons during conditioning in *Drosophila*. Thus DA could trigger signaling cascades that affect the storage of information about the conditioned stimulus. In the honey bee, OA appears to be the modulatory transmitter which conveys information about rewarding sucrose stimuli and induces medium- to long-term modifications in interneurons during associative olfactory learning. Electrical stimulation of an identified octopaminergic cell, the ventral unpaired median VUMmx1 neuron, can substitute for the sucrose reward during olfactory conditioning (Hammer, 1993). This neuron has extensive arborizations in different brain regions, including the antennal lobes and the mushroom bodies. Microinjections of OA into these two neuropiles of the bee brain confirmed that OA in fact induces associative learning. Thus, a picture emerges, where aversive learning depends on dopamine, whereas reward learning depends on octopaminergic signalling. In both cases, the mushroom bodies are essential integrative centres for these rather complex behaviours. The exact molecular and cellular substrates underlying this very interesting behaviour are nevertheless not understood yet.

1.5. *Drosophila* tools used in neurobiology

A very useful genetic tool for study of gene function in *Drosophila* is the P-element transposition system (Rubin and Spradling, 1982). P-elements have been utilized to knock out genes as well as to insert genes into the *Drosophila* genome. This allows the study of genetics, developmental biology, neurobiology, and medicine.

Drosophila provides an excellent model system to study of biogenic amines and their receptors due to the availability of various mutant lines, driver lines and effector lines that are specific for amine systems. Driver lines and effector lines are the two essential components make the binary system GAL4/UAS system (Brand and Perrimon, 1993b). With the GAL4/UAS system (Fig.5) genes can be expressed in temporally and spatially restricted manner.

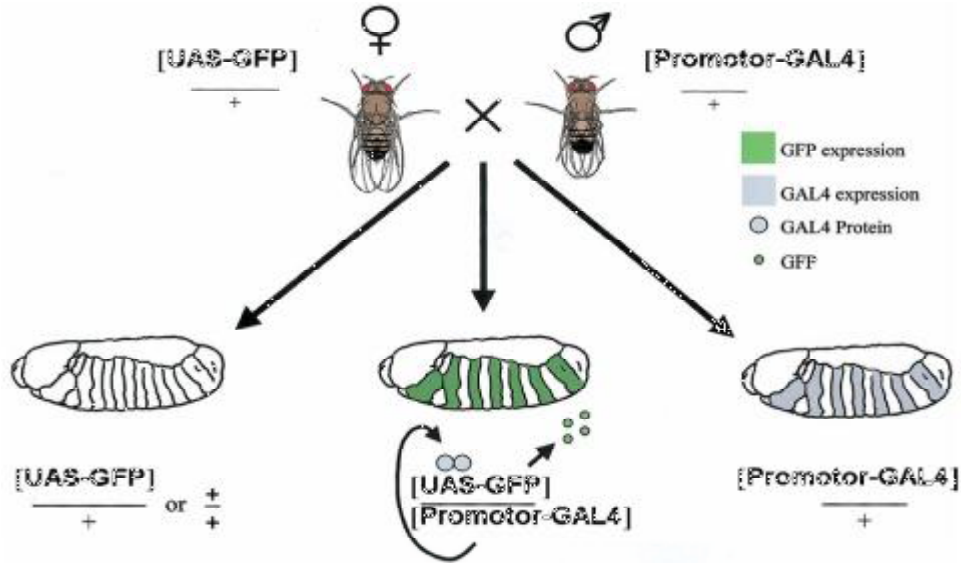

Figure 5: The bipartite UAS/GAL4 system in *Drosophila*
When females carrying a UAS responder (UAS-GFP) are mated to males carrying a GAL4 driver , only progeny containing both elements of the system express the responder in a transcriptional pattern that reflects the GAL4 pattern of the respective driver (modified from (Duffy, 2002).

To learn more about the physiological relevance of a certain gene, constructs carrying the gene of the yeast transcription factor GAL4 can be inserted in the *Drosophila* genome. In these line, which are called driver lines, GAL4 expression is driven by promoters previously cloned upstream of the GAL4 gene and subsequently inserted into the *Drosophila* genome by germline integration. Independent from these lines are other transgenic lines that allow targeted overexpression of any gene of interest. There, the GAL4 binding site (UAS) with many options of reporter genes are produced. The gene of interest is under transcriptional control of GAL4, meaning that it is only expressed if Gal4 is present. Thus, crossing these two lines will bring both partners, Gal4 and UAS element, together in the F1 generation, but

only in those cells, where the corresponding promotor is active. This yields a targeted expression pattern totally depending on the expression pattern of the driver line. Countless different combinations of crossing are possible, which combine a wealth of different driver lines with different anatomical localizations (e.g. only in the brain or only in the muscles) with also countless different effector lines (e.g. GFP or overexpression of human diseases relevant proteins etc.). A recent and extremely versatile update of the Gal4/UAS system has been the introduction of UAS-RNAi lines that allow targeted down regulation of any gene of interest. These lines contain a double-stranded hairpin construct under UAS control. Even more versatile was the introduction of a series of 22.000 transgenic lines covering the almost entire genome, which has been made available to the public via the Vienna *Drosophila* Research Center (Dietzl *et al.*, 2007).

The information regarding the expression pattern of biogenic amine receptors within the different insects tissues (including CNS) are very important from different points of view and has important implications for comparative and evolutionary physiology and biochemistry as well as serving as new targets for insecticides. Numerous data have been collected but the data are not complete, thus there is a growing need for these informations to be used for further, downstream studies and applications. To fill this gap, the physiological relevance of the different receptors has to be elucidated. As already pointed out, the fruit fly *Drosophila* melanogaster is ideally suited for this purpose, because it can be manipulated with great ease and speed.

To get access to the pharmacological properties of biogenic amine receptors, their heterologous expression in cell culture systems is required. To achieve this, full-length clones of all relevant genes coding for these receptors have to be cloned into mammalian expression vectors to get stable cell lines expressing the receptor of interest. Followed by artificial application of different lead compounds for insecticide into cells, including agonists and antagonists, reporter assay have to be optimized to allow in depth pharmacological studies. Those receptors that are most promising should be made available for high-throughput or semi-high-throughput screening assay systems.

1.6. Aim of the work

The main goal of this work was to get more accurate knowledge about the expression and function of the biogenic amine receptors in the fruit fly *Drosophila melanogaster* especially for TARs/OARs and DA receptor members. The present study has three main aspects:

1. Characterization of the temporal and spatial expression pattern of each of biogenic amine receptors using the binary system GAL4/UAS (Brand and Perrimon, 1993a). GAL4-transgenic lines carrying promoters' sequence of each bioamine receptor gene should be constructed by germline integration. These promotor-GAL4 lines should be used, together with corresponding UAS-GFP responder lines to elucidate the expression patterns in all developmental stages (larvae, pupae and adults) and in all organs in detail.
2. The major question is: Which receptor represents a potential target for insecticides. RNAi-based silencing and overexpression studies for biogenic amine receptors using GAL4/UAS system by which it is possible to interfere with gene function practically anywhere and anytime during development. RNAi experiments will be performed with different types of RNAi lines covering all genes of interest. Using them a number of phenotypical and/or behavioural parameters should be quantified.
3. Pharmacological characterization of biogenic amine receptors.

   To achieve this, full-length clones of genes coding for biogenic amine receptors are cloned into mammalian vectors. Following this, stable transgenic cell lines are established that express each gene coding for a biogenic amine receptor. Application of different lead compounds for insecticides should unravel the pharmacological features of these very important molecules.

2. Materials and methods

2.1. Materials

2.1.1. Drosophila lines

2.1.1.1. GAL4-Lines (Bloomington stock centre http://flystocks.bio.indiana.edu/).

- Y [1]W[*]; P{w [+mC] =tubP-GAL4}LL7/TM3, sb [1].

2.1.1.2. UAS-lines (Bloomington stock centre)

- P {w[+mc]+UAS-mCD8:GFP.L}LL4, y[1]w[*] P{w[+mW.hs=GawB}Iz[gal4]

2.1.1.3. RNAi-lines (Bloomington stock centre)

- CG33976: Dm Octbeta2R

2.1.2. Buffers and solutions

- *Drosophila* Ringer's solution: $CaCl_2.2H_2O$ 3mM, KCl 182mM, NaCl 46mM and Tris base 10mM were dissolved in distilled water. The pH value was adjusted to 7.2 with 1N HCl and the solution was filtered using filter paper with 0.47µm pores and autoclaved.
- Phosphate buffered saline (PBS): NaCl 137mM, KCl 2.7mM, Na_2HPO_4 4.3mM and $KH_2PO_4$1.47mM, were dissolved in 500 ml distilled water, adjusted to pH 7.5 and diluted up to 1L (1x).
- SOB-medium: 20g bacto tryptone and 5g bacto yeast extract were dissolved in 900ml distilled water; 2ml of 5M NaCl, 2.5ml of 1M KCl, 10ml of 1M $MgCl_2$ and 10ml of 1M $MgSO_4$ were added. The solution was diluted up to 1L with distilled H_2O and autoclaved.
- Paraformaldehyde in PBS (4%): 4g of paraformaldehyde were dissolved in 100ml Phosphate Buffered Saline (PBS) with aid of a hotplate stirrer. The solution was become clear on cooling before being stored at 4°C.

2.1.3. Chemicals

Agar	Carl Roth Hamburg,Germany
Agarose	Biozym (Hamburg,Germany)
Ampicillin Sodium salt	Sigma-Aldrich chemicals GmbH (Taufkirchen)
Boric acid	Carl Roth (Hamburg,Germany)

Calcium chloride	Carl Roth (Hamburg,Germany)
Diethanolamine	Acros Organics GmbH (Taufkirchen)
Dimethylsulfoxide (DMSO)	Sigma-Aldrich chemicals GmbH (Taufkirchen)
Disodium hydrogen phosphate	Carl Roth (Hamburg,Germany)
dNTP	MBI Fermentas GmbH (St.Leon-Rot)
EDTA	Applied Biosystems (Darmstadt)
Ethanol	Carl Roth (Hamburg,Germany)
Ethidium bromide	Applied Biosystems (Darmstadt)
Glucose	Carl Roth (Hamburg,Germany)
Goat serum	Sigma-Aldrich chemicals GmbH (Taufkirchen)
Hoechst stain	Sigma-Aldrich chemicals GmbH (Taufkirchen)
Isopropanol	Carl Roth (Hamburg,Germany)
LB-agar	Invitrogen Life Technologies (karlsruhe)
LB-medium	Invitrogen Life Technologies (karlsruhe)
Magnesium chloride	Carl Roth (Hamburg,Germany)
Magnesium sulphate	Carl Roth (Hamburg,Germany)
Napagin	Sigma-Aldrich chemicals GmbH (Taufkirchen)
Nile red	Sigma-Aldrich chemicals GmbH (Taufkirchen)
Paraformaldehyde	Sigma-Aldrich chemicals GmbH (Taufkirchen)
Peptone	Sigma-Aldrich chemicals GmbH (Taufkirchen)
Phalloidin	Sigma-Aldrich chemicals GmbH (Taufkirchen)
PNP (P- Nitrophenyl phosphate tablets)	Sigma-Aldrich chemicals GmbH (Taufkirchen)
RNA magic	Bio-Budget (Hamburg,Germany)
Sodium chloride	Carl Roth (Hamburg,Germany)
Sucrose	Carl Roth (Hamburg,Germany)
Tris	Sigma-Aldrich chemicals GmbH (Taufkirchen)
TritonX-100	Sigma-Aldrich chemicals GmbH (Taufkirchen)
X–GAL	Sigma-Aldrich chemicals GmbH (Taufkirchen)
Yeast extract	Sigma-Aldrich chemicals GmbH (Taufkirchen)
Zink chloride	Carl Roth (Hamburg,Germany)

2.1.4. Compounds used in pharmacological experiments (obtained either from Sigma-Aldrich chemicals GmbH (Taufkirchen) or from different researchers).

Amitraz (N,N'-[(methylimino) dimethylidyne]di-2,4-xylidine)

Chlordimeform.

Chlorpromazine (3-(2-chloro-10 H-phenothiazin-10-yl)-N, N-dimethyl-propan-1-amine)

Desmethylchlordimeform

Dopamine (4-(2-aminoethyl) benzene-1,2-diol)

Epinastine

Mianserin (*RS*)-2-methyl-1,2,3,4,10,14b-hexahydrodibenzo[*c*,*f*]pyrazino[1,2-*a*]azepine)

Metoclopramide monohydrochloride(4-amino-5-chloro-*N*-(2- (diethylamino)ethyl)-2-methoxybenzamide)

Naphazoline hydrochloride (2-(naphthalen-1-ylmethyl)-4,5-dihydro-1H-imidazole)

NC3

NC4

NC5

NC6

NC7

NC9

NC12

Octopamine (4-(2-amino-1-hydroxy-ethyl)phenol)

Phentolamine (3-[4,5-dihydro-1H-imidazol-2-ylmethyl- (4-methylphenyl)-amino]phenol)

Rauwolscine

Serotonin (5-Hydroxytryptamine or 3-(2-aminoethyl)-1*H*-indol-5-ol)

Synpherine (4-[1-hydroxy-2-(methylamino)ethyl]phenol)

Tyramine (4-(2-aminoethyl)phenol)

Yohimbine hydrochloride (17α-hydroxy-yohimban-16α-carboxylic acid methyl ester)

2.1.5. Kits

DNA purification kit	MBI Fermentas GmbH (St.Leon-Rot)
Plasmid preparation kit	Mol Biotech (Heidelberg, Germany)
PCR purification kit	MBI Fermentas GmbH (St.Leon-Rot)
SEAP assay Kit	Invitrogen Life Technologies (karlsruhe)
Gel extraction kit	MBI Fermentas GmbH (St.Leon-Rot)
The CloneJET™ PCR Cloning Kit	MBI Fermentas GmbH (St.Leon-Rot)

2.1.6. *Drosophila* media

Semi-defined medium:10g agar, 80g yeast, 20g yeast extract, 20g peptone, 30g sucrose, 60g glucose, 0.5g $MgSO_4.6H_2O$ and 0.5g $CaCl_2.2H_2O$ were dissolved into 1L with water, boiled and cooled to 60°C. Propionic acid and Napagin were added during stirring. The mixture was dispensed when the temperature reached 40-50°C.

2.1.7. Cell culture media

Advanced DMEM, Dulbecco's modified Eagle medium, was used. It was supplied with L-glutamine or GLUTAMAX™-I (GIBCO®). Twenty ml of fetal bovine serum albumin, 5ml GLUTAMAX™ and 5ml penicillin/streptomycin were added to each 500 ml bottle.

2.1.8. Enzymes

- Superscript — Invitrogen Life Technologies (karlsruhe)
- T4 DNA Ligase — MBI Fermentas GmbH (St.Leon-Rot)
- Taq Polymerease — MBI Fermentas GmbH (St.Leon-Rot)
- CIAP — MBI Fermentas GmbH (St.Leon-Rot)
- Retriction enzymes were from MBI Fermentas GmbH (St.Leon-Rot).

2.1.9. Plasmids

- pCRE-SEAP — BD Bioscience Clontech (Heidelberg)
- PpTGAL — (Provided by D. Eberl)
- pEAK10CV — Edge Biosystems (Gaithersburg, USA)

2.1.10. Antibodies

2.1.10.1. Primary antibodies

- anti GFP(1A5) - Rat monoclonal IgG — Santa Cruz Biotechnology (Heidelberg, Germany)
- N2 7A1 ARMADILLO- Mouse Anti-*Drosophila* Armadillo Protein Monoclonal Antibody, Unconjugated. — Developmental Studies Hybridoma Bank (Iowa, USA)
- Prospero (MR1A) - Mouse Anti-*Drosophila* Prospero Protein Monoclonal Antibody, Unconjugated. — Developmental Studies Hybridoma Bank (Iowa, USA)

2.1.10.2. Secondary antibodies

- § DyLight™ 488-conjugated Affinipure Donkey Anti-Rat IgG (H+L) Jackson ImmunoResearch Europe (Heidelberg, Germany).
- § DyLight™ 549-conjugated Affinipure Goat Anti-Rat IgG (H+L) Jackson ImmunoResearch Europe (Heidelberg, Germany).

2.1.11. Oligonucloetides (primers)

2.1.10.1. Primers for biogenic amine receptor gene promoters amplification

DOPR1-sense: 5`-GAG AGC GGCCGCATGGAG CTT TGG AGG TTT-3`

DOPR1-antisense: 5`-GAGAGG ATC CAC ACA CAC TTA CAC GTC ACT-3`

DOPR2-sense: 5`- GAG AGC GGC CGC TAA CTC GAT TCT CGC ATGC-3`

DOPR2-antisense: 5`-GAG AGA TCT CTG TTC CTG TGC CTG ATT CT-3`

DOPR2-like-sense: 5`- GAG AGC GGC CGC AGT TGT TCG TTG TGG TGT-3`

DOPR2-like-antisense: 5`- GAG AGA TCT CAG CCA CAT TGT CCA G-3`

OAMB –sense: 5`-GAG GCG GCC GCT GTA TGA GTG GTG CCA CAGC-3`

OAMB-antisense: 5`-GAG AAGATCTAATTGTT CGTT CCGGAACG-3`

OA2- sense: 5`- GACGAC CTC CAT TTA ACA CC-3`

OA2-antisense: 5`- TTC CTA GAA CCC AAC ATGCC-3`

OCTBeta 2R- sense: 5`- GAG AGG ATC CGG CAT CTT CGG TCC AAT ACC-3`

OCTBeta 2R-antisense: 5`- GAG AGC GGC CGC GAG TCT CGT TGT CTG GTT-3`

OCTBeta 3R-sense: 5`- GAG AGG ATC CAA TAA TCG GCG AGT GTG AGG-3`

OCTBeta 3R-antisense: 5`- GAG AGC GGC CGC CCA TGC GAG CCT GAT TAGG-3`

TyRIII-antisense (BamHI):5`- GAG AGG ATC CGG TTC ACA ATC GAG TGT GG-3`

TyrR III –sense (Not I) :5`- GAG AGC GGC CGC CTA ATG CCG GAG ATG AGT GC-3`

TyrRII -antisense (BglII):5`GAG AAG ATC TGC GGA TAG CTC ACT CAC TTA GG-3`

TyrRII –sense (NotI):5`GAG AGC GGC CGC AAC GAA TCC TGC TGA CAA GC-3`

TyrR-antisense (Bgl II):5`GAG AAG ATC TAA CTT TAG CCA CCC GCA AC -3`

TyrR-sense (Not I):5` GAG AGC GGC CGC CTT GCT GAT GCT CTG GTT GG-3`

2.1.11.2. Primers for amplification of the whole coding regions of biogenic amine receptor genes for pharmacological studies

OCTBeta 2R-cDNA-sense: 5`-GAG AGA ATT CAT GTT GTT GTG CGA CGG CTTG-3`

OCTBeta2R-cDNA-antisense: 5`-GAG AGC GGC CGC TTA TAA GTT GTC CAC CAT CTGA GAC-3`

OCTBeta3R-cDNA-sense:5`-GAG AGA ATT CAT GTCAGG GGT TAA CGT GGC TG-3`
OCTBeta3R-cDNA-antisense: 5`- GAG AGC GGC CGC TTA GAC GTA GTA GGCG TTG TACG-3`

2.1.11.3. Sequencing primers

PEAK –rev: 5` -ACC TGT CCC GCC TTGAGCT -3`
PEAK- for: 5`- CTC AGA CAG TGG TTC AAAG-3`
PpTGAL-rev: 5`-TTA GCG ACG AGT TCA CTT TGC-3`
PpTGAL-for: 5`-GTT CAA TGA TAT CCAGTG CAGT-3`

2.1.12. Equipment

Incubators	Waterbath Thermostat	Eppenodrf AG (Hamburg)
Microscopes	• Imager.Z1, Zeiss	Carl-Zeiss MicroImaging, GmbH
	• Leica TCS SP1 confocal Microsystems	Heidelberg Germany
	• Olympus	Olympus Optical Co Europa GmbH
PCR machines	bio-Rad Laboratories GmbH (München)	
Spectrophotometer	• NanoDrop(ND-1000UV/Vis-spectralphotometer Peq (Erlangen) • Multiscan MCC/340 P version 2.32	

2.2. Methods

2.2.1. *Drosophila* breeding

Maintenance and breeding of *Drosophila* were done in clear plastic vials and bottles without lid, but capped with foam bungs (Foam wads or closure). Semi defined medium supply to the flies was about one fourth of the bottles and vials. Napagin solution and Propionic acid were added to the medium to protect media from being infected. Renewal of *Drosophila* media was done every 1-2 weeks, by anaesthetizing adult *Drosophila* using carbon dioxide in the old bottle or vial for a while and moving adults into the new one.

2.2.2. Constructing GAL4 transgenic lines

2.2.2.1. Genomic DNA extraction

Drosophila larvae (5-10) were grinded in 200µl TE buffer and then added to 400µl lysis solution (DNA Extraction kit MBI Fermentas), incubated at 65°C for 5min. 600µl of chloroform was added to the pervious solution and gently emulsified by inversion (3-5) times. After centrifugation at 10,000 rpm for 2min, the upper aqueous phase containing DNA was transferred to a new tube containing 800µl of precipitation solution. This solution was mixed gently by several inversions at room temperature for 1-2 min and centrifuged at 10,000 rpm for 2 min. Supernatant was removed completely and the pellet was dissolved in 100 µl of 1.2M NaCl solution by gentle vortex. Cold ethanol was added to precipitate DNA, centrifuged at 10,000 rpm for 5min. DNA was washed once with 70% ethanol and eluted in sterile deionized water by gentle vortexing.

2.2.2.2. PCR Amplification of promoters

PCR was used to amplify promoters sequence of each bioamine receptor using a specific pair of primers designed for each one of these receptors.

The reaction is generally composed of:

10X reaction buffer (without $MgCl_2$)	5µl
$MgCl_2$ 25mM	1.5µl
dNTP mix (10mM of each dNTP)	1µl
Taq DNA Polymerase(5U/µl)	0.25µl
downstream primer (10 um/µl)	1µl
upstream primer (10 um/µl)	1µl
DMSO (optional)	2.5µl
template DNA (10-100ng/µl)	1-2µl
nuclease-free water (adjusted to a final 50µl)	

General Cycle condition:

Step	Temp	Duration	Cycle number
Denaturation	94°C	1 min	1 cycle
Denaturation	94°C	30 sec	
Annealing	50-55°C	30 sec	35 cycles
Elongation	72°C	3 min	
Final extension	72°C	10 min	1 cycle

Final soak	4°C	hold

2.2.2.3. Agarose gel electrophoresis

Agarose gels were made with 1% (w/v) agarose in electrophroesis buffer (Tris/Borate/EDTA (TBE). To make DNA bands visible for agarose gel electrophoresis, 1µl Ethidium Bromide (EtBr) was added. After electrophoresis the gel was illuminated with an ultraviolet lamp and photographed by a digital camera.

2.2.2.4. PCR purification

To each 100µl PCR mixture, 400µl of binding solution were added and mixed. The mixture was loaded on the top of spin column, centrifuged at ≥12,000xg for 1min and the flow through was discarded. Column was washed using 500µl washing buffer and reinserted into empty receiver tube. The column was centrifuged at ≥12,000xg for 1min. DNA was eluted using hot deionized water and the column was centrifuged at maximum speed for 2min.

2.2.2.5. Restriction digest

Each promoter was digested twice using two restriction enzymes of StuI, XbaI, SstII, NotI, BglII, EcoRI, KpnI, and BamHI, which cut in the multiple cloning site of the vector pPTGAl (Fig.6). Plasmids were cut twice with the same two restriction enzymes that were used to cut the promoter.

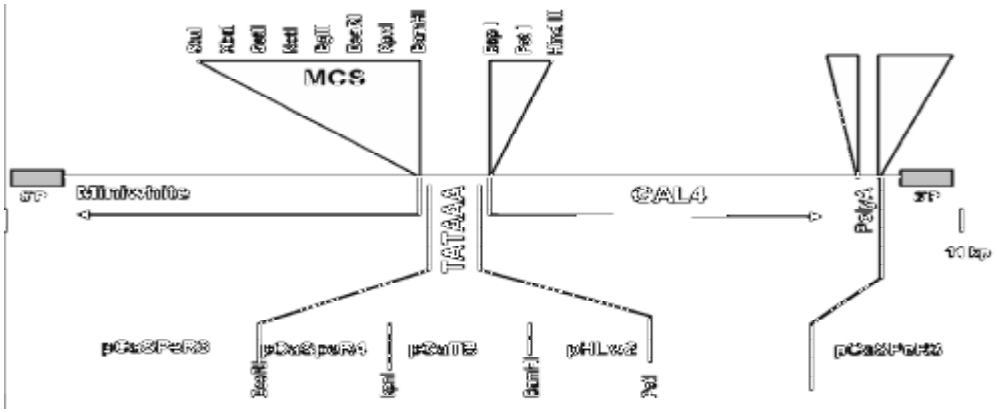

Figure 6: Map and construction of the pPTGAL vector.
The pPTGAL vector, based on CaSpeR3, contains the Gal4 coding sequences driven by a minimal promoter downstream of a multicloning site (MCS) for insertion of enhancer-containing fragments. Unique restriction sites (asterisks) include StuI, XbaI, SstII, NotI, BglII, EcoRI, KpnI, and BamHI (modified from Sharma et al. ,2002).

Restriction enzymes and suggested buffers were used according to the manufacturer's instructions (Fermentas). One unit of restriction enzyme was designed to digest 1µg of DNA

in 1 hour at 37°C in 50µl of recommended reaction buffer. One µ calf intestine alkaline phosphatase was added to the double-digested plasmid and incubated 1h at 37°C.

2.2.2.6. Ligation of promoters in pPTGAL vector

T4 ligase joins the 5' phosphate and the 3'-hydroxyl groups of double stranded DNA molecules. To estimate the vector and insert concentrations, the Nanodrop spectrophotometer was used. Ligation mixture was set up as following:

200 ng of vector DNA

600 ng of the insert

10X ligase buffer

1 µl T4 DNA ligase

Total volume was completed to 10µl with nuclease free water. The mixture was mixed by pipetting. Sticky end ligation reactions were incubated at 4°C overnight. Before transformation, the ligase was heat-inactivated by placing tube containing the ligation mix in 65°C water bath for 10 min.

2.2.2.7. Transformation into *E. coli* DH5α

Plasmid DNA can be introduced into bacteria by transformation. Competent *E. coli* cells (stock frozen at -80°C) were allowed to thaw in ice, one to three µl of ligation mixture or the control were added to *E. coli* in a separate tube and the contents of each tube were mixed gently, incubated in ice for 5min. Then the tubes were heat-shocked by incubating them in a water bath at 42°C for 90 seconds and then on ice.

2.2.2.7.1. Culture medium

Luria-Bertani (LB) medium was utilized for culturing *E. coli* transformation and conservation. To make LB- plates 20g of premix LB Agar powder, 5.0 g tryptone, 2.5 g yeast extract, 5.0 g NaCl and 7.5 g agar were dissolved in 500ml dH_2O, heated to boil for 1min while stirring, autoclaved and cooled to ~55°C. Ampicillin antibiotic was added under sterile condition (final concentration of ampicillin-sodium salt 100 mg/L). A thin layer (5mm) of LB Agar (~10mL) was poured into each plate.

2.2.2.7.2. Culture conditions

After ligation and transformation into *E. coli*, 500~800 µl of LB liquid medium were added and incubated at 37°C with continuous shaking for 30min. The *E. coli* suspension was spread on LB-amp-agar plates, dried, inverted and incubated at 37°C overnight.

2.2.2.8. DNA plasmid preparation

To obtain cells for plasmid isolation, a single colony was inoculated and cultured in 4ml LB-amp liquid medium at 37°C with continuous shaking overnight. Plasmid DNA was purified, with kit (Fermentas). Cultures were pelleted by centrifugation at maximum speed for 10 min and all traces of medium were removed. 250µl of resuspending solution (50 m/µ Tris /HCl (pH 8); 10mµ EDTA; 100µg/ml RNAase A) were added to the pellet and cells were resuspended by vortexing until complete homogeneity. Thereafter, 250µl of cell lysis solution (200mM NaCl; 1% SDS) were added and mixed gently without vortexing, incubated at room temperature for 5 min. Then 350µl neutralization solution (containing acetate and guanidine hydrochloride) were added, mixed gently and centrifuged at maximum speed for 10 min. The supernatant was loaded on the top of spin column, centrifuged at ≥ 12.000 xg for 1 min; the flow through was discarded. The column was washed twice with 70% Ethanol. The plasmid was eluted by sterile water and centrifugation at ≥ 12.000 xg for 2 min.

2.2.2.9. Sequencing

I have used sequencing Service supplied by Eurofins MWG operon. The sequences were obtained and verified using the alignment software BLAST (http:// www.ncbi.nlm.nih.gov/BLAST) of the national centre of biotechnology information (NCBI).

2.2.2.10. Injection of *Drosophila* embryos

Drosophila transgenic service supplied by BestGene Inc was used. The *Drosophila* P-element transformation based on the injection of transposon-based construct with the ***white*** and/or the ***yellow*** marker to w^{1118} or *yw* host line.

2.2.2.11. Crossing of GAL4 lines with UAS-GFP-line

Each Gal4 line obtained by germline integration was crossed with a UAS- GFP line.Then the F1-generation have been analyzed in detail and phenotypical characteristics have been quantified to elucidate the physiological significance of each receptor .

2.2.2.12. Immunohistochemistry

2.2.2.12.1. Larval and adult CNS

The CNS of first generation larvae and adults were dissected in *Drosophila* Ringer`s solution and incubated in 4% (w/v) paraformaldehyde in PBS for 1-2 hours at room temperature. Tissues were washed three times 5 min in PBS-T (0.1 % Triton-100) and blocked for 30 min in blocking buffer (1x PBS + 2% NP-40 +10% goat serum) at room temperature. The samples were incubated with the primary antibody (anti GFP rat monoclonal IgG; 1: 200 in blocking buffer) overnight at 4°C and washed three times for 5 min in PBS-T. Subsequently, the samples were incubated with the secondary antibody (donkey anti rat IgG; 1: 500 in blocking buffer) for 1-3 hours at room temperature, washed twice for 5 min in PBS-T. Final washing in PBS-T + Hoechst staining was done to stain nuclei as well. Tissues were mounted directly on slides with one drop of focus clear, incubated for 1-3 h and covered with a cover slip.

2.2.2.12.2. Digestive system

Intact guts were dissected in 1×PBS and fixed at room temperature for 45min in 4% paraformaldehyde in 1×PBS. All subsequent incubations were done in blocking buffer (1xPBS, 2% NP-40, 10% goat serum). The following antisera were used: Rat monoclonal α-GFP, 1:300, α-armadillo, 1:20 and α-Prospero, 1: 20. The guts were washed three times with PBT. The Secondary antibodies used, were Goat anti-mouse and donkey anti-rat IgG conjugated to DyLight^{TM} 488 and DyLight^{TM} 549 (1: 1000). Hoechst stain was used (diluted 1: 1000 with 1×PBS). Preparations were mounted on slides using glycerol as a mounting medium and examined using a zeiss axioimager.

2.2.2.12.3. Muscular system

Phalloidin is a fungal toxin isolated from the poisonous mushroom *Amanita phalloides.* Phalloidin is able to bind to F-actin in muscle cells. As a result of binding phalloidin, actin filament becomes strongly stabilized. Fluorescent conjugates of phalloidin are used to label actin for histological applications.

Phalloidin-TRITC P1951 was used according to the manufacturer instructions to identify actin filaments in the constructed lines showing expression in muscular tissue, by which we can judge whether the expression occurs in all or only in certain muscles.

Third instar larvae were dissected in PBS solution on a small silicone plate. Using forceps, the larvae were pinned twice at the anterior and posterior ends. Using scissors, the larvae were

splitted along the dorsal midline and gut and other organs were removed. The side walls were pinned back to expose the body wall muscles. Following dissection, the dissected larval preparation is washed twice with PBS, fixed with 4% PFA in PBS overnight at 4°C, washed three times using PBST. then blocked for 30 min in blocking buffer (1XPBS + 2%NP-40 +10 %goat serum) at room temperature Incubation with the primary antibody (anti GFP rat monoclonal IgG; 1: 200 in blocking buffer) was done overnight at 4°C then washed three times 5 min in PBST (0,1 % Triton-100). Incubation in the secondary antibody (donkey anti-Rat IgG; 1: 500 in blocking buffer), mixed with TRITC-labelled Phalloidin (0.5 µg/ml), was done for 1-3 hours at room temperature. Then, tissues were washed three times for times 5 min in PBS-T. Preparations were mounted on slides using glycerol as a mounting medium and examined using a Zeiss axioimager.

2.2.2.13. Immunofluorescence microscopy

2.2.2.13.1. Confocal microscopy

Larval and adult brain mounts were imaged using a Leica TCS SP1 confocal microscope. Images were exported as tiff-format series using the Leica confocal software. The collected Z-series were projected into a single plane image using ImageJ, Java-based processing program.

2.2.2.13.2. Immunoflorescence microscopy

Third stage larvae and adults were examined with standard fluorescence microscopy (imager.Z1, Zeiss).

2.2.3. RNA interference

Virgin females were collected from the GAL4 driver and UAS stocks and the corresponding crosses also performed in reverse orientation. About 10 males and 20 females were placed in a small vial at constant temperature (27-29°C). The animals were passed daily for 1-2 weeks. The flies were allowed to remain in the same vial two days, the use of exchangeable food vials provided a continuous food supply and provided the necessary egg collection sites. The vials were inspected daily and the relevant event and date on which they occur was noted as, the beginning of 1st larval instar, 3rd larval instar wandering, prepupation formation, pupation, eclosion and pupal lethality.

Hatchability was determined as the percentage of eggs collected that produce adults, then count number of males and females daily.

Fecundity determinations were made using female progeny from the egg collection. Ten pairs of flies were mated. Their eggs were collected and scored on the basis of total number of eggs laid every day for seven days.

2.2.4. Pharmacological characterization of octopamine receptors in human embryonic kidney cells (HEK 293 cells)

To get access to the pharmacological properties of these very important molecules, their expression in cell culture system is required. To achieve this, full-length clones of genes coding for bioamine receptors were cloned into mammalian expression vectors. Following this, stable, transgenic cell lines were established that express the complete set of these genes

2.2.4.1. Cell culture

HEK-293 cells were cultured in advanced DMEM supplemented with 4% FBS, 50µ/ml penicillin, 50g/ml streptomycin, and 2mM glutamine. Cells were grown in an incubator at 37°C with humidified 5% CO_2 and 95% air. The medium was changed every 2-3 days.

2.2.4.2. Transfection in HEK 293 cells

Transfection was carried with both, the expression vector pEAK10CV containing the gene of interest and the reporter plasmid pCRE-SEAP, where the expression of secreted alkaline phosphatase is under transcriptional control of cre-elements.

I harvested the growing HEK293 cells the day before transfection by removing and discarding the culture medium taking care to remove all traces of serum that contain trypsin inhibitors. Later, cells were rinsed with 25% (w/v) trypsin – 0.53mM EDTA solution, the flask was shaken for several seconds and then incubated at 37°C for up to 5 min to facilitate dispersal of the cells. Trypsinization was stopped by adding 5-6 ml DMEM medium. Cells were checked using microscopic analysis and further processed only if at least 95% single cells were present, if not, vigorously shaking was necessary. Then, cells were aspirated by gentle pipetting and putting appropriate aliquots into 96–well plates (150 µl each well). These cells were incubated in at 37°C until they nearly reached 60-80% confluency.

The transfection reaction concentrations that have been used typically was the Turbofect transfection reagent. 10–20 µg DNA, NaCl (final concentration 150mM NaCl), 50 µl Turbo-Fect Transfection Reagent were mixed, completed to 2ml with nuclease free water, mixed by vortexing, incubated approximately 10 min at room temperature (15–25°C) to enable

TurboFect–DNA complex to form, then transferred to the flask, and swirled gently. Cells were incubated with complexes at 37°C and 5% CO2 for about 24h.

2.2.4.3. Application of compounds

Most of applied compounds are not water–soluble, so dimethylsulfoxide (DMSO) was used as a solvent for stock solutions.

Agonists

An agonist is a type of ligand or drug that binds and activates a receptor. Stock solutions were 10^{-1}M and then a series of tenfold dilutions with 1×PBS were made ranging from10^{-3} to10^{-12} M and applied to the 96-well plates including wells without compound application. The plate with applied agonists was incubated at 37°C and 5% CO2 for about 24h.

Antagonists

A receptor antagonistic is a type of receptor ligand or drug that does not produce a biological response itself upon binding to a receptor, but blocks or inhibit agonist-mediated responses. Seven antagonists have been applied to HEK 293 cells transfected with each receptor type. The antagonist activity is examined as the ability of the antagonist to inhibit an agonist induced response. The seven antagonists were epinastine, phentolamine, chlorpromazine, metoclopramide, yohimbine, rauwolscine and mianserin, and their activities were examined by applying agonist first (10^{-1} M, octopamine) into the same concentration to all wells of 96-well plates except wells of the first row which then used as a blank, incubating the plate for 30 minutes in 37°C, 5%CO2 incubator and then applying antagonists in ten fold diluted concentrations (10^{-3} to 10^{-12} M). Plates were incubated with applied compounds at 37°C and 5% CO2 for ~ 24h. The activity was tested 24 hours post-application.

2.2.4.4. SEAP reporter assay

SEAP is a secreted form of embryonic alkaline phosphatase and thus can easily be detected in a sample of culture medium without destroying the cells. SEAP catalyzes the hydrolysis of pNitrophenyl phosphate, producing a yellow end product that can be read spectrophotometrically at 405 nm.

SEAP quantification

The protocol was used for 96-well plates. About 1 ml of culture medium of transfected cells or control cells were collected and centrifuged 5 min at 10,000 rpm. 500 µl of supernatant were transferred to a microfuge tube to eliminate cell debris. About 10 µl of supernatant were transferred into a well of a 96-well plate. 10 µl of the control served as a blank. Samples were

heated to 65°C for 5-10 min to inhibit endogenous alkaline phosphatases. 50 µl of 1X Dilution Buffer, 100 µl of 1X Assay Buffer, 20 µl of 100 mM L-homoarginine and 20 µl H_2O were added and incubation proceeded at 37°C for 10 min. Then 20 µl of Staining Solution was added, incubated at 37°C for 10 min in the dark and taken an initial reading of the OD 405 by using a Multiscan MCC/340 P spectrophotometer. Then they were reincubated at 37°C in the dark and readings were taken every 10 min.

2.2.4.5. RNA extraction

Drosophila larvae 3-5 were grinded in RNA magic solution and 200µl chloroform was added, incubated 10 min in ice, centrifuged for 10 min at 17.000xg. The upper aqueous phase was transferred into a new tube and equal amount of isopropanol was added, mixed and RNA let to precipitate for 30 min at -80°C, centrifuged at maximum speed for 30 min in 4°C. Isopropanol then poured off and the pellet washed twice using 70% alcohol. The pellet let dried for 5 min and then dissolved in nuclease free water.

2.2.4.6. cDNA synthesis

Reverse Transcription (RT reaction) have been done using the total cellular RNA. 2-4 µg were used, a reverse transcriptase enzyme (superscript SSII), gene specific primers, dNTPs and an RNase inhibitor. The resulting cDNA was used in RT-PCR reaction. The reaction has been done at 42°C for 1 hr. then the reaction heated at 70 °C to inactivate the enzyme before using the reaction in RT-PCR.

2.2.4.7. RT-PCR

The resulting cDNA is used as templates for subsequent PCR amplification using primers specific for each gene. RT-PCR was carried out by mixing all reaction components (10X PCR buffer, dNTPs, gene specific sense and antisense primers, cDNA template and taq polymerease) in one tube prior to starting the reactions.

2.2.4.8. Electrophoresis on agarose gels

PCR product was checked with 1% (w/v) agarose gel.

2.2.4.9. Restriction digests

Restriction digests were performed according to the suggestions of the manufacturer.

2.2.4.10. Transformation in *E. coli* cells DH5α

Competent *E. coli* cells were used as described before.

2.2.4.11. DNA plasmid preparation

Using plasmid preparation kit (MBI Fermentas) following the instruction enclosed.

2.2.4.12. Sequencing

The sequence analysis using the service supplied by MWG eurofin, using sense and antisense sequencing primers to sequence each insert twice and the result aligned using the web site http://www.biochem.ucl.ac.uk/cgibin/mcdonald/cgina2aa.pl.

The results of sequencing have been translated into amino acids and compared with the gene data bank obtained from the national center of biotechnology informations (NCBI) based on the amino acid sequence similarity.

2.2.4.13. Statistical analysis

Data were evaluated using Prism program. Sigmoidal dose-response curve were plotted for the percentage of the *in vitro* maximal response to an agonist in the presence or absence of an antagonist vs. the logarithm of ligand concentration. There after, statistical values were obtained automatically including the EC50 values.

3. Results

3.1. Studying spatial and temporal expression pattern of biogenic amine receptors

3.1.1. Octopamine receptors

3.1.1.1. *Oamb* expression analysis

In *Drosophila*, the gene octopamine receptor in mushroom bodies is referred by the symbol *Dmel\Oamb* (CG3856). Primers targeting a region of approximately 3kB of the presumptive promotor region of the *Oamb* gene were used to amplify this DNA (Fig.7A). The resulting PCR product (Fig.7B) was inserted into the pPTGAL vector, checked by sequencing (Sharma et al. 2002) and injected into *Drosophila* w^{1118} embryos to obtain suitable transgenic lines, which express Gal4 under control of this promotor. The injection itself was performed by the BestGene Inc corporation. To identify the expression pattern of the *Oamb* gene, the corresponding lines were crossed to a UAS-gfp line.

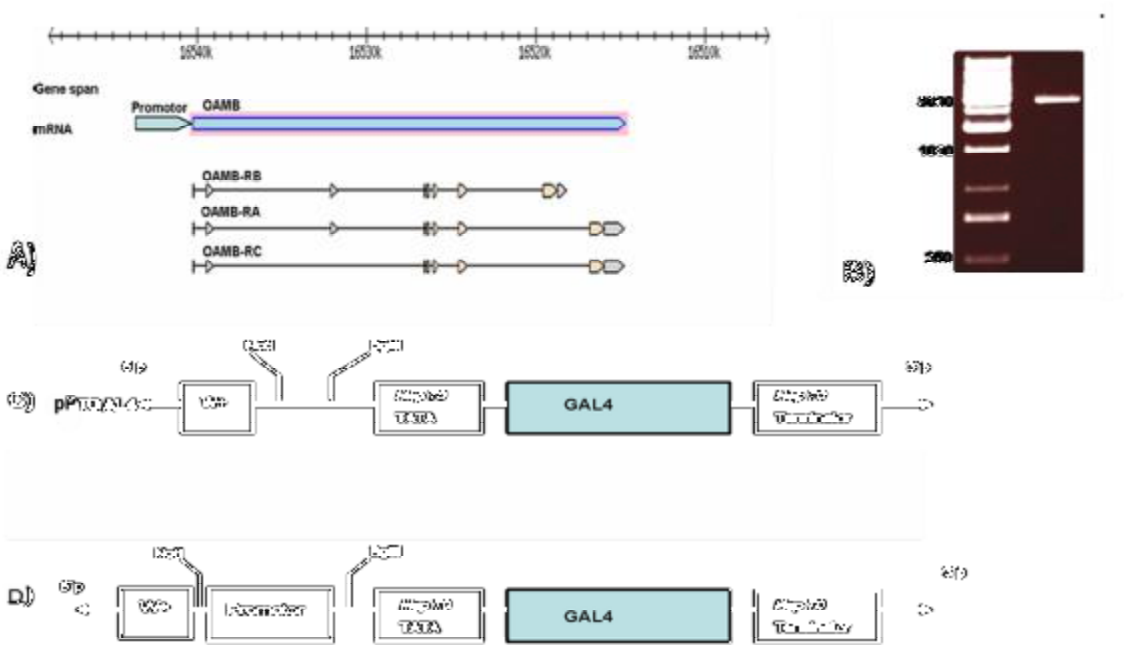

Figure 7: Generating *Oamb* promotor inserted pPTGAL4 vector.
A, schematic drawing showing *Oamb* gene model and its products. B, 1% agarose gel showing *Oamb* promotor region amplifies with PCR. C, a part of pPTGAL4 vector with GAL4 coding sequence between minimum promotor (*hsp*70 TATA) and terminal transcription sequence (*hsp*70 terminaltor). pPTGAl4 vector was prepared for ligation by double digestion with NotI and BamHI. D, schematic drawing for promotor-GAL4 -vector. The NotI/BamHI double digested promotor sequence was inserted in the NotI/BamHI double digested pPTGAL4 vector.

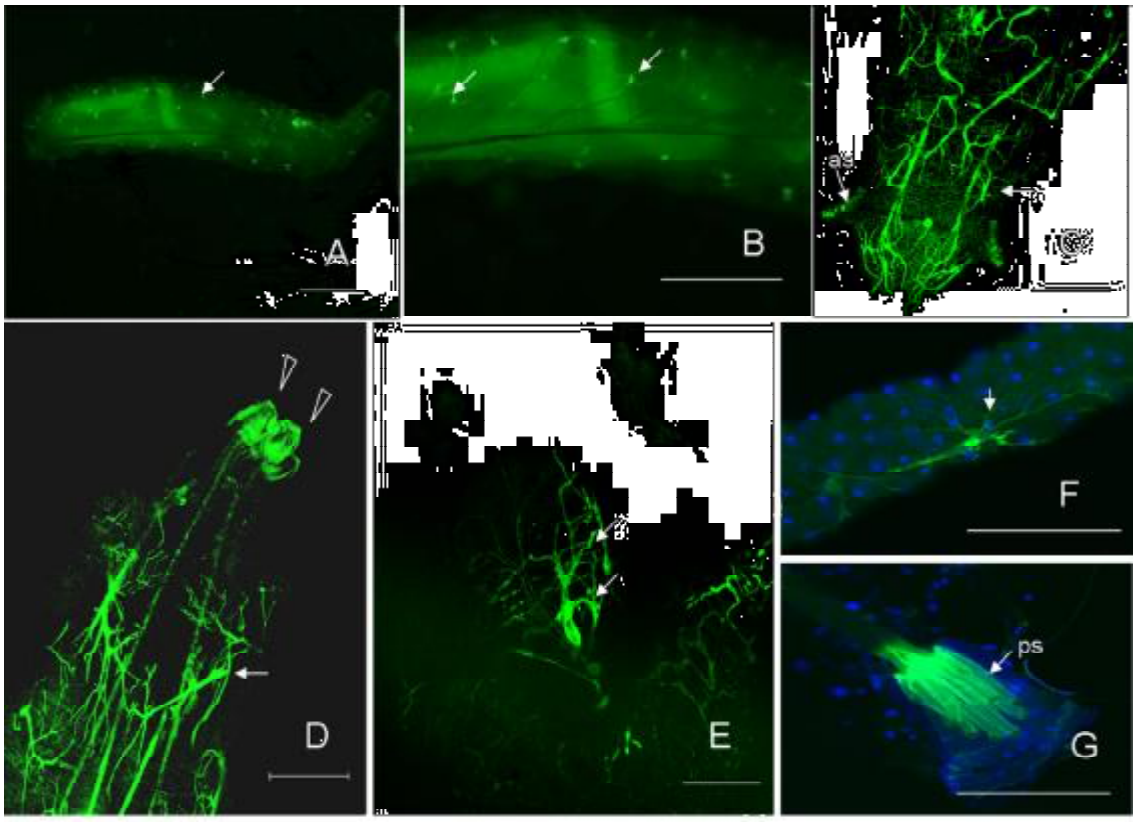

Figure 8: GFP expression pattern in *Oamb*-GAL4/UAS::GFP larval tracheal system .
A and B panel, whole L3 larvae and C-E panels are projections of confocal stacks. C, tracheal branching in the larval head. D, tracheal branches of the tail segments. (as) anterior spiracle. Arrow heads refer to posterior spiracles. E, visceral branches of trachea surrounding the proventriculus. F, visceral branches of trachea surrounding the gut. G, posterior spiracle (ps). Scale bar = 200µm.

Larvae of F1 generation showed a strong expression in the terminal branches of the tracheal system (Fig. 8), including a lot of visceral branches and transverse connectives which were visible through the cuticle of living larvae.

The tracheal expression can be seen throughout the entire system, but it appears to be confined to the terminal branches, omitting the primary and secondary branches. Most prominent is the labelling of those branches that directly contact organs, such as the gut (Fig. 8E, F). In addition, larval salivary gland strongly expressed *Oamb* (Fig. 9). In larval muscles, no obvious signs of expression were present.

In contrast, distinct *Oamb* expression was evident in the larval CNS (Fig.10). In the brain lobes, *Oamb* expression was highly enriched in the mushroom body primordia. Three parts of the mushroom bodies, the calyx, containing the somata, the pedunculus with its axonal projection and the axonal terminals lobes, could be distinguished. Two clusters of positively stained somata appeared dorsally in the base of each brain lobe. Their processes were directed to the suboesophageal ganglion and connected with transverse connectives forming a ladder-

like structure. Three *Oamb* neurons on each side arose from this structure and extended into the thoracic-abdominal ganglion, along the parallel longitudinal tracts around the midline.

Figure 9: GFP expression in *Oamb*-GAL4/UAS::GFP larval salivary glands.

In each thoracic neuromere, two pairs of strongly stained transverse *Oamb* expressing neurons could be visualized. One pair with their somata resides at the height of the dorso-lateral traces in each neuromere. They send a single transverse axon toward the midline. The somata of the other pair are located on the ventro-lateral part. They send an axon outside of the thoracic ganglia, projecting via the segmental nerves to the periphery.

The *Oamb* gene shows also expression in the adult stage. Moderate but distinctive expression appeared in leg muscles in, coxa (depressor of trochanter), trochanter (redactor muscles of femur), femur (depressor of tibia) and the middle part of tibia (depressor of tarsus) of both midleg and hind leg (Fig.11).

Adult brain shows strong *Oamb* expression in all mushroom body subdivisions (Fig12). In the optic lobe, *Oamb* neurons innervates the outer and inner medulla and the lobula. Along with *Oamb* neurons in the central brain, in the middle region of the suboesophageal ganglion and in between the antennal lobes. There is also GFP expression in the medulla, lobula and lobula plate of the optic lobes. Distinct *Oamb* immunoreactivity was evident in the thoracico-abdominal ganglion, especially in the area between the first and second thoracic ganglion and second and third thoracic ganglion and abdominal ganglion.

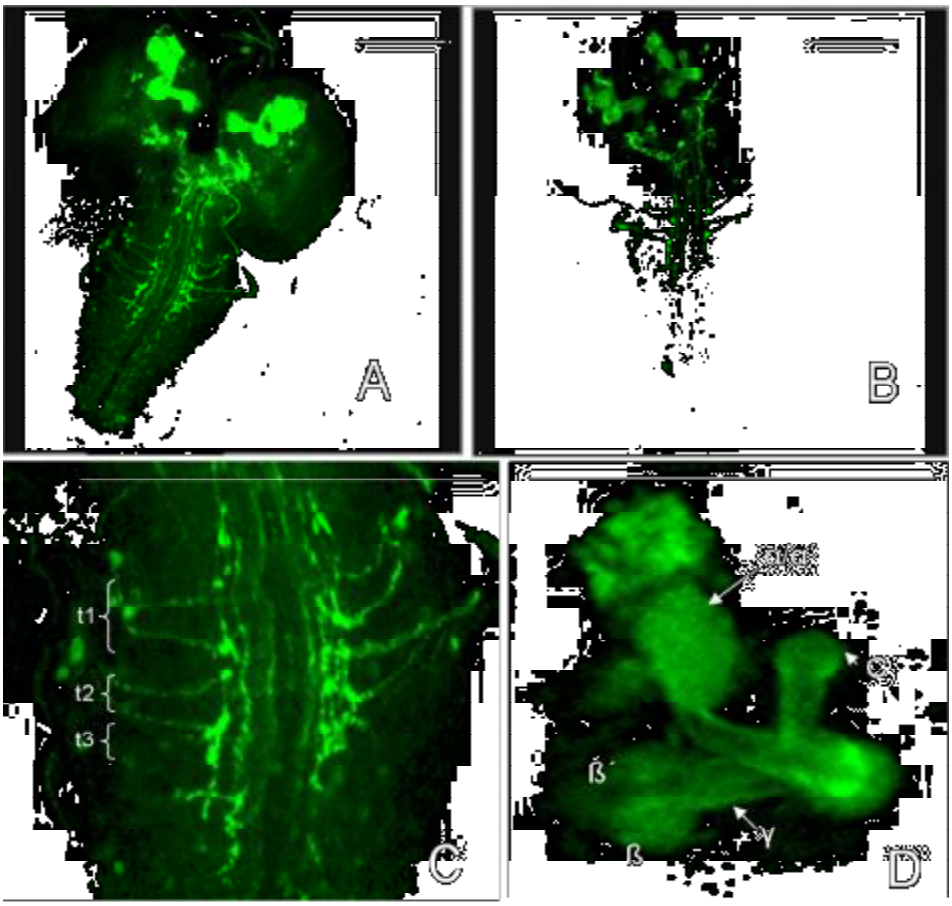

Figure 10: GFP immunoreactivity in the whole-mount CNS of third-instar larva *Oamb*-GAL4/UAS::GFP

A, projection of confocal stacks with maximum intensity. B, projection of confocal stacks with minimum intensity. C, close-up view on the thoracic neuromeres; t1, prothoracic neuromere;t2, mesothoracic neuromere; t3, metathoracic neuromere. D, close-up view on the mushroom body primordia; α/α´ lobes; ß/ß´ lobes; γ lobe; c, calyx. Scale bar = 100µm.

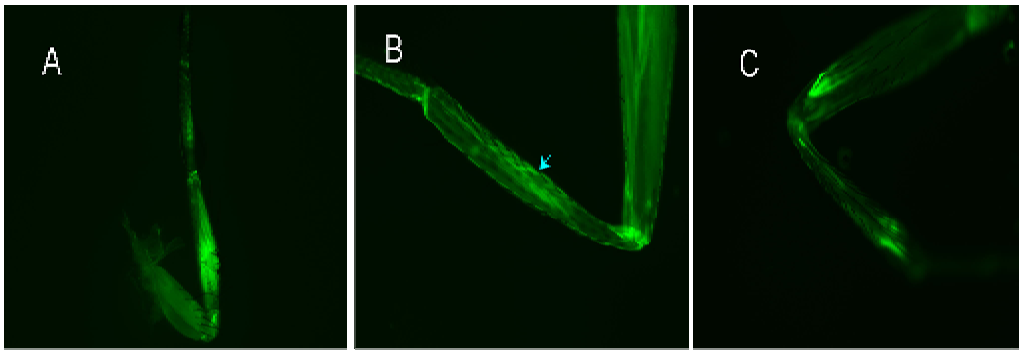

Figure 11: GFP expression pattern in leg muscles of *Oamb*-GAL4/UAS::GFP adults .

Panel A, showing strong GFP in tibia and moderate GFP in femur and tarsi of the fore leg. Panel B, showing GFP in the mid leg muscles. Arrow refers to muscles in tibial region (depressor muscle of tarsus), and panel C, GFP in the hind leg muscles, with strong GFP in the femur region.

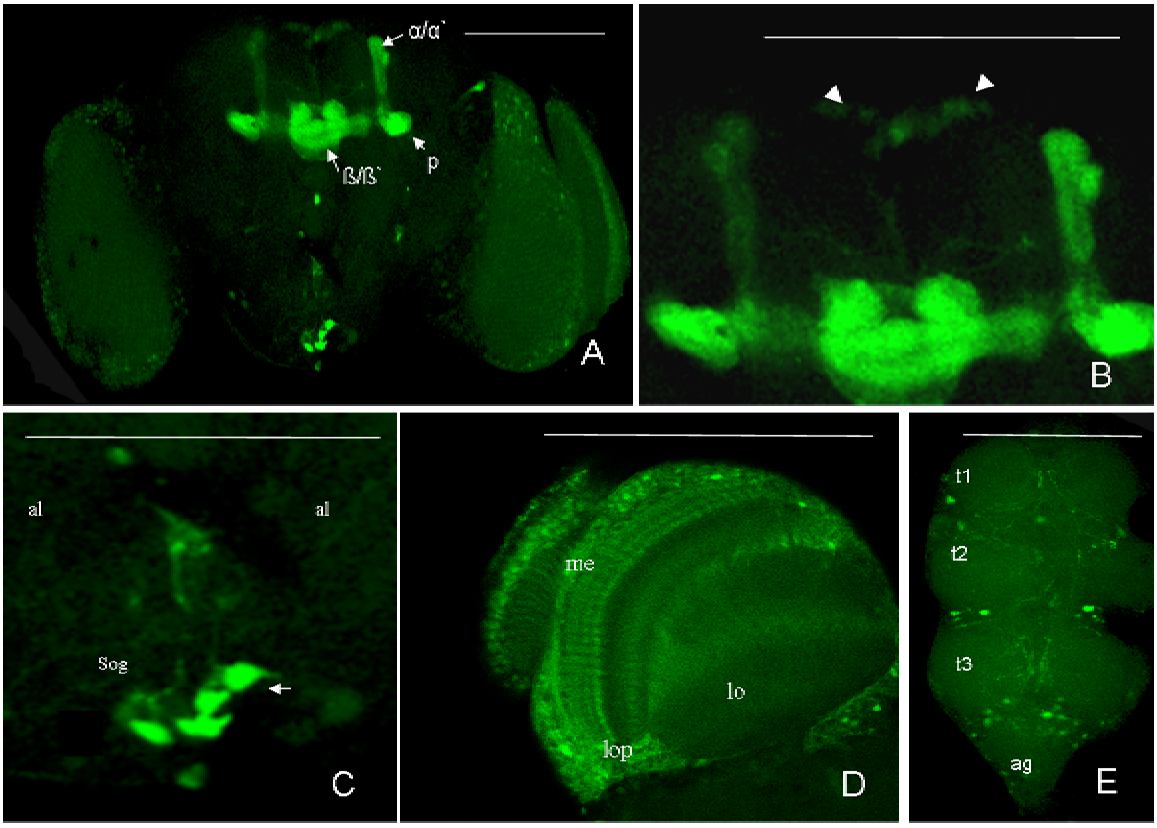

Figure 12: GFP immunoreactivity in CNS of *Oamb*-GAL4/UAS::GFP adult stage showed in projections of confocal stacks A –E .
A, Adult brain with strong GFP in mushroom bodies; α/α` lobes and ß/ß` lobes; p, pedunculi. B, close-up view on the middle of protocerebrum; head arrows refer to protocerebral bridge. C, Area between the antennal lobes (al) and in the suboesophageal ganglion (sog); arrow refer to somata. D, compound eye showed *Oamb* immunoreactivity in medulla (me), lobula (lo) and lobula plate (lop). E, *Oamb* immnuoreactivity in thoracico-abdominal ganglion; t1, prothoracic neuromere; t2, mesothoracic neuromere; t3, metathoracic neuromere; ag, abdominal ganglion. Scale bar = 150µm.

3.1.1.2. *Octß2R* expression analysis

In *Drosophila*, the gene *Octß2R* is referred by the symbol *Dmel\Octß2R* (CG33976). To explore *Octß2R* expression, *Octß2R* sense and antisense primers were used to amplify the *Octß2R* promotor region (~3200bp). This PCR product was inserted in pPTGAL vector, which was used for germline integration. Studying the expression pattern was performed using the UAS/GAL4 system. The *Octß2R* Gal4 line, in which the expression of *Octß2R* is driven in Gal4 expressing cells were crossed to a UAS-GFP line. GFP pattern was analyzed in the first generation in detail.

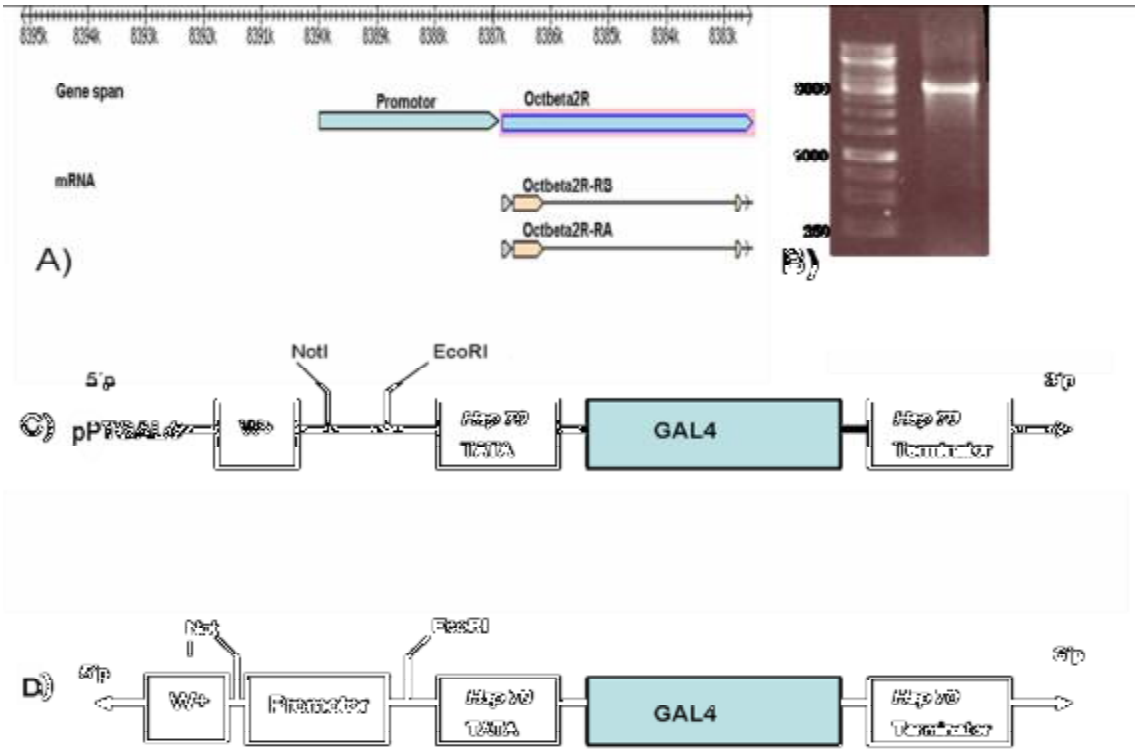

Figure 13: Generating *Octß2R* promotor inserted pPTGAL4 vector.
A, schematic drawing illustrating *Octß2R* gene model and its products. B, 1% agarose gel showing *Octß2R* promotor region amplifies with PCR. C, a part of pPTGAL4 vector with GAL4 coding sequence between minimum promotor (*hsp*70 TATA) and terminal transcription sequence (*hsp*70 terminaltor). pPTGAl4 vector was prepared for ligation by double digestion with NotI and EcoRI. D, schematic drawing for promotor-GAL4 - vector. The NotI/EcoRI double digested promotor sequence was inserted in the NotI/EcoRI double digested pPzTGAL4 vector.

Larvae show very strong *Octß2R* expression in the muscular system, including longitudinal, transverse, oblique, and acute muscles in both dorsal and ventral regions, which are visible through the cuticle of 1st- 3rd stage larvae. As showed in figure (14), the expression begins from the musculature of the larval head and ends in the musculature of the tail segments.

Larval Brain shows weak *Octß2R* expression. Weak expression could be observed in mushroom bodies. Few numbers of neurons could be detected in the other parts of the CNS.

A group of neurons from both hemispheres send axonal projections across the midline in the brain forming the inter-hemispheric bridge.

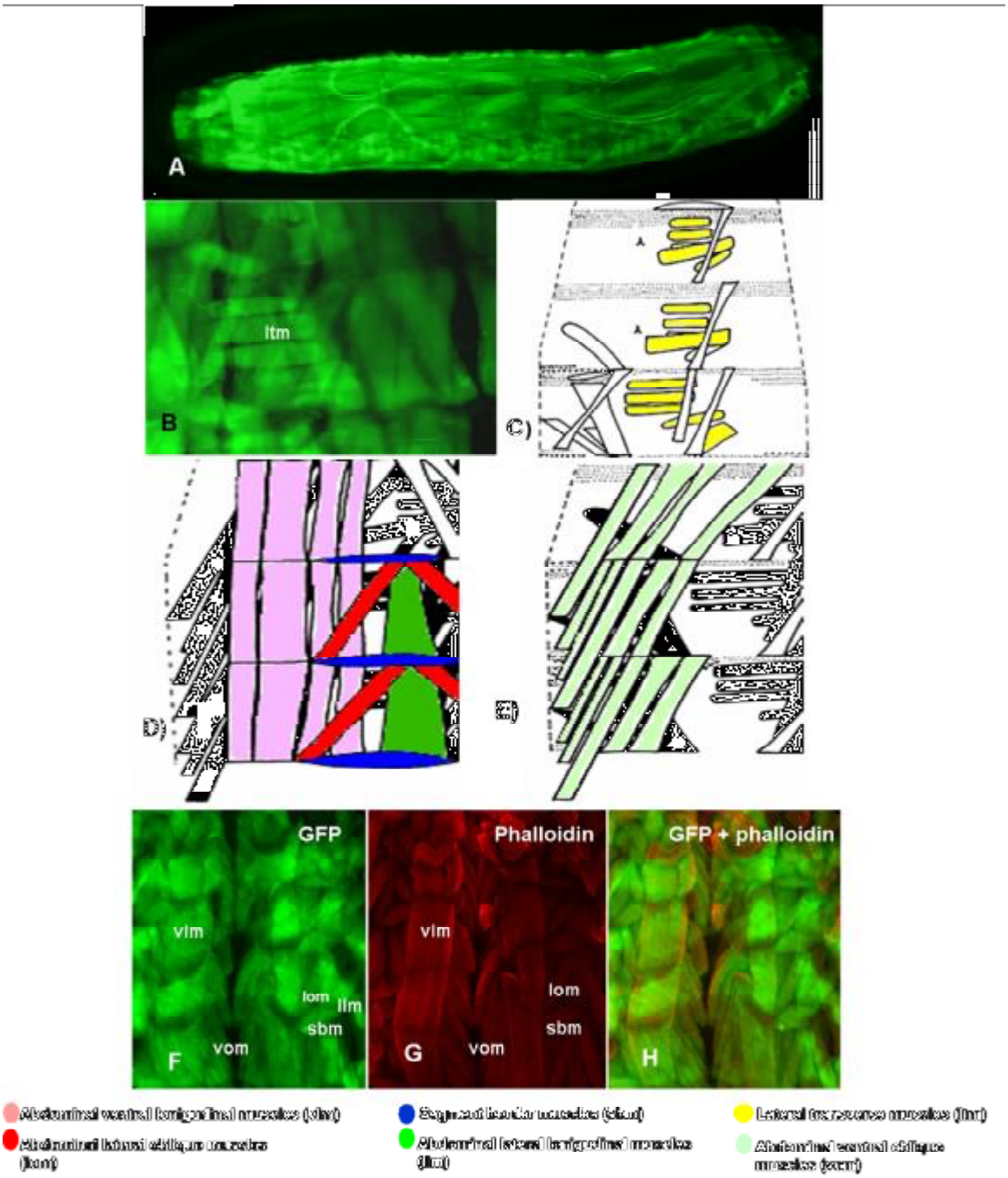

Figure 14: GAL4 expression pattern of *Octß2R* -GAL4 in the larval muscular system
A, Whole L3 larvae showing GFP in muscular system. B, close-up view of muscles of a live larva showing lateral transverse muscles (ltm). C, schematic drawing illustrating lateral view of larval musculature; yellow coloured muscles refer to lateral transverse muscles (ltm), D and E, schematic drawing illustrating lateral view of larval musculature; Pink coloured muscles refer to ventral longitudinal muscles (vlm); red coloured muscles refer to lateral oblique muscles (lom); blue coloured muscles refer to segment border muscles (sbm); green coloured muscles refer to lateral longitudinal muscles (llm); faint green coloured muscles refer to ventral oblique muscles (vom). F-H, larval musculature conjugated to the cuticle stained immunohistochemically using α GFP antibody mixed with Phalloidin; F, GFP expression pattern; G, larval musculature conjugated to the cuticle labelled with Phalloidin. H, overlay of GFP and dsRed photos (schematic drawings are modified from http://flybase.org).

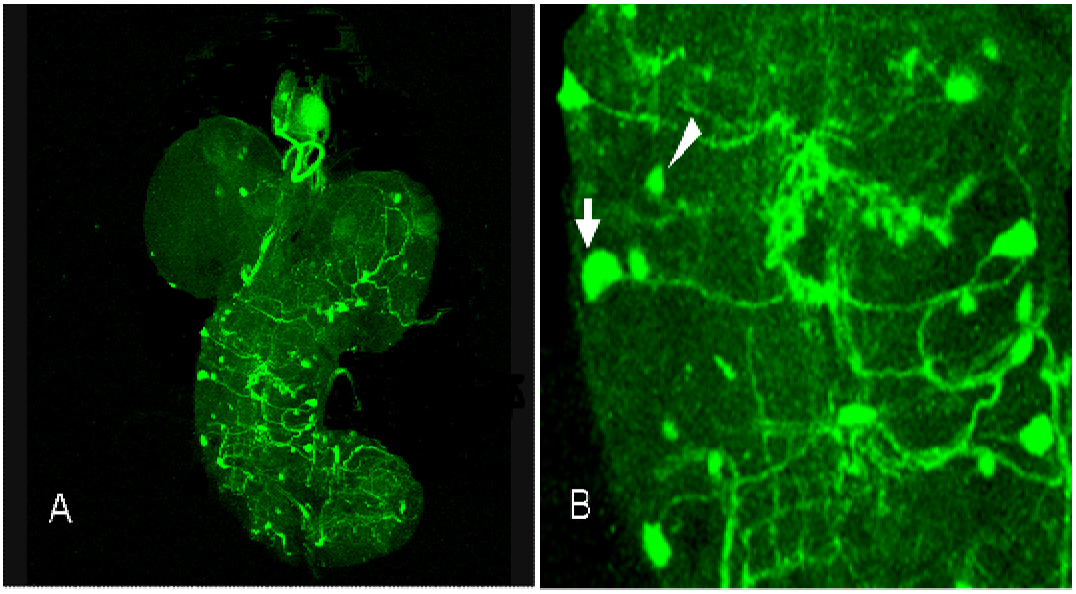

Figure 15: GFP immunoreactivity of *Octß2R* -GAL4 in the larval brain.
A, *Octß2R* immnuoreactivity showed in a whole mount larval brain. B, close –up view on the thoracic neuromeres; arrow refers somata located on the dosolateral traces, sending a neuron toward the midline; head arrow refers two the other somata that located on the ventrolateral traces; sending a neuron also toward the midline.

Adults also show also strong *Octß2R* expression in the entire abdominal musculature (Fig. 16 A,F,G). Compared to the abdominal musculature of the larva, the abdominal musculature of the adult fly shows less expression. Dorsally there is a single layer of short longitudinal muscles, varying in number between 15 and 25 per segment. With their anterior end these muscles insert in the middle of a tergite, with their posterior end at the antecostal ridge of the posteriorlly adjacent segment. Ventral longitudinal muscles are reduced to two fibres that span the entire length of the segment. Lateral transverse muscles form a dense array of 12-15 thin, parallel fibres that insert at the tergites (dorsally) and sternites (ventrally), respectively.

Leg muscles show *Octß2R* expression in coxa (intracoxal depressor and intracoxal levators of trochanter), in the trochanter (redactor muscle of femur), in femur (levators and depressors of tibia) muscles, especially at the end of femur near the site of articulation with the tibia and tibial region (levator and depressor muscles of tarsus) as shown in Figure (16 B,C,D). The depressor muscle of tarsus shows *Octb2R* expression only at its base, near the site of articulation with tarsi.

Antennae show strong *Octß2R* expression in the 3rd antennal segment, which may be due to glial cells or olfactory receptor neurons. Salivary glands and head musculature of adults show strong *Octß2R* expression (Fig, 17).

Strong GFP could be seen in the female reproductive system, in both virgin and mated females, in the three sperm-storing organs, spermathecae and seminal receptacle (Fig 18).

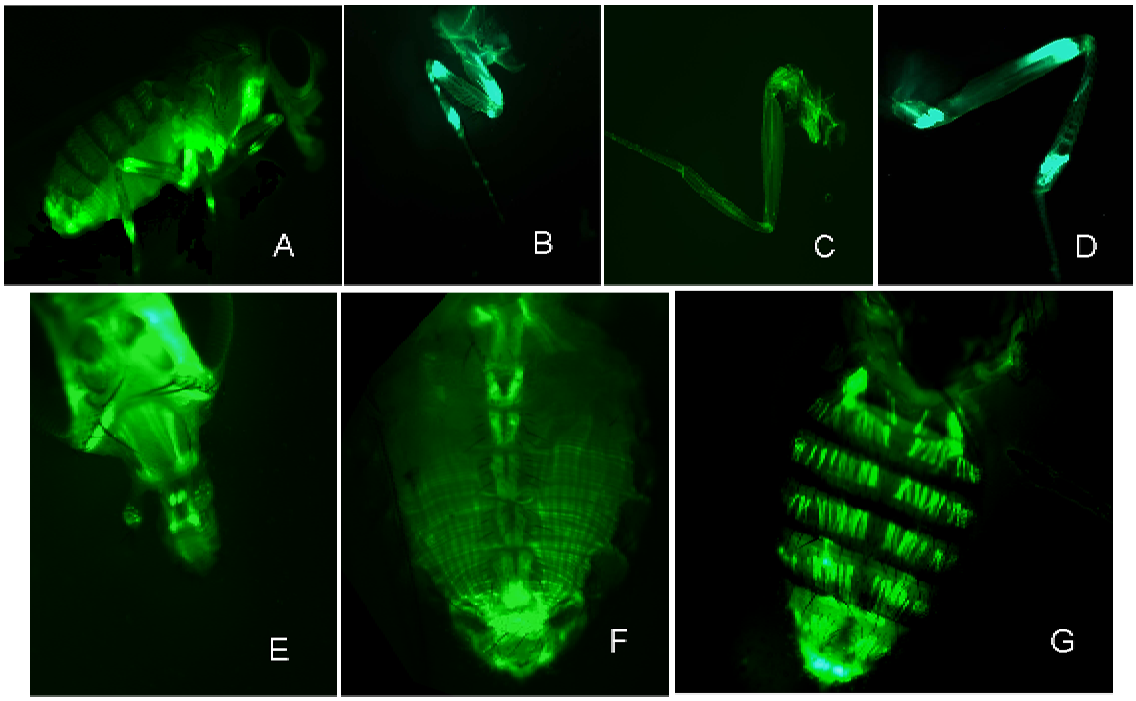

Figure 16: GFP expression pattern in musculature of *Octß2R* -GAL4/UAS::GFP adult stage.
A, lateral view of adult female. B-D, showing expression in leg muscles. B, fore leg, C, middle leg and D, is hind leg. E, showing the expression in the muscles of the head region. F, ventral view of abdominal region transverse muscles in each abdominal segment. G, dorsal view of abdominal region showing 12-15 short, thin, parallel longitudinal muscle fibers in each abdominal segment.

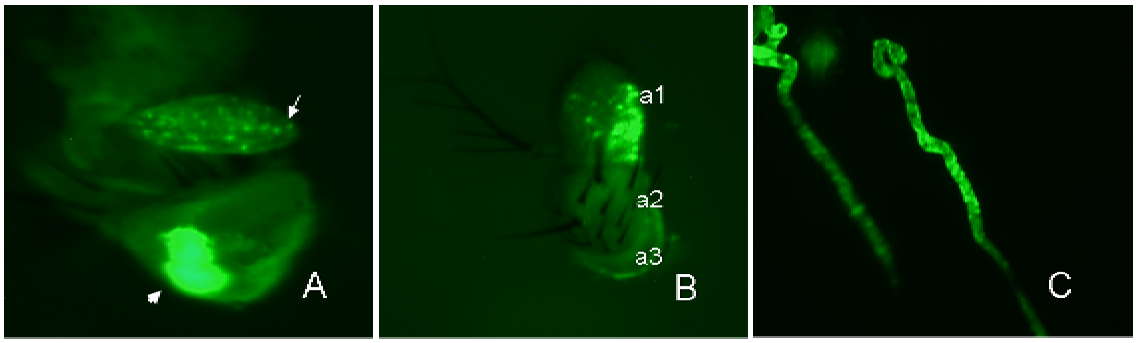

Figure 17: GFP expression pattern in musculature of *Octß2R* -GAL4/UAS::GFP adult stage.
A, showing the expression in the maxillary palp (arrow);head arrow refers to proboscis. B, showing the expression in antenna; a1, antennal segment 1; a2, antennal segment 2; a3, antennal segment3. C, showing the GFP expression in adult salivery glands.

Strong *Octß2R* was seen, in the male reproductive system (Fig. 19), in the male accessory gland .The secretions of the male accessory gland are very important for fertility, it also affect female egg production, oviposition, and possibly sperm storage.

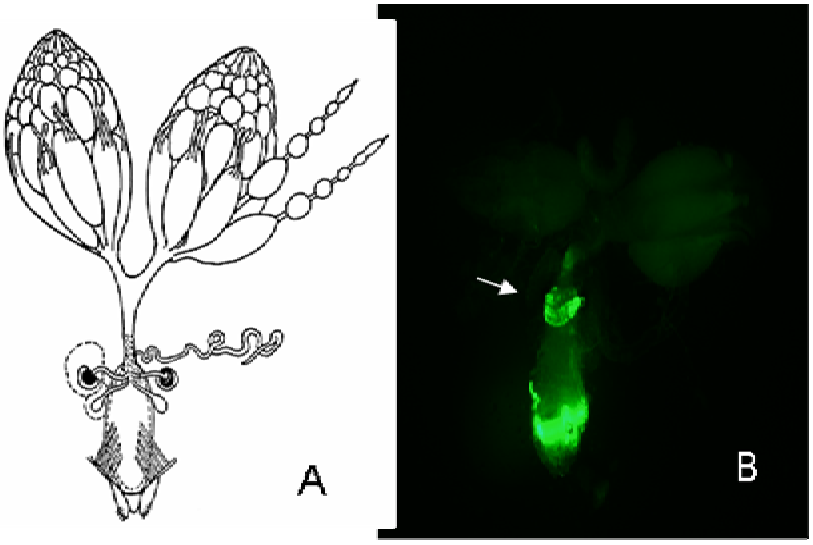

Figure 18: GFP expression pattern in *Octß2R* -GAL4/UAS::GFP female reproductive system.
A, schematic drawing illustrating female reproductive system. B, female reproductive system; arrow referring to sperm storing organs (schematic drawing is modified from http://flybase.org).

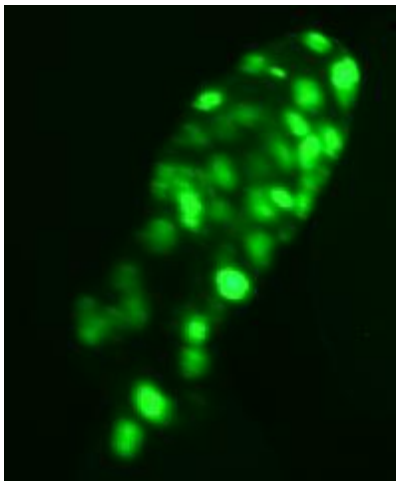

Figure 19: GFP expression pattern in *Octß2R* -GAL4/UAS::GFP male reproductive system.

In the adult brain, mushroom bodies have strong *Octß2R* signals (Fig 20). Two large clusters of varicose ramifications could be seen in the contralateral superior protocerebrum. Many groups of neurons could be distinguished, the first group of transverse neurons crosses the

midline dorsal to the fan shaped body and innervates the protocerebral bridge. Two large somata appear on the midline above the protocerebrum bridge, they send an axons along the midline. From the ventrolateral oesophagus, a thick axon runs laterally into the ipsilateral half, projecting into the cervical connectives. The second group of neurons, which project posteriorlly, some with twisted processes, bilaterally innervates the optic lobes. A conspicuously thick neuron projects from the anterior superior median protocerebrum, passes the posterior margin of the antennal lobe and ends ipsilaterally in the suboesophageal ganglia. A pair of somata, one on each side, could be seen in the ipsilateral inferior lateral protocerebrum where it sends a neuron to the ventrolateral protocerebrum.

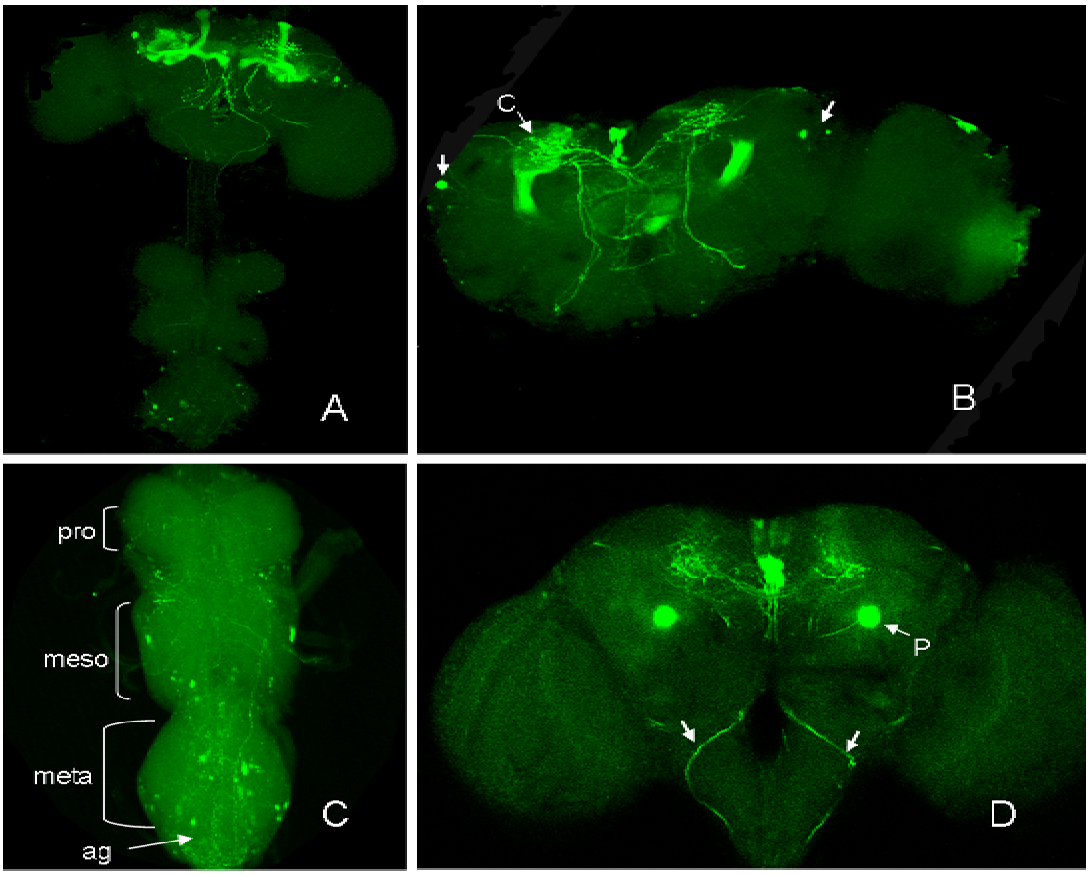

Figure 20: GFP immunoreactivity in CNS of *Octß2R* -GAL4/UAS::GFP adults showen in projection of confocal stacks (A-D).
A,whole CNS. B, *Octß2R* immunoreactivity in adult brain; (C), mushroom bodies calyces; Arrows refer to pair of somata could be seen in the ipsilateral inferior lateral protocerebrum where each send a projection to ventrolateral protocerebrum. C, *Octß2R* exists in the thoracico abdominal ganglion; pro, prothoracic neuromere; meso, mesothoracic neuromere; meta, metathoracic neuromere; ag, abdominal ganglion. D, *Octß2R* immunoreactivity in adult brain; P, pedunculi; arrows refer to a pair of *Octß2R* neurons pass the posterior margin of the antennal lobe and end ipsilaterally in the suboesophageal ganglion.

3.1.1.3. *Octß3R* expression analysis

In *Drosophila*, the gene *octß3R* is referred by the symbol *Dmel\Octß3R* (CG42244). To isolate the putative promotor region (~3100bp), corresponding oligonucleotides were used. The promotor region was double digested with NotI and EcoRI restriction enzymes and directly inserted into the pPTGAL vector, which was prepared accordingly. This vector was used for germline transformation of w^{1118} flies. Studying the expression pattern was performed using the UAS /GAL4 binary system. The *Octß3R*-Gal4 lines were crossed to UAS-GFP driver line. The GFP expression pattern in the first generation was analysed in details.

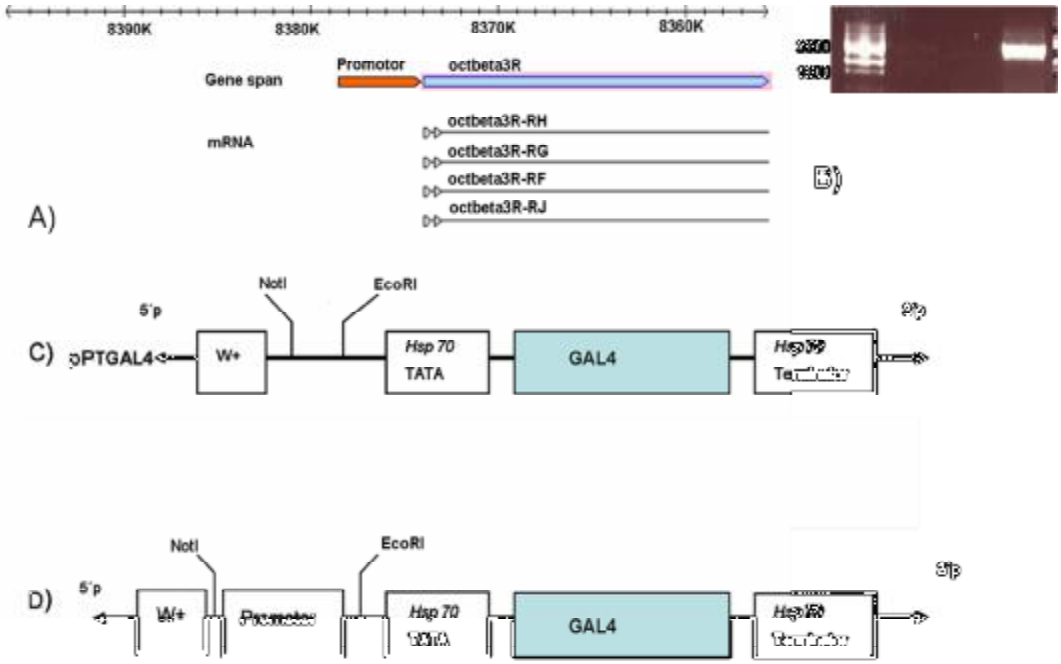

Figure 21: Generating *Octß3R* promotor inserted pPTGAL vector
A, schematic drawing illustrating the *Octß3R* gene model and its products. B, 1% agarose gel showing *Octß3R* promotor region amplified with PCR. C, a part of pPTGAL vector with GAL4 coding sequence between minimum promotor (*hsp*70) and terminal transcription sequence (*hsp*70 terminator). pPTGAL vector was prepared for ligation by double digestion with NotI and EcoRI. D, schematic drawing for promotor-GAL4 - vector. The NotI/EcoRI double digested promotor sequence was inserted in the NotI/EcoRI double digested pPTGAL4 vector.

The larval stage generally shows weak *Octb3R* expression. Scattered sensilla which are aligned at more or less regular intervals can be found in each hemisegment (Fig.22A,B). These sensilla are composed of three types; hairs or bristles (sensilla trichoidea, sensilla chaetica), pegs (sensilla basiconica, sensilla coeloconica), and pits or papillae (‘‘papilla sensilla,’’ in some cases classified as sensilla campaniformia).

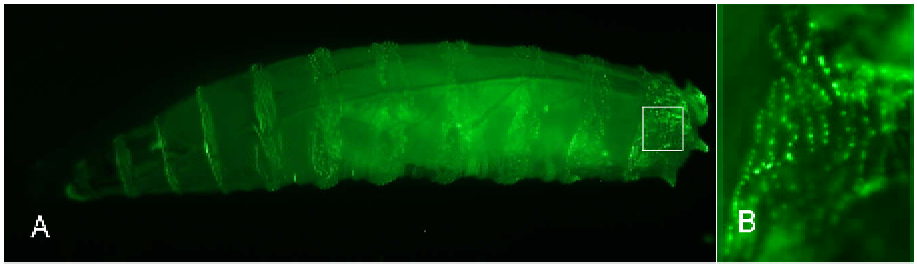

Figure 22: GFP expression pattern in of the *Octß3R* -GAL4/UAS::GFP third larval stage
A, the whole mount third stage larva. B, close view of the posterior part of the larval body showing the scattered distribution of the sensilla.

The thoracic sensilla in *Drosophila* larvae may represent mixed hygro-/temperature receptors, based on the ultrastructural resemblance of these organs with sensilla of other insects (classified as styloconical or basiconical sensilla), which have been investigated electro-physiologically (Altner *et al.*, 1981; Hartenstein, 1988). Moderate *Octb3R* expression can be observed in the larval CNS (Fig.23A,B). The strongest expression could be found in mushroom bodies. GFP-positive somata are located on the dorsolateral traces and along the midline in the thoracic and abdominal neuromere.

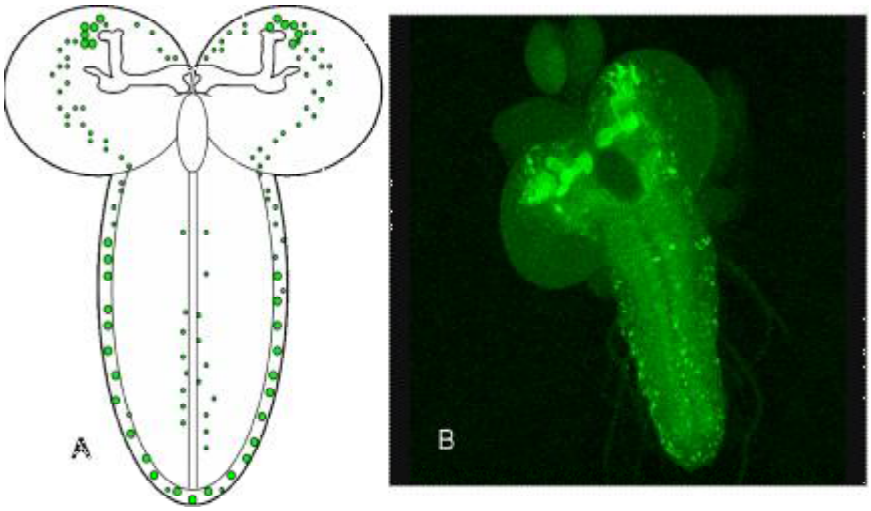

Figure 23: GFP immunoreactivity in the CNS of the *Octß3R* -GAL4/UAS::GFP larval stage.
A, schematic drawing illustrating the GFP expression pattern in the larval brain; somata could be seen on the dorsal surface of each hemisphere especially those conjugated to the α/α´ lobes of mushroom body. Somata could also be seen in the thoracico-abdominal ganglion along the midline and along the dorsolateral trace. B, maximum intensity projection of confocal stacks of GFP expression of larval CNS. Strong GFP could be seen in mushroom body.

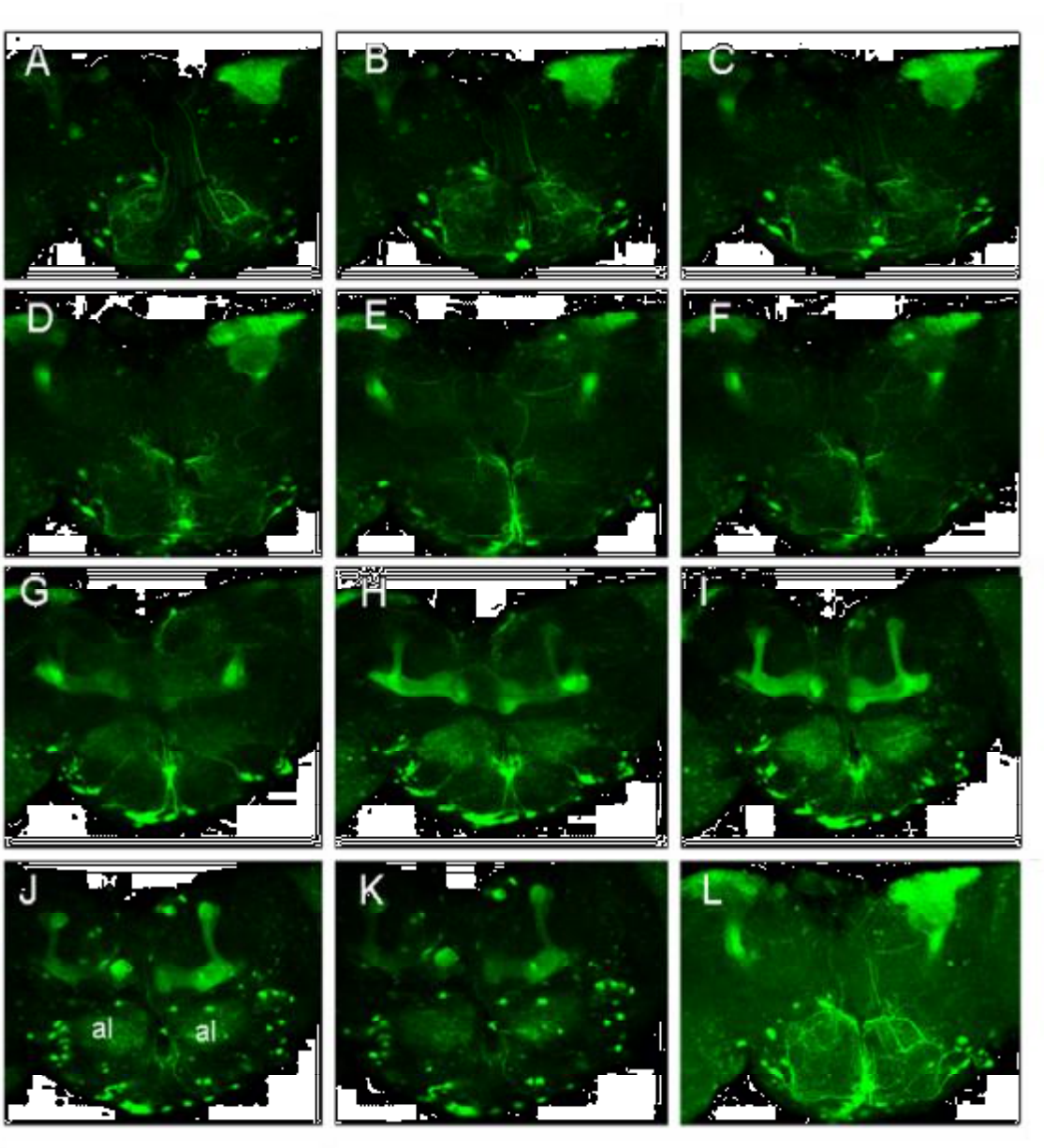

Figure 24: GFP immunoreactivity in the *Octß3R* -GAL4/UAS::GFP adult CNS.
A-L, optical sections showing the innervation of the central brain by *octß3R*. A, arrows refer to two dorsal unpaired median somata. B and C, arrow refers to a cluster of somata located in the mechanosensory center; sending projections passing the antennal lobes toward middle region. D, spiny arborizations surrounding the esophagus foramen (oes); cx, calyx of mushroom body. E and F, innervation of the protocerebrum; arrow refers to a neurite extended in the lateral posterior protocerebrum. G, arrow refers to the position of the ventral unpaired median soma; head arrows refer to two pairs of somata, one pair each side, located in the mechanosensory center. H, head arrow refers to cluster of somata located in the posterior region of the sog send projections toward the midline. I, *octß3R* expression in the mushroom body substructures and ellipsoid body. J and K, a lot of somata could be seen in the subesophageal and the antennal ad mechanosensory center. Most of them sent projections toward the mid line. L, a thick neuron projected from the dorsal unpaired median soma bifurcate near the mid line, each branch extend to the antennal lobe, rolling inside and ascend out of the antennal lobe toward the median protocerebrum.

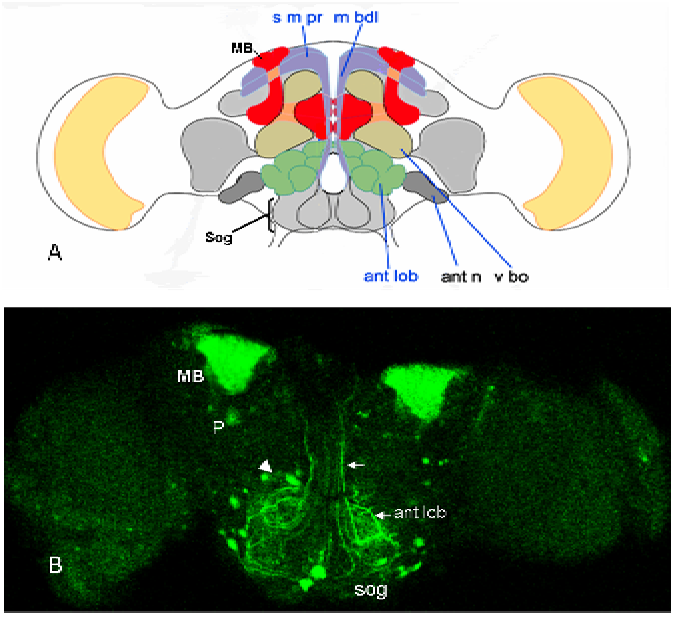

Figure 25: GFP immunoreactivity in the *Octß3R* -GAL4/UAS::GFP adult brain.
A, schematic drawing illustrating *Drosophila* brain centres. B, projection of confocal stacks illustrating the bulky expression of *octß3R* in the antennal lobes , mechanosensory center and subesophageal ganglia. Arrow refers to the neuron that roll up inside the antennal lobe and ascend to the median protocerebrum. Head arrow refers to somata that could be seen in the antennal lobe. MB, mushroom body; p, pedunculus; ant lob, antennal lobe; ant n, antennal nerve; Sog, subesophageal ganglion; m bdI, median bundle; smpr superior median protocerebrum; v bo, ventral body (schematic drawing is modified from http://web.neurobio.arizona.edu/Flybrain) .

In the adult brain, bulky expression of *octß3R* could be seen in the antennal lobes, mechanosensory center and subesophageal ganglion (fig.24,25). Distinct *Octb3R* expression was seen in the mushroom bodies and the ellipsoid body. Two dorsal unpaired median somata could be seen posteriorlly along the midline. A thick neuron projected from the dorsal unpaired median soma bifurcate near the mid line, each branch extends to the antennal lobe, rolling inside and ascends out of the antennal lobe toward the median protocerebrum. A cluster of somata located in the mechanosensory center; sending projections passing the antennal lobes toward middle region. Spiny arborizations surrounding the esophagus foramen (oes). Positively expressed cluster of somata located in the posterior region of the sog send projections toward the midline.

3.1.1.4. *Oa2* expression analysis

In *Drosophila*, the gene octopamine receptor2 is referred by the symbol *Dmel\oa2* (CG6919). The putative promotor region was amplified by PCR (~1500bp). The amplificate was inserted into the pJET vector (MBI Fermentas). The pJET vector was then prepared by double digestion with NotI/BamHI and the insert transferred to pPTGAL, which was prepared

accordingly. The *oa2*-Gal4 line, in which the expression of *oa2* drives Gal4 was crossed to UAS-GFP Driver line. GFP expression in the first generation was analyzed in details.

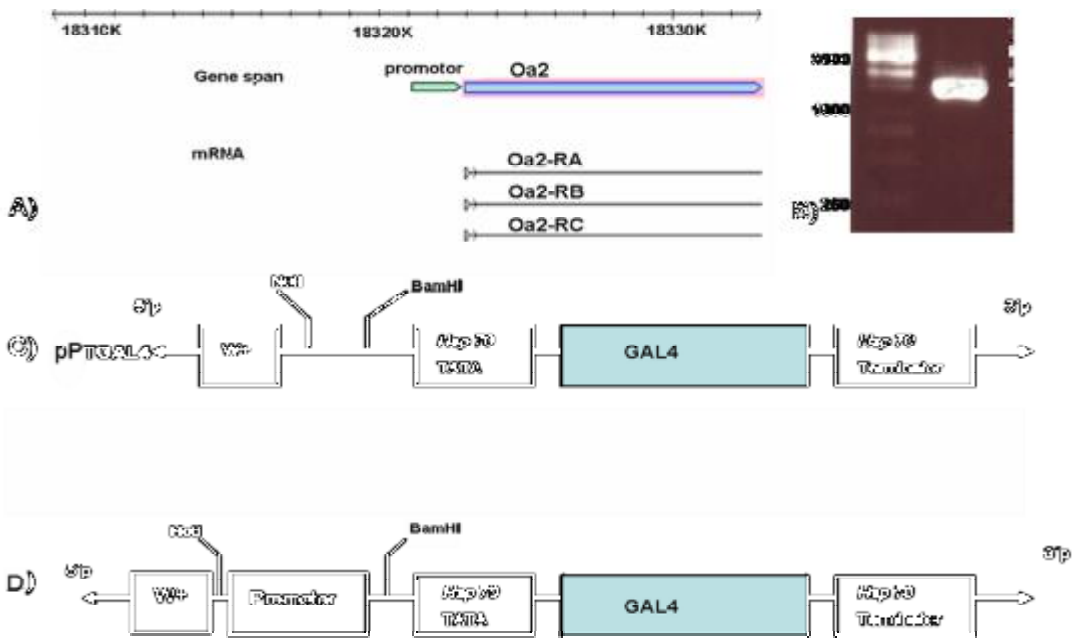

Figure 26: Generating *oa2* promotor inserted pPTGAL vector.
A, schematic drawing illustrating the *oa2* gene model and its products. B, 1% agarose gel showing *oa2* promotor region amplified with PCR. C, a part of pPTGAL vector with GAL4 coding sequence between minimum promotor (hsp70 TATA) and terminal transcription sequence (hsp70 terminaltor). pPTGAL vector was prepared for ligation by double digestion with NotI and BamHI. D, schematic drawing for promotor-GAL4 -vector. The NotI/BamHI double digested *oa2* promotor sequence was inserted in the NotI/BamHI double digested pPTGAL4 vector.

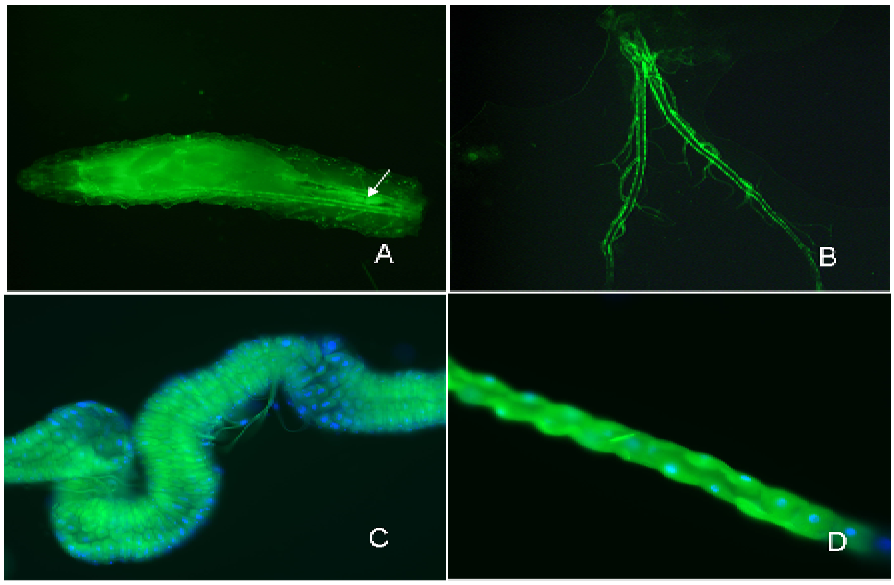

Figure 27: GFP expression pattern in the *oa2*-GAL4/UAS::GFP in the larval stage.
A, the whole third stage larva; arrow refers to the GFP expression pattern in the main branches of trachea. B, GFP expression pattern in dissected tracheal system. C, GFP expression pattern in midgut cells; nuclei (blue) were stained by Hoechst staining. D, GFP expression pattern in the malpighian tubule; nuclei were stained by Hoechst staining.

In the larval stage very strong *oa2* expression could be seen (Fig. 27), especially in the main branches of the tracheal system, which are visible through the cuticle of living larvae. Strong GFP expression could be seen in the midgut cells and in the malpighian tubules.

Very strong expression could be seen in the larval CNS (Fig.28). Scattered somata located on the dorsal surface of each hemisphere express the *oa2* receptor gene. The somata of the thoracic *oa2* neurons reside ventro-medially in the cortex beneath the centro-intermediate trace. The abdominal ganglia contain three morphological different *oa2* expressing groups of neurons. The first group of *oa2* neurons consists of bilateral pairs of dorso-lateral neurons with three somata, composing a cluster and residing at the height of the dorso-lateral traces in each neuromere from abdominal ganglion 1 to 8. The second group of *oa2* expressing neurons is located bilaterally in each abdominal neuromere. Typically, a pair of *oa2* expressing neurons resides in each of the abdominal neuromers, except for the last two ganglia. The somata of these abdominal *oa2* expressing neurons are ventro-laterally on the ventro-lateral trace. The third group comprises ventral paired median *oa2* neurons, their somata are located in the cortex beneath the ventro-median tracts. Outside of the ventral ganglion, these pair of neurons join and project together via the segmental nerves to the periphery.

Strong GFP expression could be seen in the larval eye anlage, which are stem cell-like progenitors (neuroblasts) of the protocerebrum. The eye anlage remains part of the surface epithelium until later in embryogenesis, give rise to adult eye and inner and outer optic lobes.

In the adult stage, strong GFP expression could be seen in the wing veins (Fig. 29). The venation pattern consists of five longitudinal veins and cross veins which are thick cuticular regions providing structural support and nervous /heamolymph conduits.

Strong *oa2* expression could be seen in adult CNS (Fig. 30). A pair of cluster of somata, one each side, located at the pars intercerebralis which are the major insulin producing cells in the fly (Rulifson *et al.*, 2002). Some of their projections project laterally along with the median bundle, these right and left projections cross each other, forming a chiasma and continue projecting till the ventromedial part at the base of antennal lobes. Other neurons, from those which are projecting along the median bundle, project laterally and pass the antennal lobe toward the optic lobes where they extend in strongly labelled ramifications. Mushroom bodies moderately express *oa2*. Scattered and strongly labelled somata are located laterally in the subesophageal ganglion (sog). Strongly labelled somata surrounded the antennal lobes could be seen. Many somata are scattered around the protocerebral bridge and the core of α and β lobes of mushroom bodies.

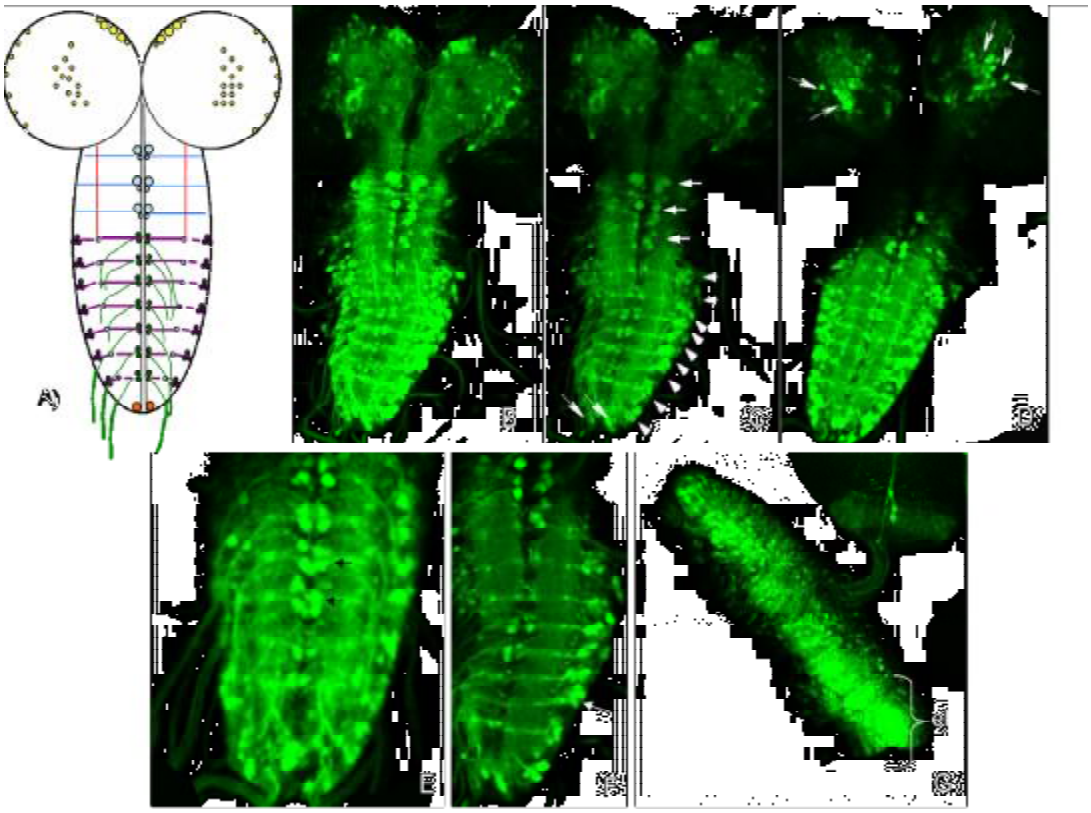

Figure 28: GFP immunoreactivity in the CNS of the *oa2*-GAL4/UAS::GFP larvae.
A, schematic drawing illustrating the *oa2* expression in the larval CNS. B, maximal intensity projection of confocal stacks. C, average intensity projection of confocal stacks; arrows refer to somata in thoracic neuromeres; head arrows refer to somata clusters located on the dorso-lateral traces in each abdominal neuromere. D, projection of confocal stacks; arrows refer to somata which are located on the dorsal surface of each hemisphere. E, close view of the last six abdominal neuromeres; black arrows refer to somata locate in the cortex beneath the ventro-median tracts, their projecting neurons join and project together via the segmental nerves to the periphery. F, close view of the abdominal neuromeres; arrow refer to the lateral clusters of somata located on the dosolateral trace in each neuromere. G, confocal image of GFP expression in larval eye anlage; el, eye anlage.

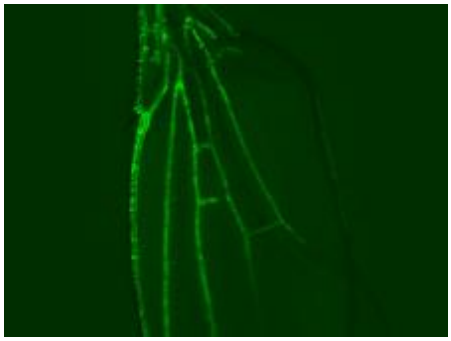

Figure 29: GFP expression pattern in the wing venation of the *oa2*-GAL4/UAS::GFP adults.

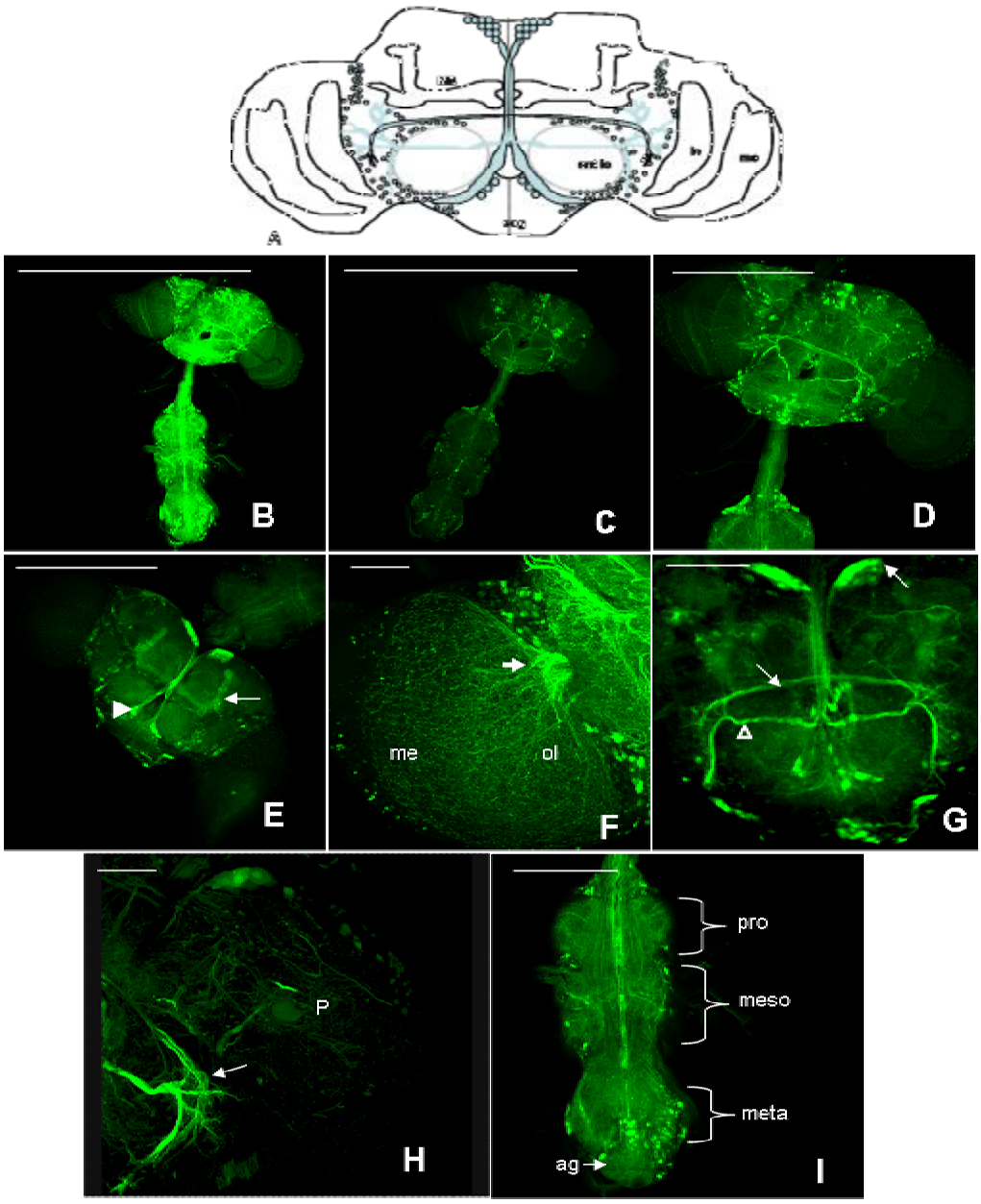

Figure 30: GFP immunoreactivity in the CNS of *oa2*-GAL4/UAS::GFP adults.
A, schematic drawing illustrating the *oa2*expression in the adult brain; MB, mushroom body; lo, lobula; me, medulla; ant lo, antennal lobe; sog, suboesophageal ganglion. B, maximal intensity projection of confocal stacks illustrating the *oa2* expression pattern in the whole CNS. C, average intensity projection of confocal stacks illustrating the *oa2* expression pattern in the whole CNS. D, close view on the brain. E, close up view of the brain; arrow refer to the moderately expressed mushroom body; head arrow refer to projections run laterally along with the median bundle, these right and left projections cross each other forming chiasma and continue projecting till the ventromedial region at the base of antennal lobes. F, close view on the optic lobe; the lobula (lo), lobula plate and medulla (me) are innervated by *oa2* neurons; arrow refers to the main and strong expressed neuron. G, close view on the middle part of the brain; right arrow refers to cluster of somata located at the pars intercerebralis which are the major insulin producing cells in the fly (Rulifson et al., 2002); middle arrow refers to strong expressed great commissure connecting the brain hemispheres; isosceles arrow refers to neuron projecting along the median bundle, project laterally and pass the antennal lobe toward the optic lobes where they extend in strongly labelled ramifications. H, strong labelled intercalating ramifications of the great commissure and the neurons that innervate the optic lobe; arrow refers to those intercalating ramifications. I, GFP expression pattern in the thoracic-abdominal ganglion; pro, prothoracic ganglion; meso, mesothoracic ganglion; meta, metathoracic ganglion; ag, abdominal ganglion. Scale bar = 50µm.

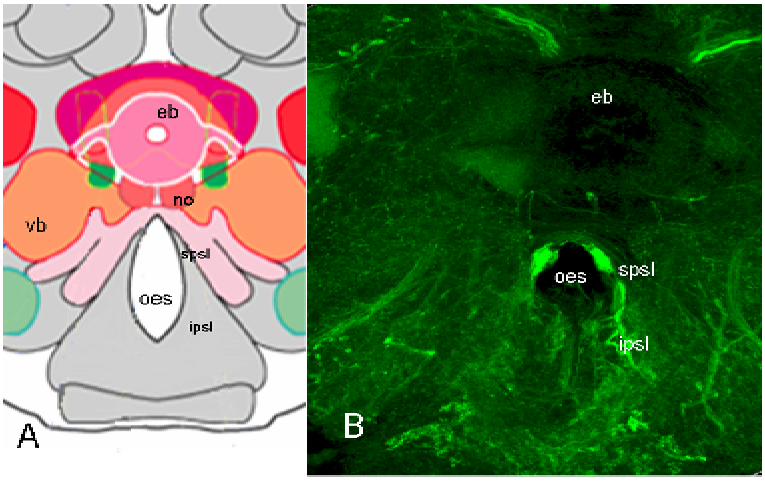

Figure 31: GFP immunoreactivity in the central complex in the brain of the *oa2*-GAL4/UAS::GFP adults.
A, schematic drawing illustrating the central complex and suboesophageal ganglion; eb, ellipsoid body; vb, ventral body; no, noduli; spsl, superior posterior slope surrounding the esophagus (oes); ipsl, inferior posterior slope surrounding the esophagus. B, confocal image showing close view of central complex; fine OA2 positive ramifications could be confined in the posterior region of ellipsoid and noduli (no). Dense ramifications spread in the superior (spsl) and inferior posterior slope surrounding the esophagus foramen
(schematic drawing is modified from **http://web.neurobio.arizona.edu/Flybrain/html/atlas/index.html**).

A great commissure could be seen connecting the adult brain hemispheres, sending strong labelled ramification toward the optic lobe. The lobula, lobula plate and medulla in the optic lobe are innervated by *oa2* neurons. In *Drosophila*, central complex located at the interhemispheric junction, consists of four structures; protocerebral bridge, fan-shaped body, ellipsoid body and pair of noduli. Relatively weak expression was confined in central complex (Fig.31), however, some ramifications innervated the ellipsoid and paired noduli could be seen.

3.1.2. Dopamine receptors

3.1.2.1. *DopR* expression analysis

In *Drosophila*, the gene Dopamine receptor is referred by the symbol *Dmel\DopR* (CG9652). To amplify the *DopR* promotor region (~800bp) corresponding sense and antisense oligonucleotides were used. The DNA containing the promotor region was inserted into the pJET vector (MBI Fermentas) via directional cloning using NotI and BamHI restriction sites. Following verification of correct integration by sequencing, the insert was transferred into the pPTGAL vector, which was used for production of transgenic lines by germline integration (injection service BestGene). Studying the expression pattern was performed using the UAS

/GAL4 system (Brand and Perrimon, 1993a). The *DopR*-Gal4 line was crossed to a UAS-GFP responder line, thus allowing to visualize expression of the DopR gene by GFP expression.

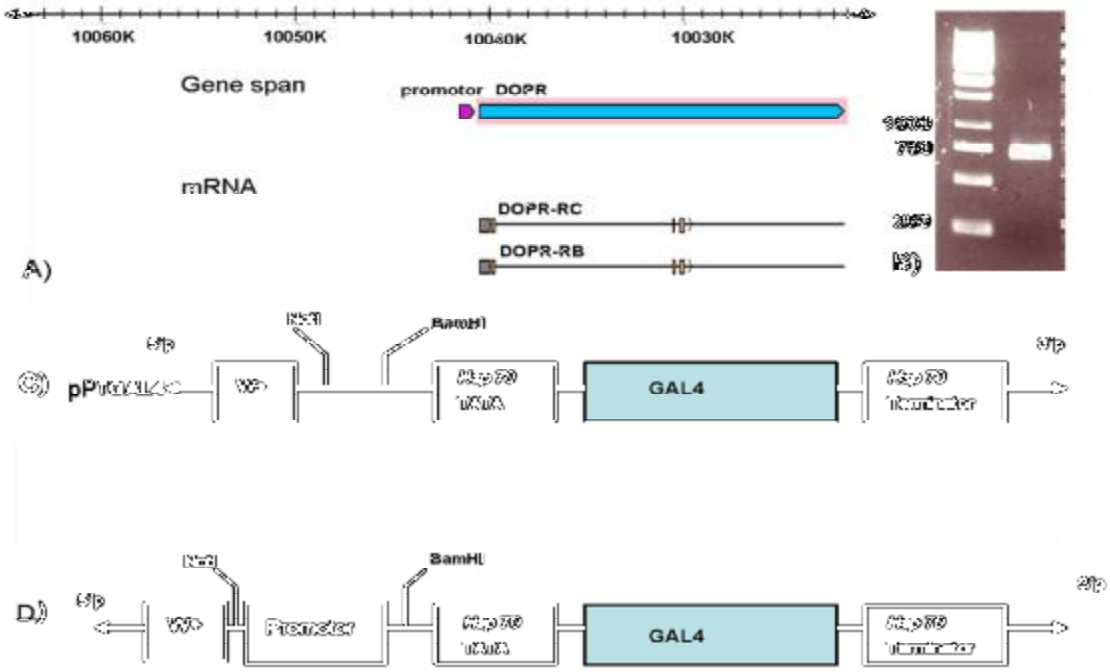

Figure 32: Generating *DopR* promotor inserted pPTGAL vector.
A, schematic drawing illustrating the *DopR* gene model and its products. B, 1% agarose gel showing *DopR* promotor region amplified with PCR. C, a part of the pPTGAL vector with the GAL4 coding sequence between a minimum promotor (*hsp*70) and termination sequence (*hsp*70 terminaltor). The pPTGAL vector was prepared for ligation by double digestion with NotI and BamHI. D, schematic drawing of the vector construct. The NotI/BamHI double digested *DopR* promotor sequence was inserted into the NotI/BamHI double digested pPTGAL vector.

The *DopR* expression pattern was analyzed in detail in the larval and adult progeny from this cross. Strong GFP expression could be seen in the larval salivary gland, which was even visible through the cuticle. Distinct expression was also found in the larval fat body. Strong GFP was seen in the larval gut (Fig.33). To identify the cells within the gut that express the *DopR*, I performed immunohistochemical studies with three different primary antisera; anti-GFP, anti-prospero and anti-armadillo to label specific intestinal cells. Interspread among the monolayer of intestinal cells are enteroendocrine cells, which express different peptides. Most of enteroendocrine cells express the transcription factor prospero and also the ß-catenin homologue Armadillo. Most of the Armadillo- positive cells show strong *DopR* immunoreactivity.

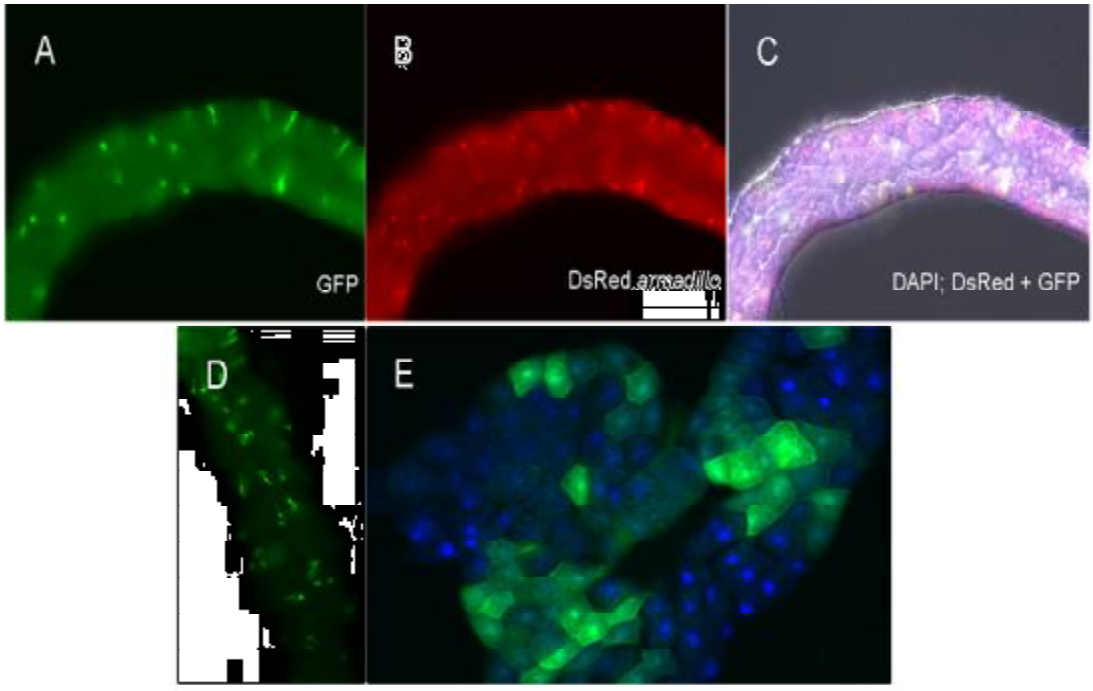

Figure 33: GFP expression pattern in the *DopR*-GAL4/UAS::GFP larval stage.
A, GFP expression pattern in the gut. B, the same gut is co-labelled with α armadillo antibodies (DsRed channel). C, overlay of DsRed and GFP; nuclei are stained with DAPI (blue). D, close view of the gut showing the GFP expression pattern. E, GFP expression pattern in the larval fat body; nuclei are stained with DAPI (blue).

GFP expression pattern of the *DopR* in larval brain appear as connected bundles in the brain cortex because secondary small axon traces travel radially connecting the *DopR* positive somata within the hemisphere (Fig.34). These *DopR* expressing somata are located on almost all neuropile secondary traces including; medial dorsoposterior, lateral dorsoanterior, medial dorsoanterior, lateral dorsoposterior traces which are located dorsally in each hemisphere; centromedial and centroposterior which are located in the centre of the neuropile; basolateral anterior, basolateral ventral and basolateral posterior traces in the base of each brain hemisphere. Strongly expressed somata are also located in the thoracico-abdominal ganglion. The outline detecting optic lobe also expressed *DopR*. Strongly expressing somata are also located dorsally on the optic lobe. Two large and strong expressed somata also located on the medial dorsoposterior in the hemisphere. Some of the strongly expressed neurons project from the neuropile toward the optic lobe.

In the adult stage strong GFP expression could be seen in the thoracic region, which is due to strongly expressing flight muscles (fig. 35).

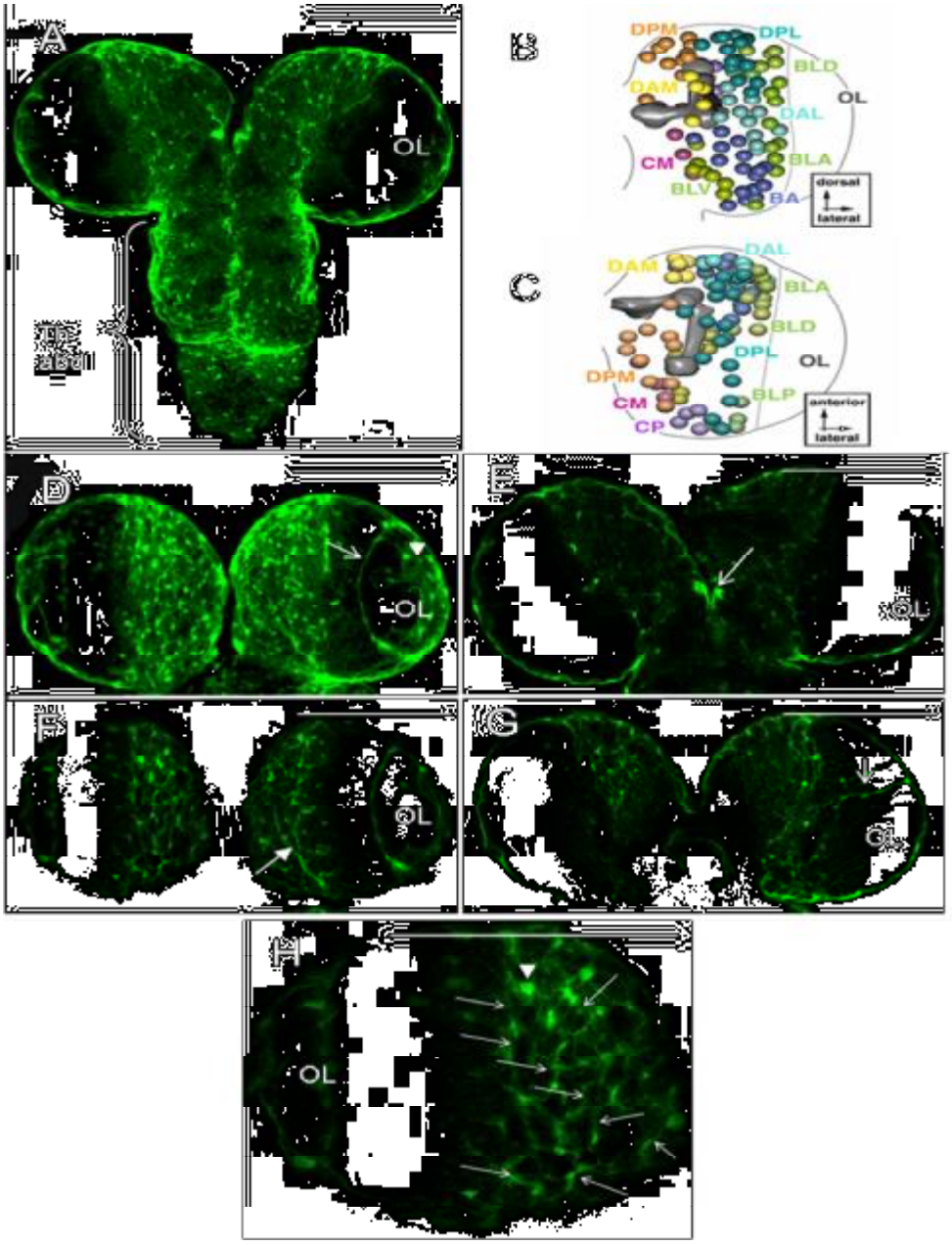

Figure 34: GFP immnuoreactivity in the CNS of the *DopR*-GAL4/UAS::GFP larval stage.

A, projection of confocal stacks illustrating the GFP expression pattern in the CNS of 3rd instar larva. The GFP was seen in the surface of the brain hemisphere and cortex and neuropile regions; OL, optic lobe; Th abd, thoracico-abdominal ganglion. B and C, 3D models of brain hemisphere (B, dorsal view ; C, anterior view) showing hemisphere regions located by colored spheres; the outline of the optic lobe is indicated by gray line; mushroom body indicated by shaded dark gray; (DPM), medial dorsoposterior; (DPL), lateral dorsoposterior; (DAM), medial dorsoposterior; (DAL), lateral dorsoanterior;(DPL), lateral dorsoposterior; (DPM), medial dorsoposterior; (BLA), basolateral anterior;(BLD), basolateral dorsal;(BLP), basolateral posterior; (BLV), basolateral ventral; (CM), centromedial (Pereanu and Hartstein; 2006). D, projection of confocal stacks showing close view on the larval brain hemispheres. Strong expressed somata located in central neuropile; arrow refer to the GFP in outline of the optic lobe; head arrow refer to group of somata located dorsally on the optic lobe. E-G, confocal stacks. E, arrow refer to pair of large and strong expressed somata located medial dorsoposterior, one each hemisphere. F, arrow refers axons projected in the centroposterior (CP) and centromedial in the neuropile. G, arrow refers to a projection from a soma located in the neuropile toward the optic lobe. H, close view on one brain hemisphere; arrows refer to several axons located in the central neuropile; head arrow refer to somata located in the medial drosoposterior (DPM) in the cortex. Scale bar = 150µm.

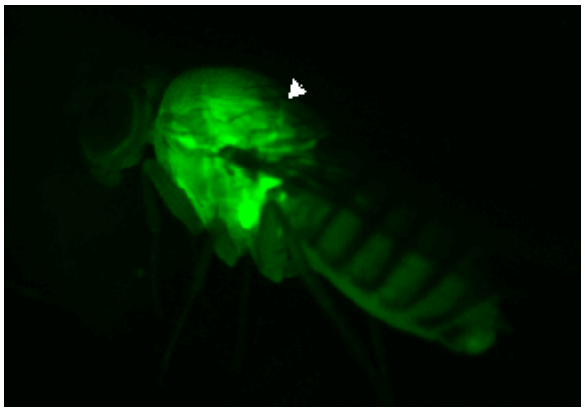

Figure 35: GFP expression pattern in the whole *DopR*-GAL4/UAS::GFP adults.
Arrow refers to the GFP in flight muscles.

In the adult brain, the *DopR* positive somata and axons could be seen almost everywhere in the supra- and subesophageal ganglia as well as in the optic lobes (Fig. 36 and 37). Mushroom body substructures strongly express *DopR*. Within the interhemispheric junction, strong GFP expression could be seen in the central complex substructures including; the outer margin of the fan-shaped body; some positive *DopR* neurons including somata which innervate the ellipsoid body; noduli and some axonal projections connecting the central complex substructures. Dense ramifications spread in the superior and inferior posterior slope surrounding the esophagus foramen. Strong GFP expression was seen in the optic lobe including lobula, lobula plate and inner- and outer medulla.

Two large somata could be seen in the ventro-medial part of the subesophageal ganglion. *DopR* positive neurons project from posterior inferior lateral protocerebrum into the ventromedial protocerebrum. In addition, *DopR* positive neurons project from posterior inferior lateral protocerebrum towards the midline. Strongly expressing somata are also located in the lateral protocerebrum and in the ventrolateral part of the antennal lobe and antennal nerve. A cluster of strongly expressed somata is located in the ventrolateral protocerebrum. Positive *DopR* neurons ramified bilaterally into the ventromedial protocerebrum, they have their somata located on the midline of the subesophageal ganglion with mirror symmetry. They can be divided into three neuromeres (mandibular, maxillary, and labial) in the gnathal segment. Therefore, these subclusters are named VMmd, VMmx and VMlb from anterior to posterior. The GFP expression is strong in both VMmx and VMlb but it is moderate in the VMmd cluster. The secondary neurons turn ventrally to descend through the cervical connective. These descending axons terminate in all three thoracic ganglia and abdominal ganglia (Fig.37).

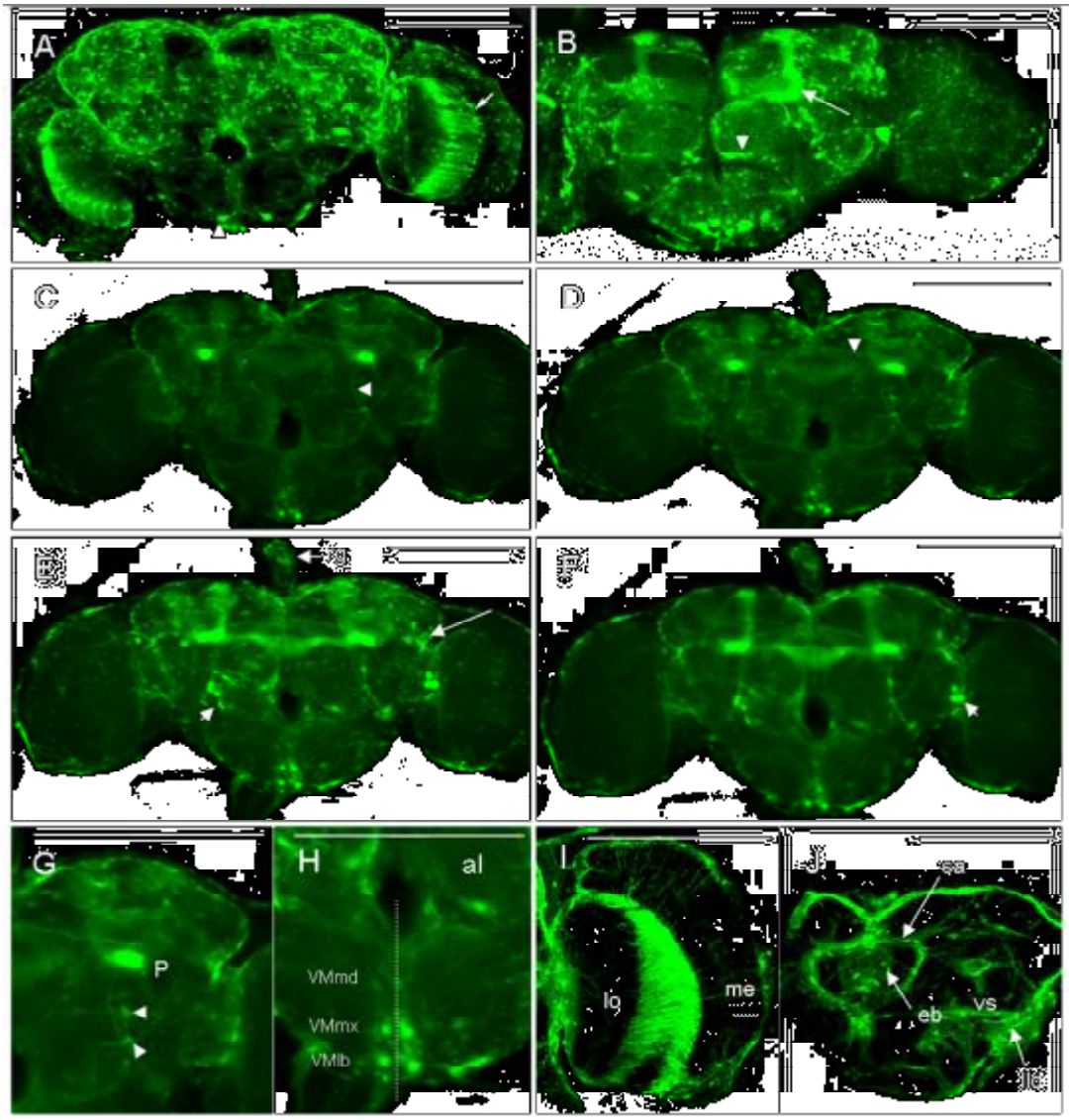

Figure 36: GFP immnuoreactivity in the *DopR*-GAL4/UAS::GFP adult brain.
A, maximal intensity projection of confocal stacks which was collected at 1.5µm steps; arrow refers to GFP expression the medulla region of the optic lobe; head arrow refers to two large somata that could be seen in the ventro-medial of the subesophageal ganglion. B, maximal intensity projection of confocal stacks which was collected at 1µm steps; arrow refers to the strong GFP expression in the mushroom body; head arrow refers to the strong expressed somata located on the ventromedial of the antennal lobes. C-F, confocal sections of the brain. C, arrow refers to *DopR* positive neuron projecting from posterior inferior lateral protocerebrum into the ventromedial protocerebrum; D, arrow refers to *DopR* positive neuron projects from posterior inferior lateral protocerebrum toward the midline. E, arrow refers to strong expressed somata located in the lateral protocerebrum; short arrow refers to somata located in the ventrolateral of the antennal lobe and antennal nerve. F, head arrow refers to a cluster of strong expressed somata located in the ventrolateral protocerebrum. G-J, single optical sections of distinct brain regions. G, single optical section illustrating close view of the anterior protocerebrum. H, close view on subesophageal ganglion; al, antennal lobe; VMmd, VMmx and VMlb refer to the three somata subclusters along the midline of the subesophageal ganglion which represent three neuromeres (mandibular, maxillary and labial). These somata send a projection toward the supra oesophageal ganglion; dashed line indicates the midline of the subesophageal ganglion. Scale bar = 150.

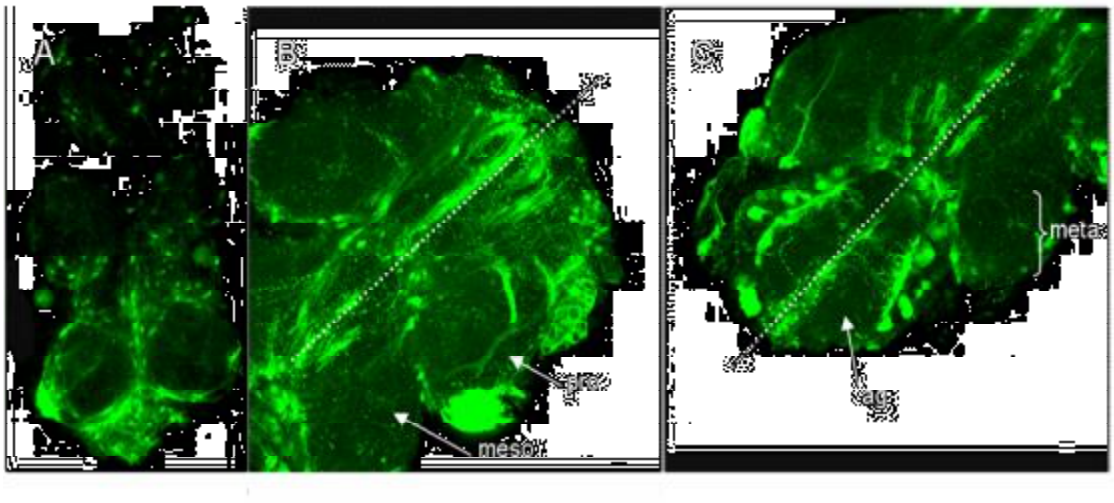

Figure 37: GFP immnuoreactivity in the thoracico abdominal ganglion of the *DopR*-GAL4/UAS::GFP adult stage.
A, GFP expression pattern in the whole thoracico abdominal ganglion. B, oblique view from the anterior so as better to visualized the beginning (pro- and meso- thoracic ganglia) of the thoracico abdominal ganglion. The thoracico abdominal ganglion is tilted about 45° to the right; the dashed line indicates the midline of the thoracico abdominal ganglion; pro, prothoracic ganglion; meso, mesothoracic ganglion. C, oblique view from the posterior so as better to visualized the bottom (metathoracic ganglion and abdominal ganglion) of the thoracico abdominal ganglion. The thoracico abdominal ganglion is tilted about 45° to the right; the dashed line indicates the midline of the thoracico abdominal ganglion.

3.1.2.2. *DopR2* expression analysis

In *Drosophila*, the gene Dopamine receptor2 is referred by the symbol *Dmel\DopR2* (CG18741). As described for the other receptor genes, the *DopR2* promotor region (~ 3000 bp) was amplified by PCR. This amplificate was directly inserted into the pPTGAL vector (fig.38) via NotI and BamHI restriction sites. This vector was used for making transgenic lines via germline integration into w^{1118} flies (BestGene). Studying the expression pattern was performed using the UAS/GAL4 binary system. The *DopR2*-Gal4 lines were crossed to UAS-GFP responder line and larval and adult stage of the first generation were analyzed in detail. Strong GFP expression could be seen in the larval gut cells (Fig. 39A). The tracheal system of larvae shows strong GFP expression, which could be seen through the cuticle (Fig. 39 B). It is present in the three major parts of the tracheal system; the primary airways, the secondary airways, and the blind ending terminal ones. Terminal branches strongly express GFP. They are very thin extensions contacting almost every single cell.

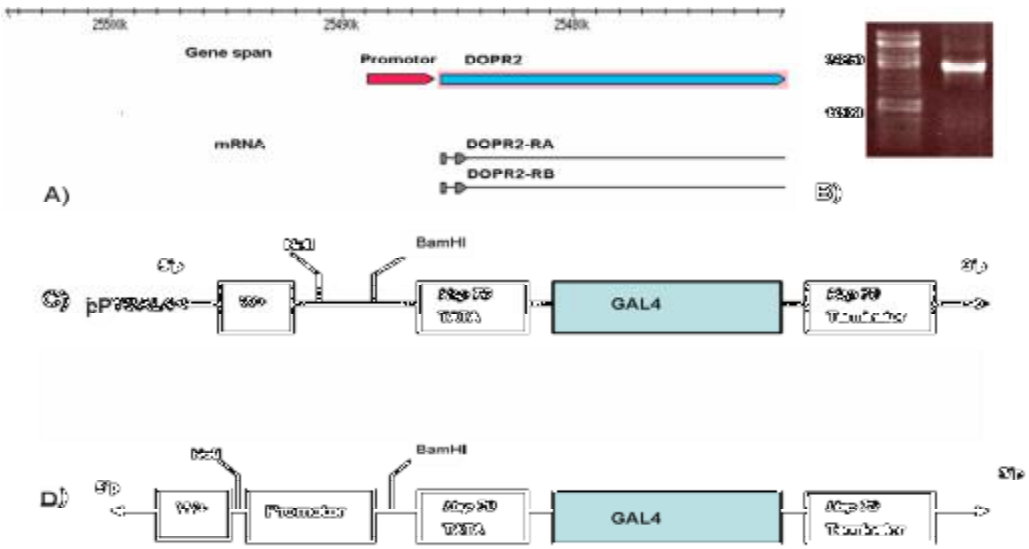

Figure 38: Generating *DopR2* promotor insertion pPTGAL vector.
A, schematic drawing illustrating *DopR2* gene model and its products. B, 1% agarose gel showing *DopR2* promotor region amplified with PCR. C, a part of pPTGAL vector with GAL4 coding sequence between minimum promotor (*hsp*70) and termination sequence (*hsp*70 terminator). pPTGAL vector was prepared for ligation by double digestion with NotI and BamHI. D, schematic drawing of the promotor-GAL4-vector. The NotI/BamHI double digested *DopR2* promotor sequence was inserted into the NotI/BamHI double digested pPTGAL vector.

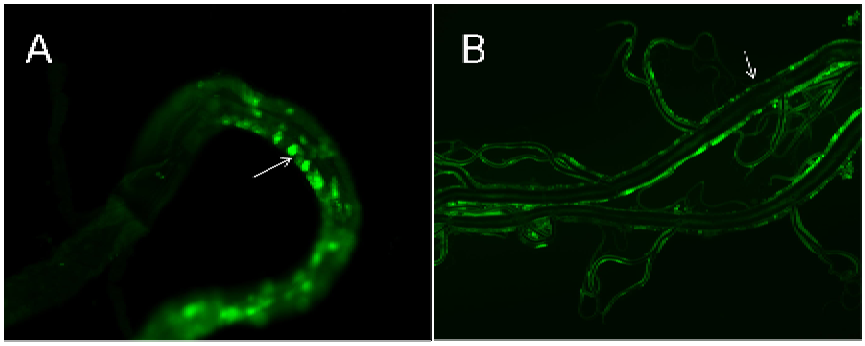

Figure 39: GFP expression pattern in distinct tissues of the *DopR2*-GAL4/UAS::GFP larvae.
A, GFP expression pattern in the larval gut; arrow refers to GFP expressed intestinal cells. B, GFP expression pattern in the larval tracheal system.

Distinct *DopR2* expression was detected in the larval CNS (Fig. 40). Huge numbers of somata could be detected in the medial dorsoposterior and lateral dorsoposterior in each brain hemisphere with non-mirror symmetry. These short axons including somata form a dense meshwork structure. From these somata, a moderately labelled projection travel to the optic lobe. *DopR2* positive somata, axons and ramifications could be seen in the centromedial and basolateral ventral part of the brain hemisphere. They are conjugated with final branches of

the tracheal system. In the thoracico abdominal ganglia, each thoracic neuromere contains two pairs of *DopR2* transverse neurons. These neurons are located laterally.

The ventral ganglion contains two morphologically different *DopR2* transverse neuronal groups: the first *DopR2* containing neuronal group consists of a pair of dorso-lateral neurons with somata residing at the height of the dorso-lateral tracts in each neuromere from the 1st to the 7th abdominal ganglia which are parallel with very fine branches of the tracheal system. In each abdominal ganglion, neurons from both sides join in one plexus beneath the centro-intermediate tracts and project together via the segmental nerves to the periphery.

These somata which are located on the dorsolateral trace, project into at least 4 regions. Each *DopR2* neuron in the thoracic and abdominal ganglia sends a neurite beneath the transverse projection. These neurites from both sides join in proximity to the ventro-median tracts. These joining *DopR2* containing neurites form extensive arborisations along the midline between the dorso-median and ventro-median tracts.

In the adult stage, terminal branches of the tracheal strongly express GFP. They are very thin extensions contacting in many tissues almost every single cell. As shown in (fig.41) the fine branches of trachea supply legs and visceral branches supply the gut.

The adult CNS showed strong *DopR2* expression (Fig. 42). Mushroom body substructures are strongly labelled with GFP. Thick and strong expressing ramifications and projections spread all over the protocerebrum, especially in the anterior superior medial protocerebrum, with their somata located in the ventrolateral protocerebrum (vlpr). A cluster of somata located in the anterior superior medial protocerebrum sends three groups of projections; those extending to the ventrolateral region of the protocerebrum; projections extending laterally to innervate the optic lobes; and the third group of these projections ascend along the midline innervating the central complex substructures and the interhemispheric junction. GFP expressing somata located in the superior and inferior posterior slope in the suboesophageal ganglion (sog). Two *DopR2* positive neurons are located in the anterior superior protocerebrum with axon projecting laterally to the optic lobe. Strong GFP expression could be seen in the lobula (Lo) as well as the inner and outer medulla (me) in the optic lobe.

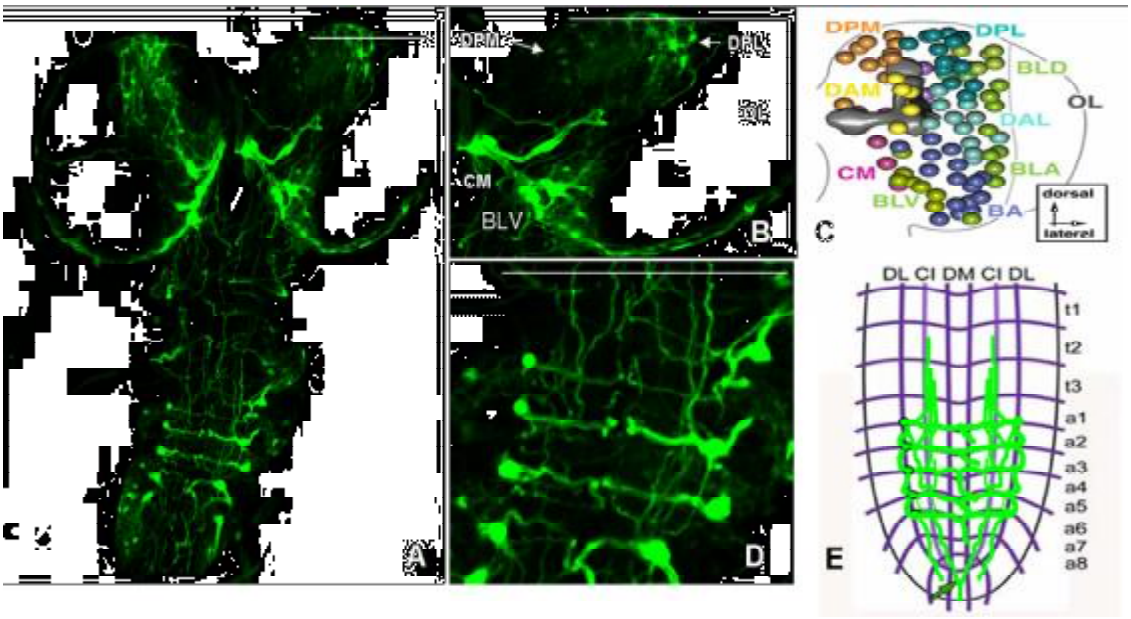

Figure 40: GFP immnuoreactivity in the CNS of *DopR2*-GAL4/UAS::GFP larvae.
A,B and D, projection of confocal stacks illustrating the *DopR2* expression. A, GFP expression pattern in the whole mount larval CNS. B, projection of confocal sections of one brain hemisphere; *DopR2* expressed by the surface of the brain hemisphere; short axons including somata were seen in the medial dorsoposterior and lateral dorsoposterior regions of the brain hemisphere which form dense meshwork. C, 3D models of the dorsal view of brain hemisphere showing hemisphere regions located by colored spheres; the outline of the optic lobe is indicated by gray line; mushroom body indicated by shaded dark gray; (OL), optic lobe. (DPM), medial dorsoposterior; (DPL), lateral dorsoposterior;(DAM), medial dorsoposterior; (DAL), lateral dorsoanterior; (BLA), basolateral anterior;(BLD), basolateral dorsal;(BLP), basolateral posterior; (BLV), basolateral ventral; (CM), centromedial (Pereanu and Hartenstein; 2006). D, close view of the DopR2 neurons laterally located in the thoracicoabdominal neurons with their projections to the medial traces. E, schematic drawing of the GFP expression pattern in the thoracico abdominal ganglia; the main traces in the thoracico abdominal ganglia are the dorsolateral trace, the centro-intermediate trace and the dorsomedial trace; (t1-t3) first, second and third thoracic neuromeres.; (a1-a8) the first to the eight abdominal ganglia. Scale bar = 150µm.

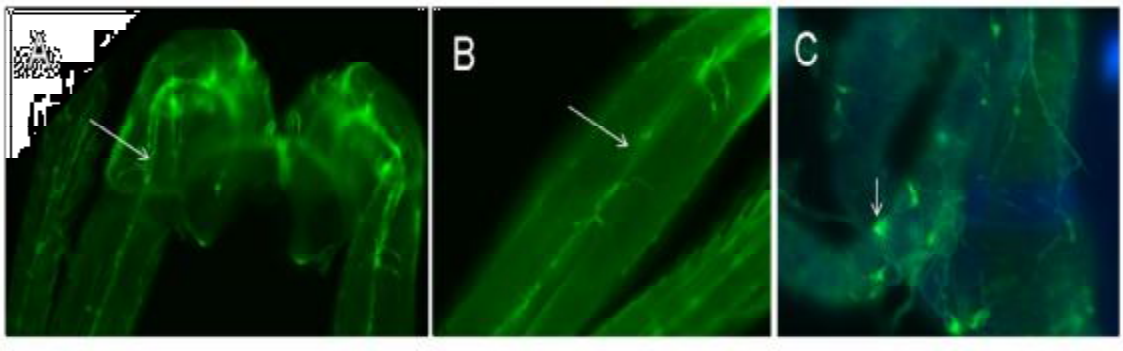

Figure 41: GFP expression pattern in the fine terminal branches of the tracheal system in the *DopR2*-GAL4/UAS::GFP adult stage.
A and B, arrows refer to the tracheal branches supplying the legs of adult stage. C, arrow refers to the fine visceral branches of the tracheal system supplying the gut.

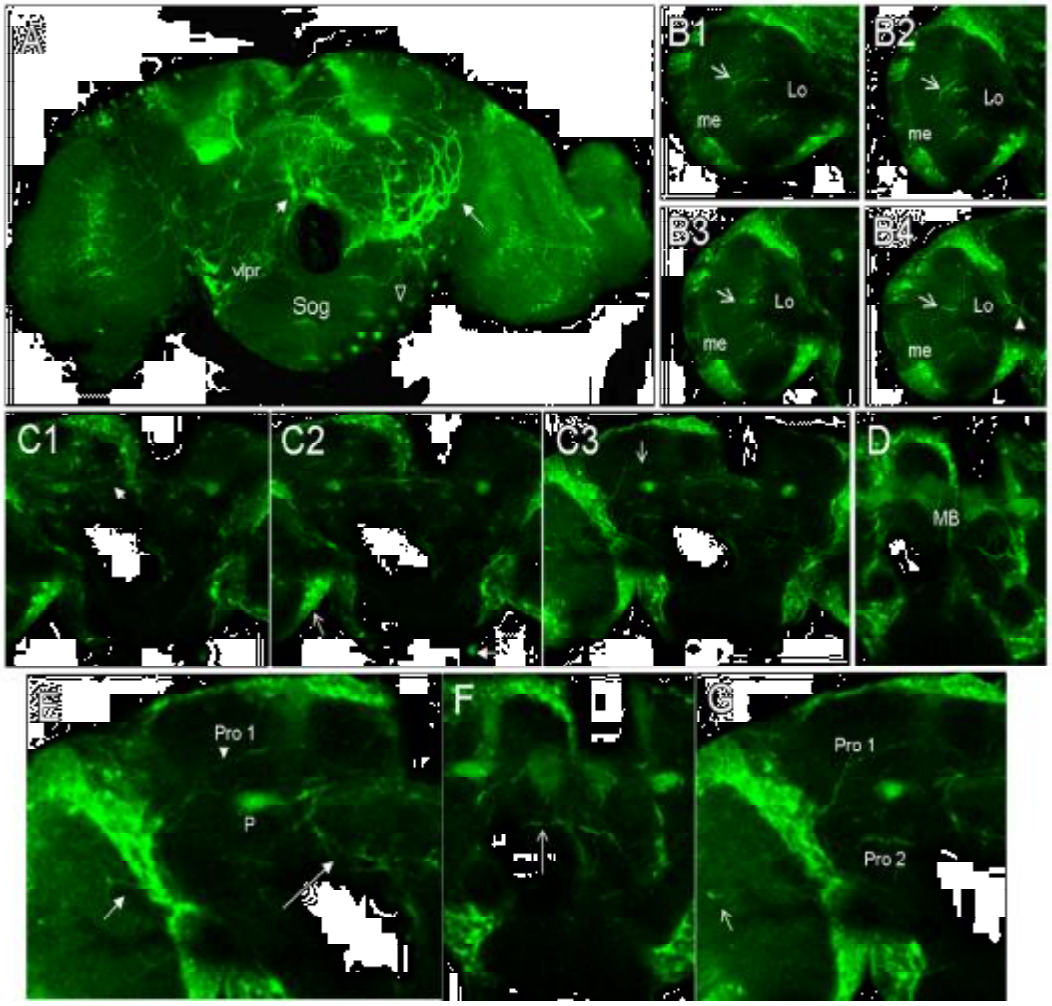

Figure 42: GFP immunoreactivity in the *DopR2*-GAL4/UAS::GFP adult brain.
A, projection of confocal stacks illustrating the GFP expression pattern in the adult brain; long arrow refer to GFP labels thick and strong expressed ramifications and projections spread all over the protocerebrum with their somata located in the ventrolateral protocerebrum (vlpr); short arrow refer to a pair of somata located in the anterior superior medial protocerebrum sending projections to the ventrolateral region of the protocerebrum and to the optic lobes; empty head arrow refers to GFP expressed somata located in the superior and inferior posterior slope in the suboesophageal ganglion (sog). B1-B4, single optical sections of the ipsilateral optic lobe illustrating ramifies, showed by arrows with the same position and angle in the four sections, in the lobula (Lo); the inner and outer medulla (me). B4, head arrow refers to a single axon project laterally to the optic lobe. C1-C3, confocal sections of the central brain; C1, arrow refers to *DopR2* positive neurons located in the anterior protocerebrum with an axon projects laterally to the optic lobe; C2, arrow refers to strong expressed somata located in the lobula of the optic lobe; C3, arrow refers to an axon located in the superior protocerebrum project laterally to optic lobe. D, a single confocal section illustrating GFP expression in the mushroom body (MB). E-G, single optical sections of distinct brain regions. E, magnifications of the protocerebrum; which contains ramifies surrounding the central complex substructures referred by long arrow; pro1 refers to an axon project laterally to the optic lobe; the short arrow refers to this axon within the optic lobe; p, pedunculus. F, arrows refers to axons pass the midline of the protocerebrum. G, pro1 and pro2 refer to axons innervating the optic lobes.

3.1.2.3. *D2R* expression analysis

In *Drosophila*, the gene Dopamine 2-like receptor is referred by the symbol *Dmel\D2R* (CG33517). The *D2R* promotor region was amplified by PCR (~ 3500 bp). This PCR product was double digested with NotI/BgIII restriction enzymes and directly inserted into the pPTGAL vector (fig.43), which was used for germline transformation. As already described, the expression pattern was studied using the Gal4/UAS-system via crossing the corresponding lines with UAS-gfp.

In the larval stage very strong *D2R* expression is seen in the tracheal system, which is visible through the cuticle of living larvae (fig 44). In addition, fine tracheal branches which contact the viscera are also GFP-positive. Strong GFP was also seen in the salivary glands. In the digestive system, strong expression was found in the foregut, atrium, pharynx and oesophagus. Within the pharynx, pharyngeal muscles are peculiarly positive. No expression was seen in the rest of the foregut. Strongly expressing muscles stripes could be seen in the hindgut.

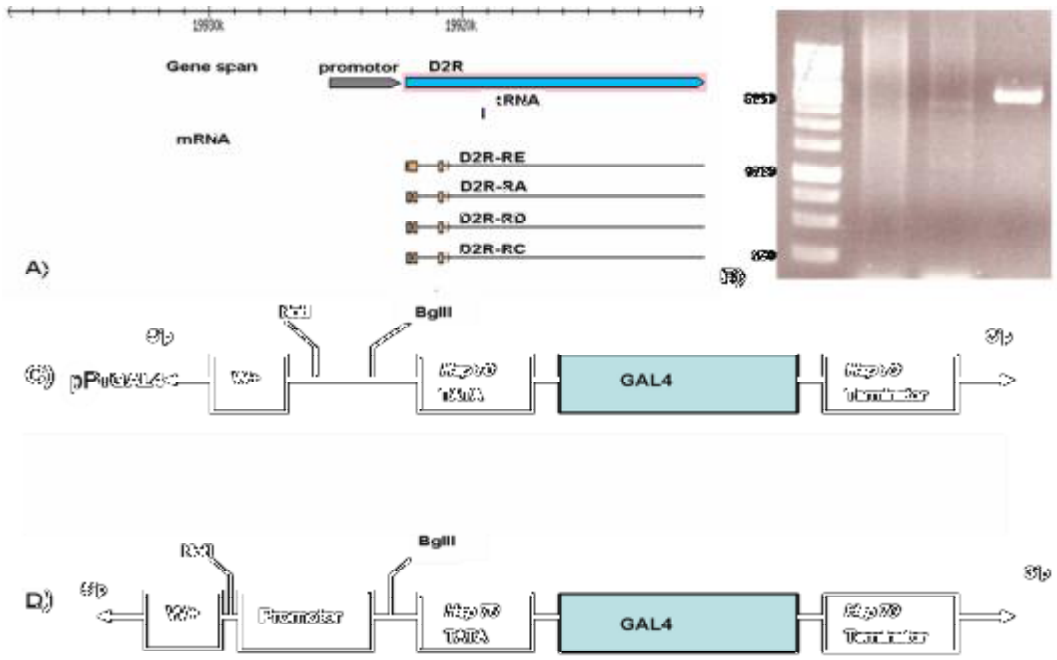

Figure 43: Generating *D2R* promotor inserted pPTGAL4 vector

A, schematic drawing illustrating the *D2R* gene model and its products. B, 1% agarose gel showing *D2R* promotor region amplified with PCR. C, a part of pPTGAL vector with the GAL4 coding sequence between a minimum promotor (*hsp*70) and terminal transcription sequence (*hsp*70 terminaltor). pPTGAL vector was prepared for ligation by double digestion with NotI and BgIII. D, schematic drawing of the promotor-GAL4 -vector. The NotI/BgIII double digested *D2R* promotor sequence was inserted in the NotI/BgIII double digested pPTGAL vector.

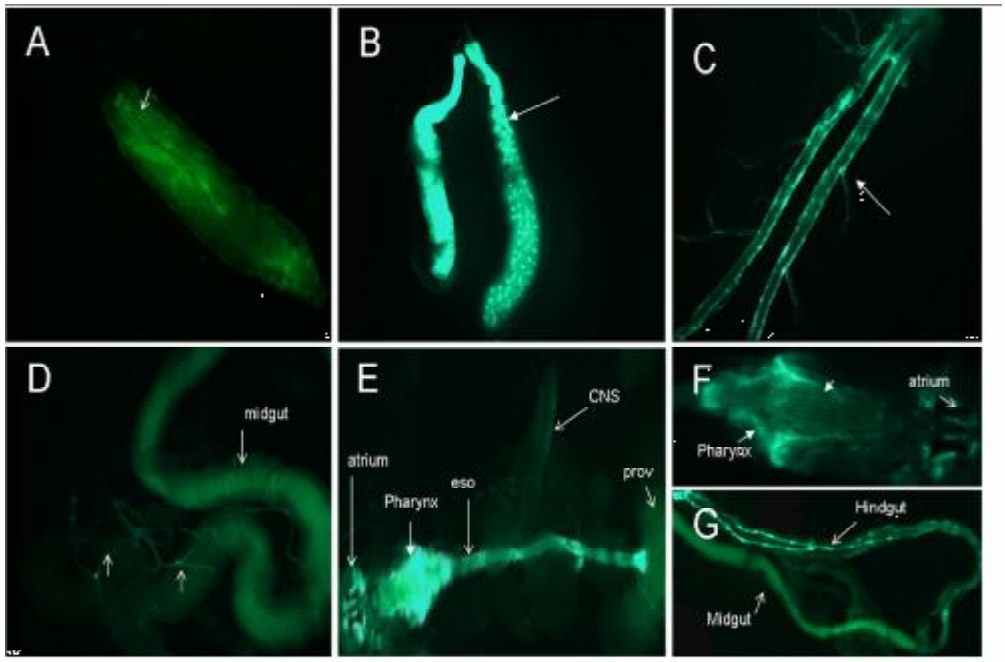

Figure 44: GFP expression pattern in the *D2R* -GAL4/UAS::GFP larval stage
A, the whole third stage larvae; arrow refers to GFP labeling the tracheal system. B, GFP expression pattern in the larval salivary gland. C, GFP expression pattern in the tracheal system. D, GFP labels the fine visceral branches of trachea supplying the gut. E, GFP labels the anterior region of the foregut including the atrium, pharynx and oesophagus. F, magnification of the pharyngeal region; arrow refers to the pharyngeal muscles. G, mid- and hindgut region; long arrow refers to two muscle strips along the hindgut.

In the larval CNS, strong GFP was seen in CNS (Fig. 45). Moderate GFP was seen in mushroom body substructures including: β/β´ lobes, GFP expression pattern in the α/α´ lobes appears as a cap over the lobes and GFP expression appears as a cap over the calyx of mushroom body. Somata and projections could be seen allover the brain hemisphere. Strongly expressing somata could be seen in the thoracicoabdominal ganglia along the midline, they send transverse projections toward the dorsolateral trace and some of their projections come out of the brain to the periphery.

Large and strong *D2R* expressing somata were seen in the dorsoanterior neuropile region and dorsoanterior surface of the brain hemispheres. They send axons toward the interhemispheric junctions. Most of these axons come out of the brain.

Strong GFP expression could be seen in the larval eye anlage, which are stemcell-like progenitors (neuroblasts) of the protocerebrum. They delaminate from the ectoderm and form a proliferating cell layer. The eye anlage remains part of the surface epithelium until later in embryogenesis, giving rise to adult eye and inner and outer optic lobes.

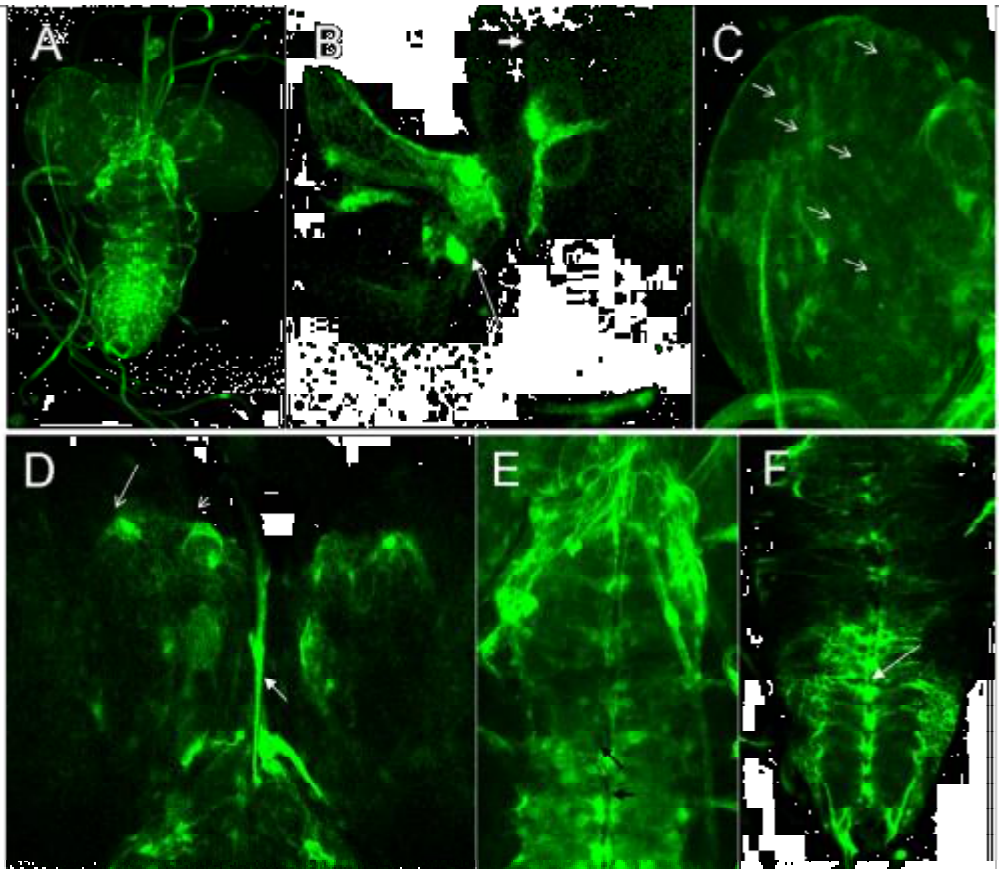

Figure 45: GFP immunoreactivity in the CNS of the *D2R* -GAL4/UAS::GFP larval stage.

A, maximum intensity projection of confocal stacks illustrating the GFP expression pattern in larval CNS. B-F, close ups of different optical sections.B, GFP expression pattern in eye anlage; arrow refers to eye anlage which appear as a stem-like projection of the protocerebrum. C, close up view of one brain hemisphere; arrows refer to somata which are distributed everywhere in all hemisphere regions. D, close up view of the brain hemispheres and interhemispheric junction; short down arrow refers to GFP expression pattern in the α/α´ lobes of mushroom body which appear as a cap over the lobes; long down arrow refers to the GFP expression in the calyx of mushroom body which appear as a cap over the calyx; left arrow refers to the GFP expression along the midline of the interhemispheric junction. E, close up view on the somata and neurons in the thoracic neuromeres; black arrows refer to *D2R* expressed somata. F, close up view on the GFP expression pattern in the thoracicoabdominal ganglia; arrow refers to strong expressed and large in size somata which are located along the midline in each abdominal neuromere. Each somata send a projection ipsilaterally toward the dorsolateral trace.

In adult CNS, Mushroom body substructures could not be distinguished, but some positively stained projections adjacent to the mushroom body could be identified (Fig.47). Some of these projections extend medially toward the fan-shaped body of the central complex which may suggest that these projections serve as neural circuits linking the central complex with the mushroom body to facilitate the flow of informations.

Receptor expressing somata conjugated with the pedunculi of the mushroom body send thick projections that extend toward the anterior superior protocerebrum, passing the antennal lobe.

This projection could not be seen after passing the antennal lobe which may suggest that it connects the mushroom body with the antenna and antennal nerve.

Another structure displaying strong *D2R* expression was the central complex. The central complex located at the interhemispheric junction consists of four interconnected substructures, protocerebral bridge, fan-shaped body, ellipsoid body and pair of noduli. From the central complex very strong expressing neurons extend up along the brain midline, which may be the main central complex out put. Positive expressing projections adjacent to noduli extend laterally in each hemisphere toward the optic lobes and their arborisations extend around the esophagus foramen. *D2R* positive cell clusters were found in the entire lateral protocerebrum, posterior lateral protocerebrum, posterior inferior lateral protocerebrum and ventrolateral protocerebrum forming dense meshwork connecting these regions. Cluster of somata located along the ventral midline of the subesophageal ganglia are also present.

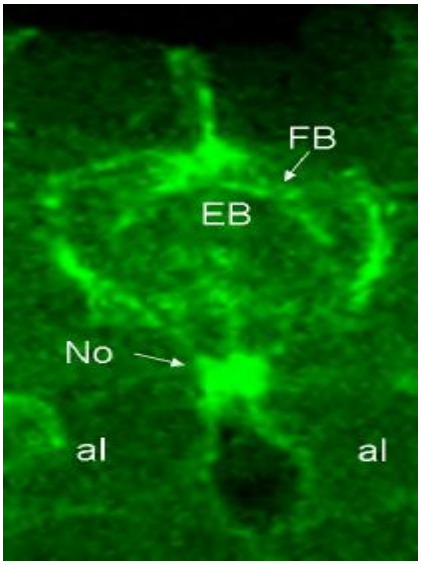

Figure 46: GFP immunoreactivity in the central complex substructures *D2R* - GAL4/UAS::GFP adult brain.
FB, Fan-shaped body. EB, ellipsoid body. No, paired noduli.

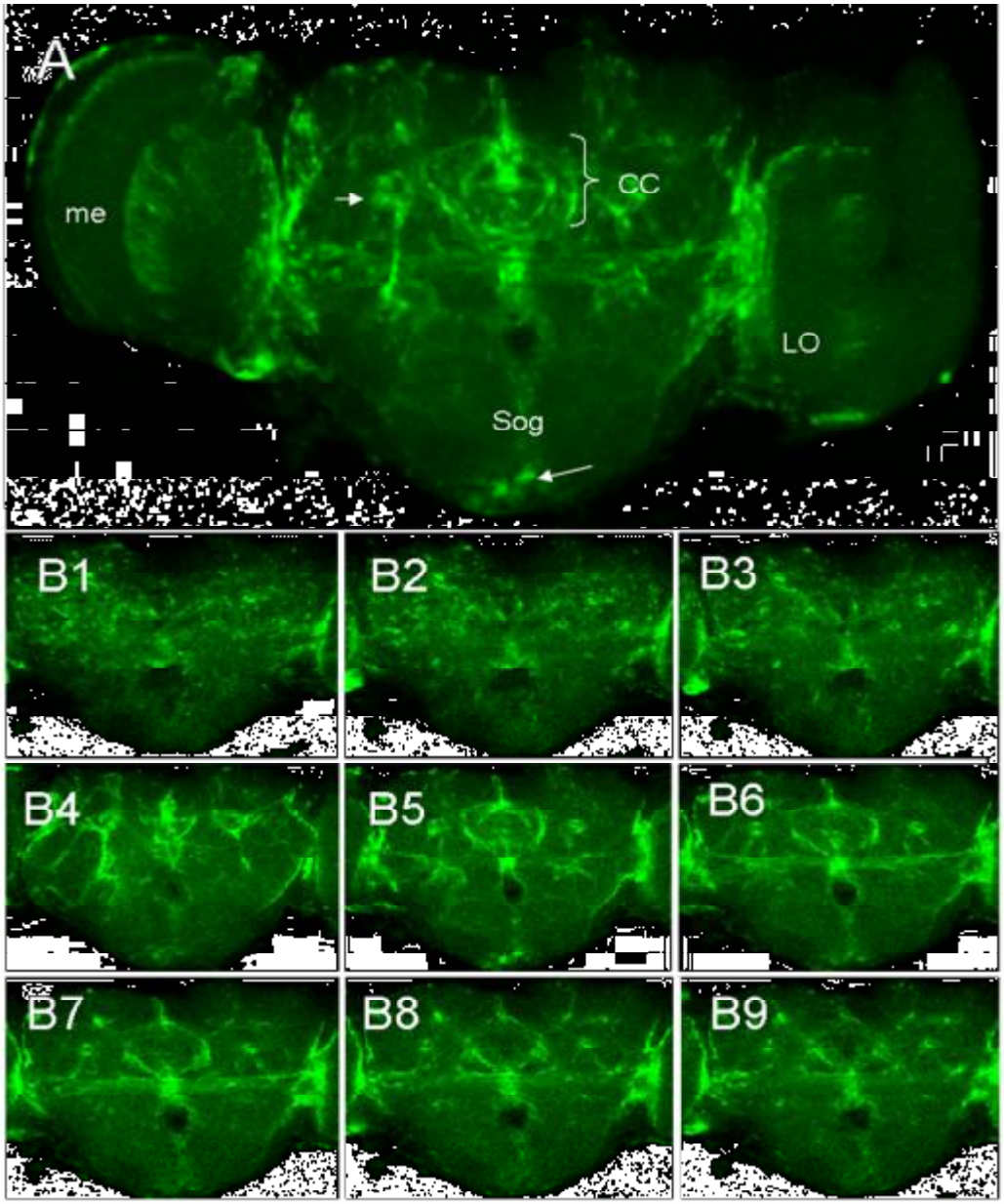

Figure 47: GFP immunoreactivity in the *D2R* -GAL4/UAS::GFP adult brain.
A, Z-projection of confocal stacks (optical sections); CC, central body complex. Me, medulla and Lo, lobula of optic lobe; sog, subesophageal ganglia; short arrow refers to positive expressed somata conjugated with the pedunculi of the mushroom body which project into thick axon extend toward the antennal lobe; long arrow refers to cluster of somata located along the ventral midline of the subesophageal ganglia. B1-B9, optical sections of the central brain.

3.1.3. Tyramine receptors

3.1.3.1 *TyrR* expression analysis

In *Drosophila*, the gene tyramine receptor is referred by the symbol *Dmel\TyrR* CG7485. To amplify the *TyrR* promotor region (~ 4000 bp), corresponding *TyrR* sense and anti-sense oligonucleotides were used. The DNA containing the promotor region was inserted into the

pPTGAL vector as described before, and was used for the production of transgenic lines by germline integration (injection service BestGene Inc.). Studying the expression pattern was performed using the UAS/GAL4 system (Brand and Perrimon, 1993a). The *TyrR*-GAL4 line was crossed to a UAS-GFP responder line, thus allowing visualizing the expression of the *TyrR* gene by GFP expression.

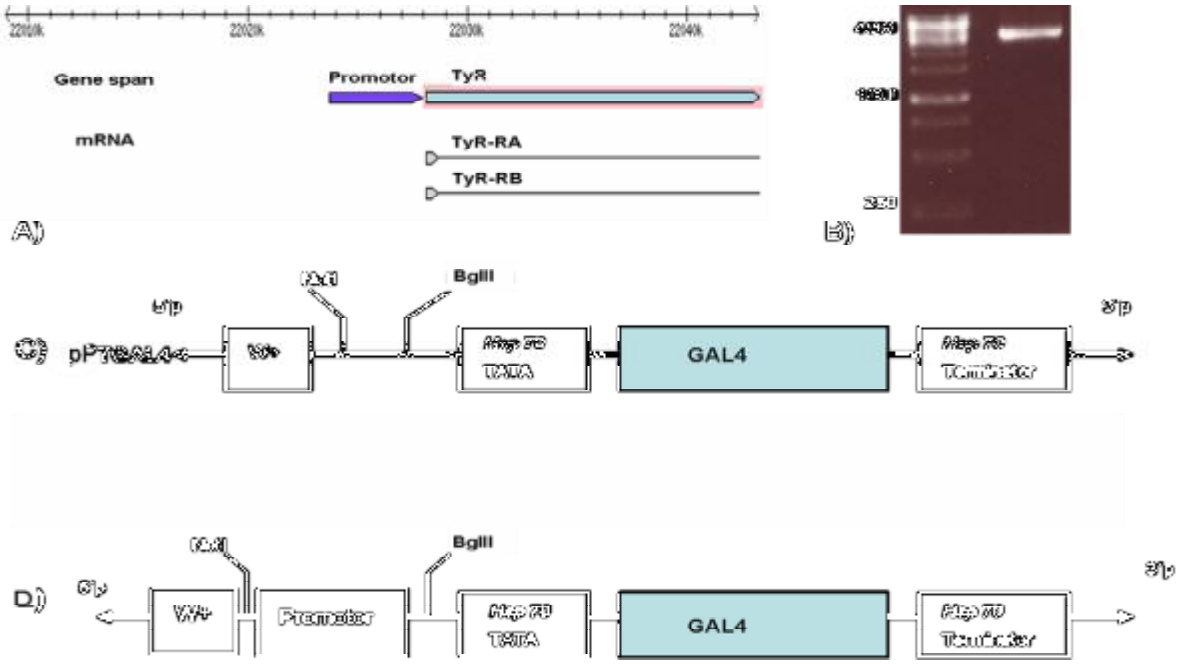

Figure 48: Generation of the *TyrR* promotor containing pPTGAL4 vector
A, schematic drawing illustrating the *TyrR* gene and its products. B, 1% agarose gel showing *TyrR* promotor region amplified with PCR. C, a part of the pPTGAL vector with the GAL4 coding sequence between a minimum promotor (*hsp*70) and termination sequence (*hsp*70 terminator). The pPTGAL vector was prepared for ligation by double digestion with NotI and BgIII. D, schematic drawing of the vector construct. The NotI/BgIII double digested *TyrR* promotor sequence was inserted into the NotI/BgIII double digested pPTGAL vector.

The GAL4 protein under the control of *TyrR*-promotor is expressed in the larval circulatory system (Fig.49A, B1, B2), which appears as a narrow simple blind-ending unbranched tube extending along the dorsal midline of the larval body that divides into anterior aorta and posterior heart. Aorta is lined by inner thin contractile myoepithelial cells (cardiocytes) followed by outer non-contractile pericardial cells. The GFP signal of the outer layers appears to be stronger than that of the inner layer. To identify the cells within the heart that express the *TyrR*, I performed immunohistochemical studies for the heart with two different primary antisera; anti-GFP, anti-bruchpilot nc82 (Fig.50).

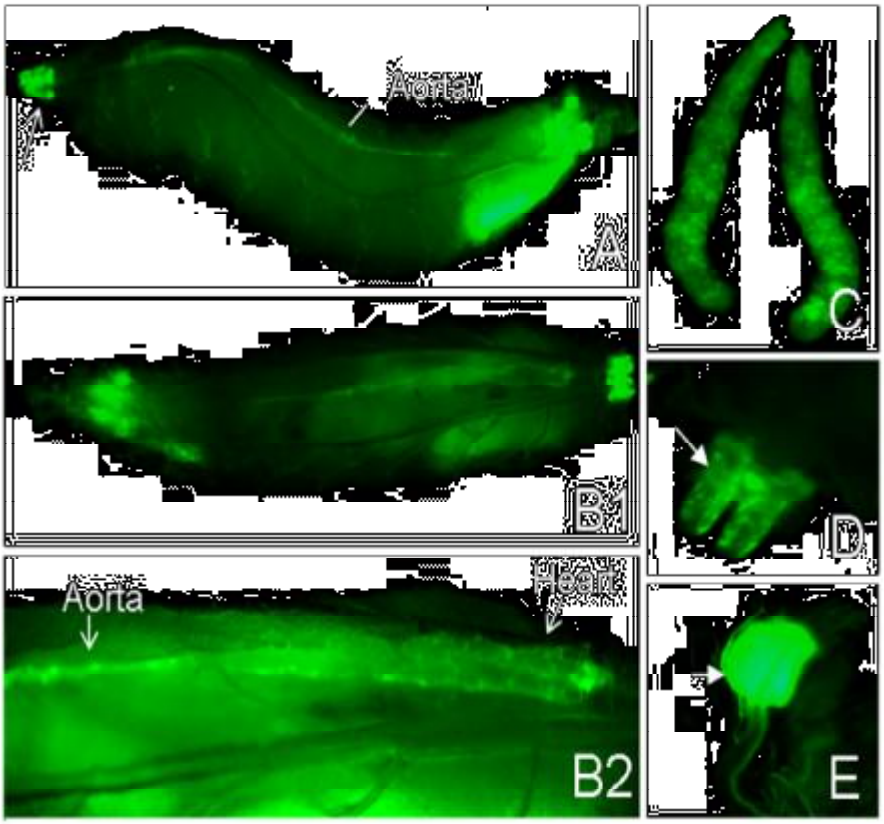

Figure 49: GFP expression pattern in the *TyrR*-GAL4/UAS::GFP in larvae.
A, lateral view of the third larval stage showing the GFP along the dorsal aorta which extend in the whole length of the larval body; arrow refers to the posterior spiracle. B1 and B2, GFP expression pattern in the larval heart. GFP could be also seen in the salivary gland (C), posterior spiracle (D), and enclose the anterior spiracle (E).

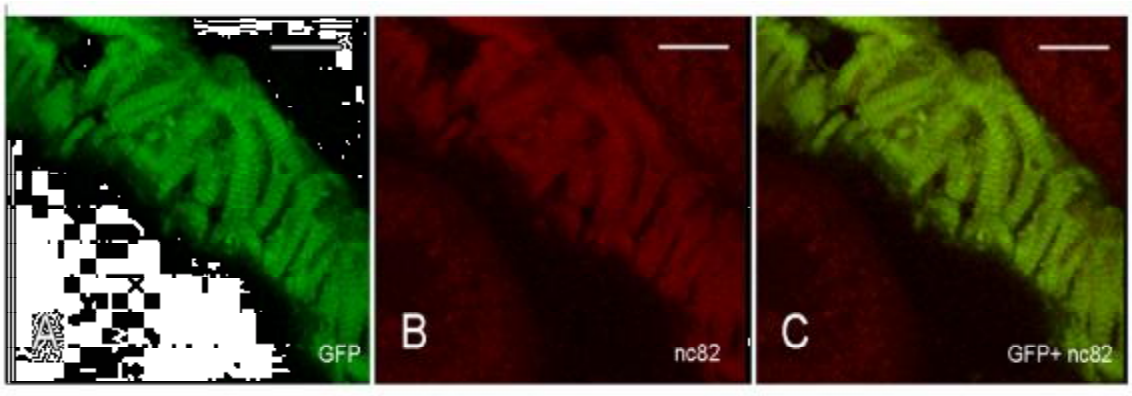

Figure 50: Projection of confocal stacks illustrating the GFP imunoreactivity in the *TyrR*-GAL4/UAS::GFP heart muscles.
The heart muscles were stained immunohisto-chemically with two primary antibodies, anti-GFP panel A and nc82 which is anti-bruchpilot panel B. Panel C, the overlay of both channels.
Scale bar = 10 µm.

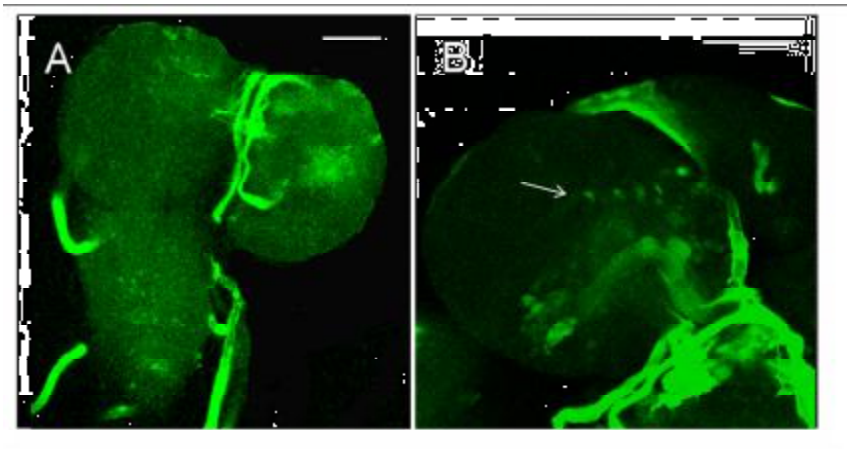

Figure 51: GFP immunoreactivity in the *TyrR*-GAL4/UAS::GFP larval CNS.
A, Very weak expression could be seen in the whole CNS. B, GFP expression pattern in one of the brain hemispheres; weak expression could be seen in the mushroom body sub-structures; arrow refers to few somata clusters appearing in the lateral dorsoposterior and medial dorsoposterior regions of the brain hemisphere. Scale bar = 50µm.

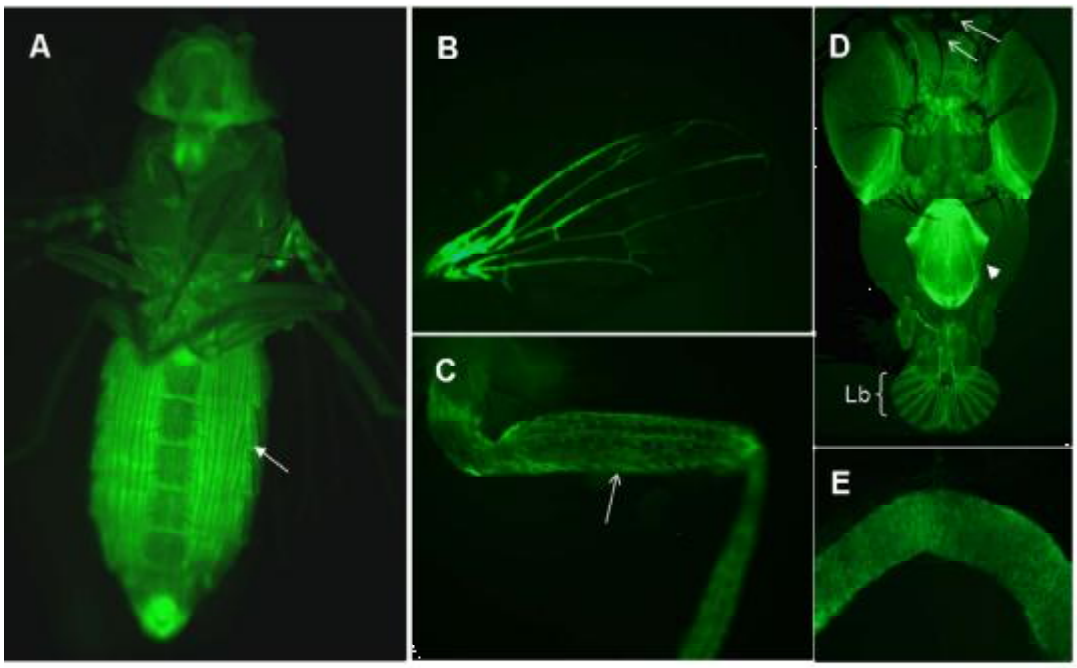

Figure 52: GFP expression pattern in the *TyrR*-GAL4/UAS::GFP adults.
A, adult female; arrow refers to moderately expressed ventral abdominal muscles. B, expression in the wing venations. C, adult Drosophila leg; arrow refers to the GFP in the location of the sensilla. D, whole amount of adult head; long arrows refer to the GFP in the ocelli; head arrow refers to strong GFP in the clypeus; GFP could be visualized in the labellum especially in the psuedotrachea. E, GFP also was seen in the gut cells.

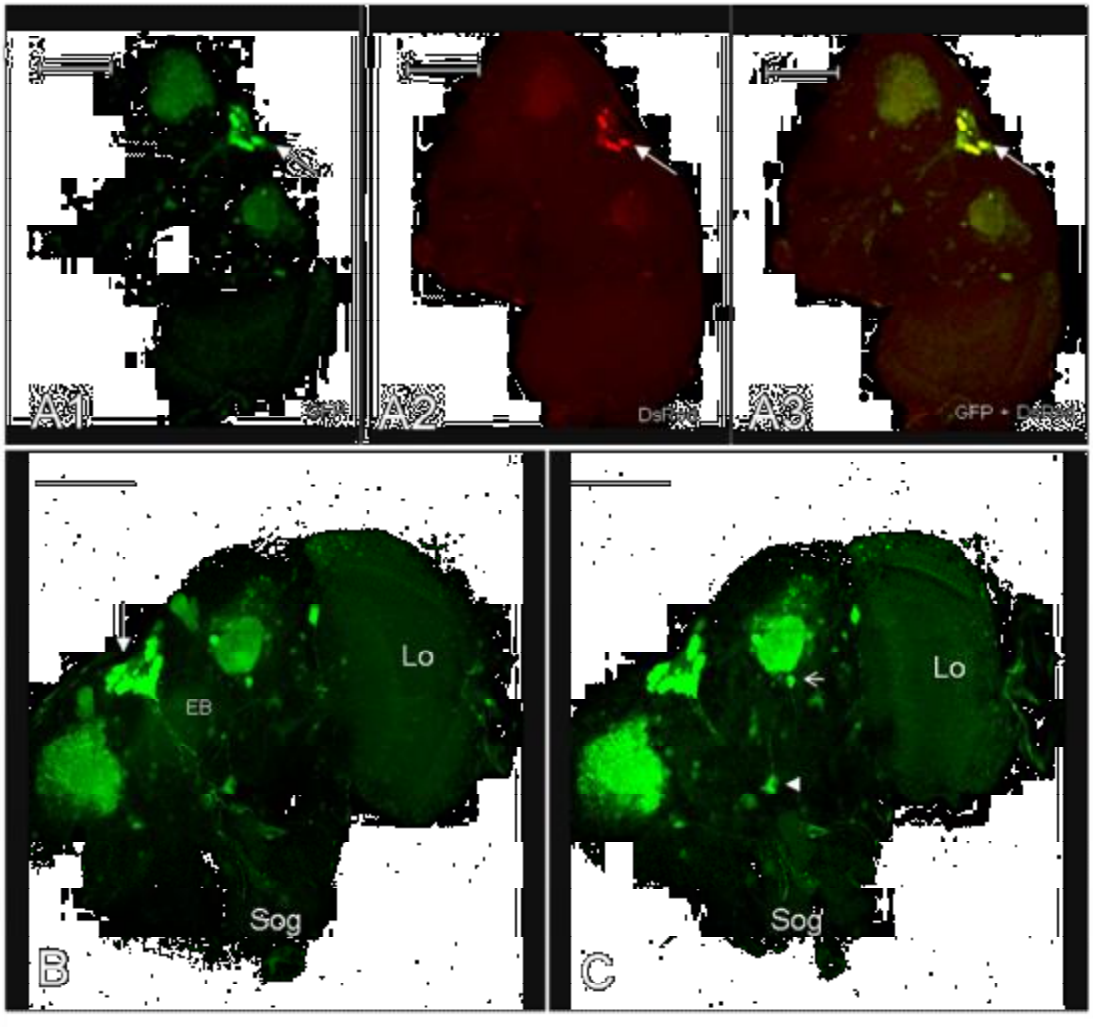

Figure 53: GFP immunoreactivity in the *TyrR*-GAL4/UAS::GFP adult brain.
A1-A3, Expression pattern of *TyrR* in the adult brain. A1, GFP expression pattern; A2, the brain was stained with nc82 antibody and; A3, the overlay of both channels. B and C, GFP expression pattern in adult brain. B, arrow refers to the clusters in pars intercerebralis, which are the insulin producing cells; EB, ellipsoid body; Lo, optic lobe; sog, subesophageal ganglion. C, arrow refers to somata conjugated with the mushroom body; head arrow refers to a pair of somata located on the superior slope of the oesophageal foramen. Scale bar = 100µm.

Very weak expression was seen in the larval CNS (Fig.51). Mushroom body substructures and few somata located in the lateral dorsoposterior and medial dorsoposterior regions of the brain hemisphere.

In adults, GFP is visible in the abdominal muscles (Fig.52A), wing venation (Fig.52B), leg conjugated with sensilla (Fig.52C) and in gut cells (Fig.52E). In the head region strong GFP was also seen in the ocelli and proboscis (Fig.52D) as well as in the labellum and psuedotrachea.

In the adult CNS, strong GFP expression could be seen in a pair of clusters of somata, one each side, located at the Pars intercerebralis (Fig. 53) which are the major insulin producing cells in the fly (Rulifson et al., 2002). Mushroom body sub-structures are strongly labelled with GFP and somata clusters conjugated with mushroom body are also strongly expressed. Moderate expression is seen in the ellipsoid body.

3.1.3.2. *TyrRII* expression analysis

In *Drosophila*, the gene tyramine receptor II is referred by the symbol *Dmel\TyrRII* (CG16766). To amplify the *TyrRII* promotor region (~ 3700 bp), corresponding *TyrRII* sense and anti-sense oligonucleotides were used. The DNA containing the promotor region was inserted into pPTGAL vector as described before, which was used for the production of transgenic lines. Studying the expression pattern was performed using the UAS/GAL4 system (Brand and Perrimon, 1993a). The *TyrRII*-GAL4 line was crossed to a UAS-GFP responder line, thus allowing to visualize the expression of the *TyrRII* gene by GFP expression.

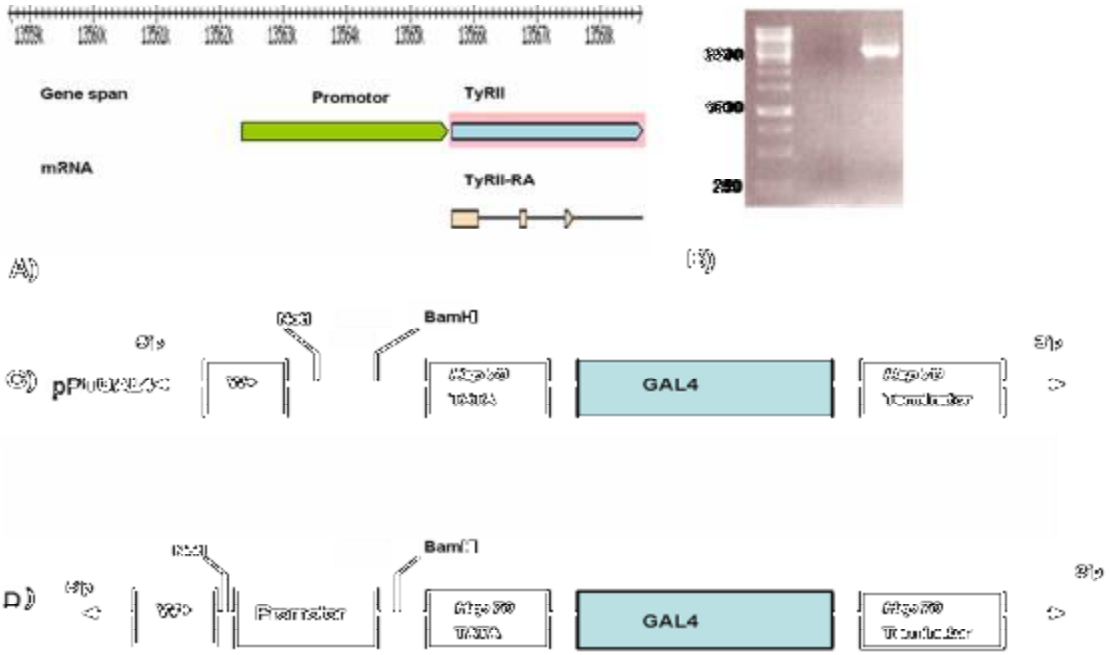

Figure 54: Generating *TyrRII* promotor inserted pPTGAL4 vector.
A, schematic drawing illustrating the *TyrRII* gene model and its products. B, 1% agarose gel showing *TyrRII* promotor region amplifies with PCR. C, a part of the pPTGAL vector with the GAL4 coding sequence between a minimum promotor (*hsp*70) and termination sequence (*hsp*70 terminaltor). The pPTGAL vector was prepared for ligation by double digestion with NotI and BamHI. D, schematic drawing of the vector construct. The NotI/BamHI double digested TyrR promotor sequence was inserted into the NotI/BamHI double digested pPTGAL vector.

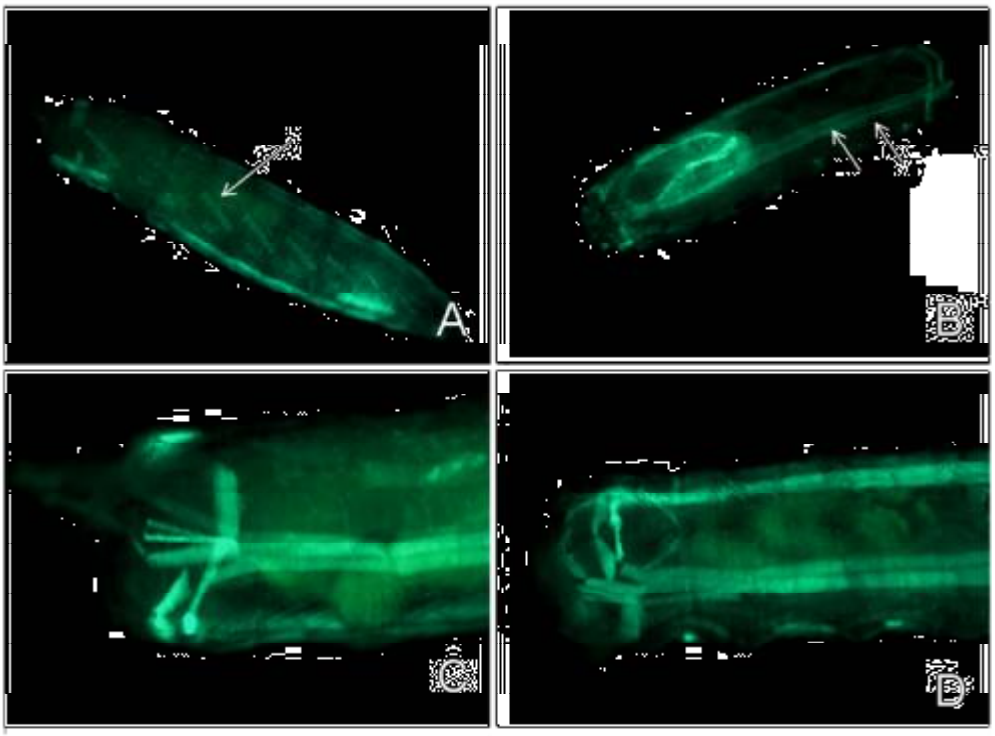

Figure 55: GFP expression pattern in the *TyrRII*-GAL4/UAS::GFP musculature of larvae.

A, lateral view of the whole larva; arrow refers to lateral oblique muscles. B, arrows refer to GFP expression in the ventral longitudinal muscles in each body hemisegments from the head to the tail region. C, close lateral view on the musculature of the tail region, which is associated with the anus and the posterior spiracle. D, close ventral view on the musculature of the tail region.

Larvae show strong *TyrRII* expression in certain muscles (Fig.55), including strong expression in the ventral longitudinal muscles in each body hemisegments from the head to the tail region and also strong expression is seen in the musculature of the tail region which is associated with the anus and the posterior spiracle. Moderate expression could be seen laterally in both sides in lateral longitudinal and lateral oblique muscles compared with ventral longitudinal muscles.

Strong expression is seen in the striated, syncytial gut muscle fibers surrounding the gut epithelium (Fig. 56A,B), including a single layer of circular muscles, which are flat and multinucleate, surrounding the foregut. The visceral musculature of the hindgut, like that one of the esophagus, is circular, with irregular diagonal and longitudinal branches given off by the circular strands which can be assumed to function during defecation as well as for water reabsorbtion. Strong expression is also seen in the tracheal system of larvae (Fig. 56C).

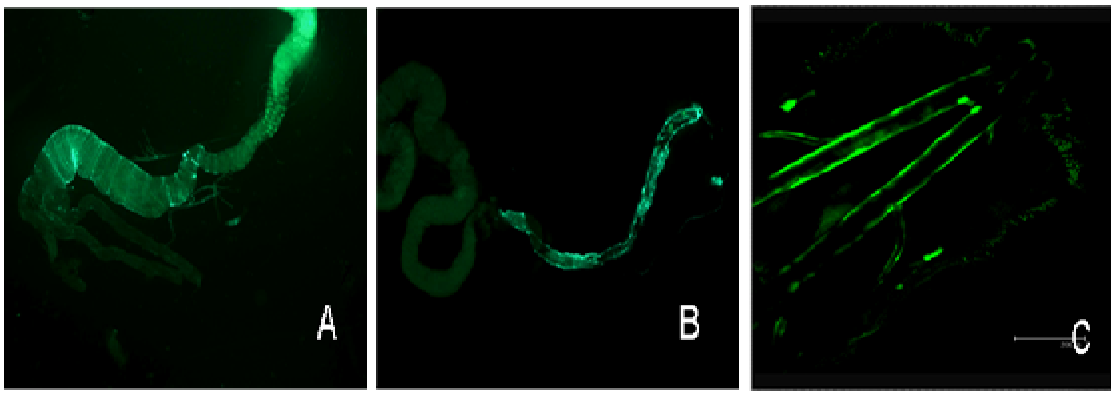

Figure 56: GFP expression pattern in the *TyrRII*-GAL4/UAS::GFP larvae.
A, GFP expression in the flat multinucleated circular muscles surrounded the foregut. B, GFP expression pattern in the musculature of the hindgut. C, GFP expression in the larval tracheal system.

Immunohistochemical analyses revealed that the larval CNS profusely expresses *TyrRII* (Fig. 57). Moderate expression was detected in the cortex of the brain hemispheres and in the mushroom body. Strong expression in somata forming clusters adjacent to the calyx of mushroom body in the dorsomedial anterior and dorsomedial posterior regions of the brain hemisphere. A strong *TyrRII* positive projection with a soma comes out from this cluster in both sides toward the interhemispheric junction. Three ventral unpaired median somata are present in each segment in the subesophageal, thoracic and abdominal neuromeres. In addition to the unpaired median somata, each thoracicoabdominal neuromere had a pair of small dorsal somata located on the dorsolateral trace and a pair of somata located on the dorsolateral trace of each thoracicoabdominal neuromere.

Adults showed strong GFP expression in the male reproductive system (Fig. 58).

Adult CNS shows strong *TyrRII* expression (Fig. 59-61). It is seen in the brain cortex, optic lobes, the protocerebrum, central complex, oesophageal foramen, antennal lobe, mushroom body substructures and subesophageal ganglion. In the central complex the fan-shaped body (FB), the noduli (no) and the ellipsoid body (EB) are strongly innervated. Conspicuously dense ramifications spread in the superior and inferior posterior slope surrounding the esophagus foramen and those ramifications are located directly posterior to the great commissure. Antennal lobe and antennal nerve and outer and inner medulla in the optic lobe also show *TyrRII* expression.

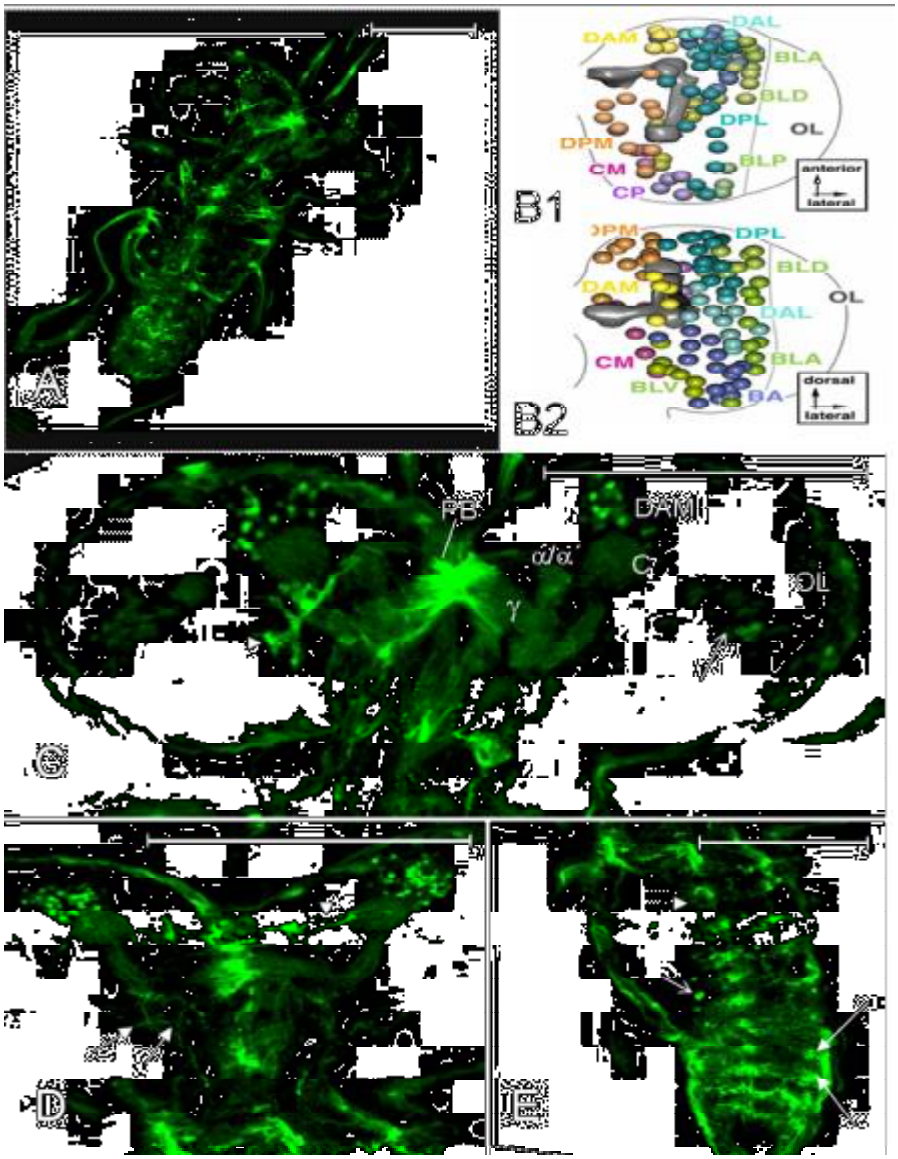

Figure 57: GFP immunoreactivity in the *TyrRII*-GAL4/UAS::GFP larval CNS.
A, projection of confocal stacks illustrating the GFP expression pattern in the whole mount larval CNS. B1 and B2, 3D models of brain hemisphere (B, dorsal view ; C, anterior view) showing hemisphere regions located by colored spheres; the outline of the optic lobe is indicated by gray line; mushroom body indicated by shaded dark gray; (DPM), medial dorsoposterior; (DPL), lateral dorsoposterior;(DAM), medial dorsoposterior; (DAL), lateral dorsoanterior; (DPL), lateral dorsoposterior; (DPM), medial dorsoposterior; (BLA), basolateral anterior;(BLD), basolateral dorsal;(BLP), basolateral posterior; (BLV), basolateral ventral; (CM), centromedial (Pereanu and Hartstein; 2006). C, close view on the brain hemispheres; strong GFP is found in the interhemispheric junction containing the protocerebral bridge (PB); mushroom body has GFP expression in all substructures including γ lobe, α/α´ lobes, calyx (c) and pedunculi. Strong expressed somata forming cluster adjacent to the calyx of mushroom body in the dorsomedial anterior (DAM) and dorsomedial posterior regions of the brain hemisphere. Moderately expressed somata are located in the dorsoanterior region of the brain hemisphere which referred by an arrow and in the optic lobes (Lo). D, close view on the interhemispheric region; Head arrow refers to strong *TyrRII* projection with a soma comes out from the dorsomedial-interiorly located somata cluster in both sides toward the interhemispheric junction; arrows refer to fine neuronal processes adjacent to the mushroom body extended posteriorlly around the midline. E, GFP expression in the thoracico-abdominal ganglia; head arrow refers to the position of unpaired median somata located along the dorsomedial trace of the subesophageal, thoracic and abdominal neuromeres; arrow refers unpaired small median somata located on the centrolateral trace of each thoracicoabdominal neuromere; filled head arrows refer to somata located on the dorsolateral trace of each thoracicoabdominal neuromere. Scale bar = 150µm.

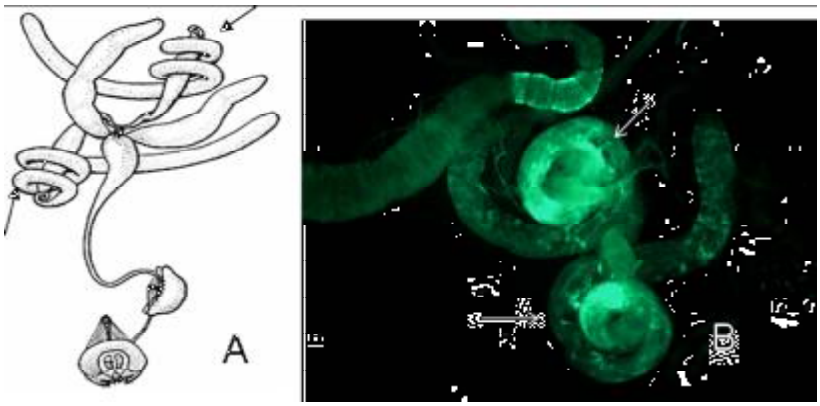

Figure 58: GFP expression pattern in male and female reproductive system of *TyrRII*-GAL4/UAS::GFP adult.
A, schematic drawing showing structure of male reproductive system. B, GFP expression pattern in testes which is referred by arrows (schematic drawing is modified from http://flybase.org).

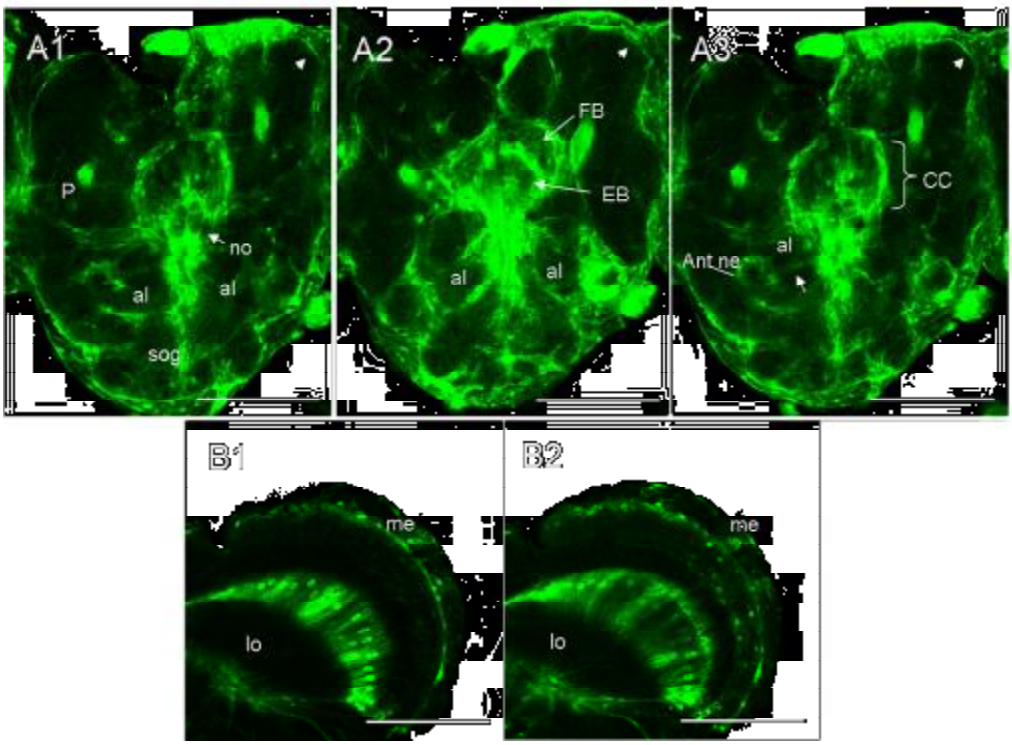

Figure 59: GFP immunoreactivity in the *TyrRII*-GAL4/UAS::GFP adult brain.
A1-A3, single optical sections of the central brain; in the central complex the fan-shaped body (FB), the noduli (no)and the ellipsoid body (EB) are strongly innervated; conspicuously dense ramifications spread in the superior and inferior posterior slope surrounding the esophagus foramen and those ramifications are located directly posterior to great commissures; A1, the subesophageal ganglion (sog) is innervated by *TyrII*, the GFP could be seen along the ventral midline of the sog from which fine neuronal processes extending throughout the sog; strong GFP which was seen in the cortex is referred by head arrow in all optical stacks; p, pedunculi; A3, antennal lobe (al) is innervated, a fine commissure arising from the oesophageal foramen is directing into the antennal lobe is referred by arrow; strong GFP could also be seen in the antennal nerve(Ant ne); cc, the central body complex; B1 and B2, single optical sections of the optic lobe; the outer and inner medulla (me) in the optic lobe are innervated while the lobula (lo) of the optic lobe is not innervated by the GAL4-expressing cells. Scale bar = 150µm.

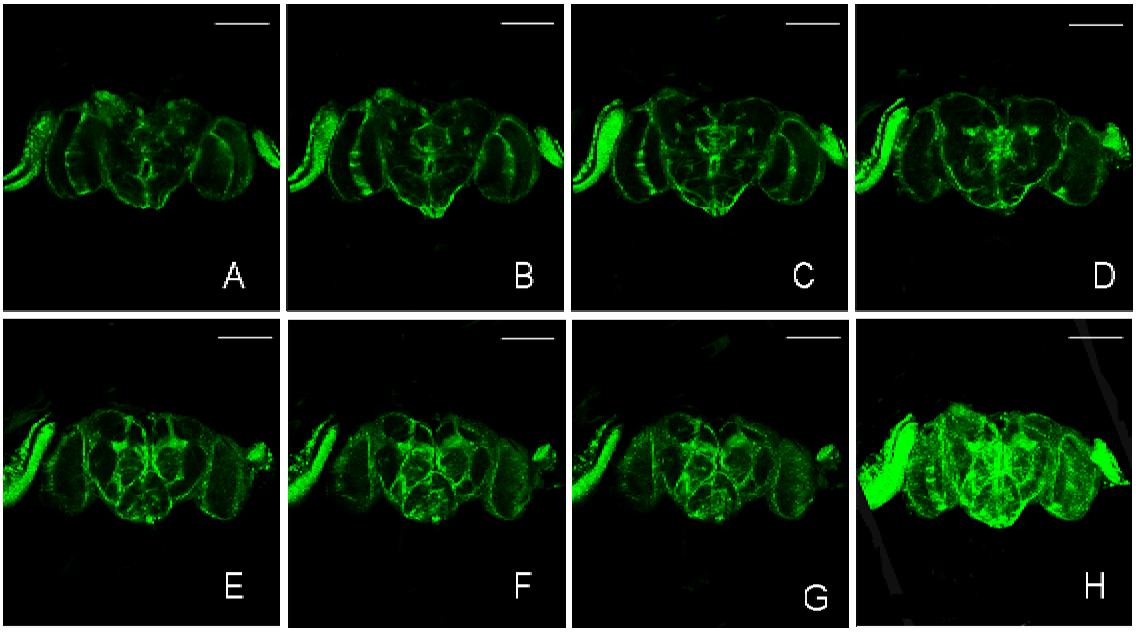

Figure 60: GFP immunoreactivity in the *TyrRII*-GAL4/UAS::GFP adult brain shown in confocal stacks.
Focusing on these stacks reveal that the *TyrRII* expression appear in optic lobes, protocerebrum, central complex , oesophageal foramen, antennal lobe, mushroom body substructures and subesophageal ganglion which could be more obviously detected from the Z-projection of those confocal stacks, H, in which the GFP expression appear allover the brain. Scale bar 150 µm.

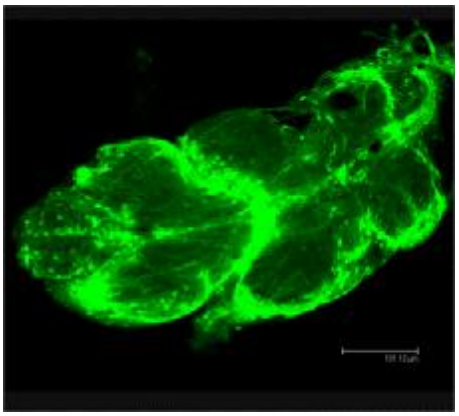

Figure 61: GFP immunoreactivity in thoracico-abdominal ganglion of *TyrRII*-GAL4/UAS::GFP adult stage shown by a projection of confocal stacks.
Scale bar = 100µm

3.1.3.3. *TyrRIII* expression analysis

In *Drosophila*, this gene is referred by the symbol *Dmel\CG7431*. To amplify the *TyrRIII* promotor region (~3200bp) corresponding *TyrRIII* sense and anti-sense oligo-nucleotides were used. The DNA containing the promotor region was inserted into the pPTGAL vector as described before.

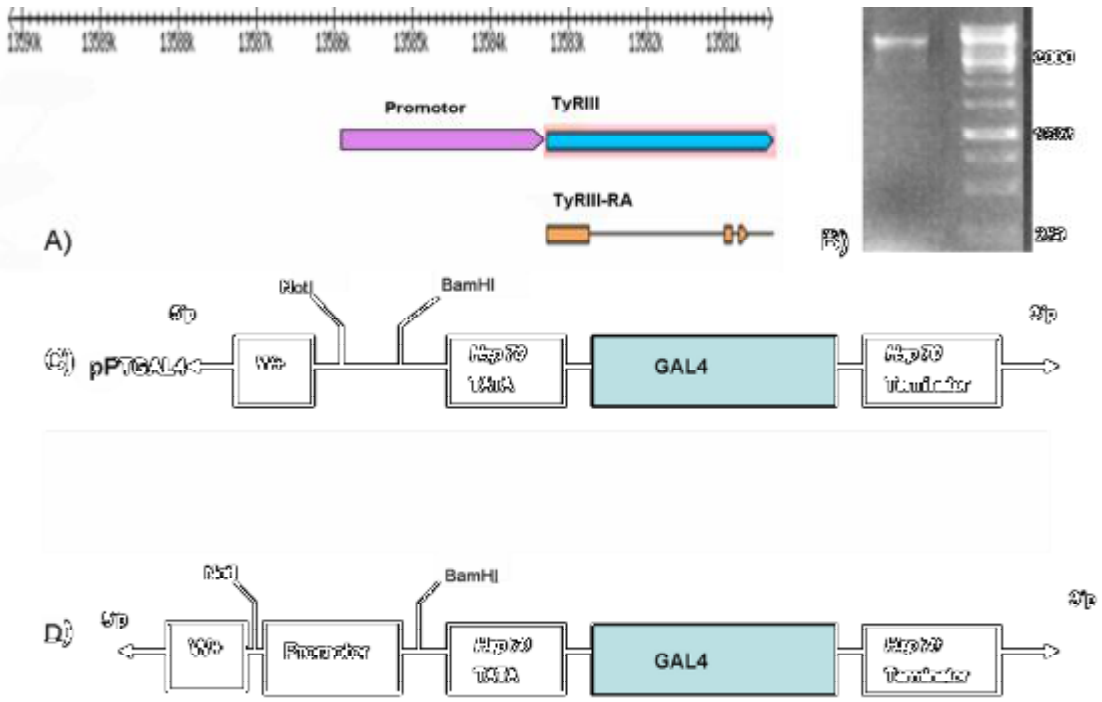

Figure 62: Generating *TyrRIII* promotor inserted pPTGAL4 vector.
A, schematic drawing illustrating the *TyrRIII* gene model and its products. B, 1% agarose gel showing *TyrRIII* promotor region amplifies with PCR. C, a part of the pPTGAL vector with the GAL4 coding sequence between a minimum promotor (hsp70) and termination sequence (hsp70 terminaltor). The pPTGAL vector was prepared for ligation by double digestion with NotI and BamHI. D, schematic drawing of the vector construct. The NotI/BamHI double digested *TyrRIII* promotor sequence was inserted into the NotI/BamHI double digested pPTGAL vector.

Larvae show strong *TyrRIII* expression in oenocytes (Fig. 63). They are large cells attached to the basal surface of the lateral epidermis. They are arranged in clusters of ~6 cells per abdominal hemi-segment. Using Nile Red (Nile blue oxazone) staining, which stains intracellular lipids, oenocytes were found to contain lipid droplets. Regions of the gut, including the proventriculus and anterior gut, malpighian tubules and salivary glands also display strong GFP expression (Fig.64).

In the larval CNS, the whole neuropile strongly expresses GFP (Fig.65), mainly in the mushroom bodies. Strongly expressed arborizations are visualized around the esophagus. Strong GFP expression could also be seen in the thoracico-abdominal ganglion. Three pairs of somata, one pair in each thoracic neuromere, reside ventro-medially in the cortex beneath the centro-intermediate trace. Each soma sends a neuron toward the dorsolateral trace. GFP-positive somata are located on the dorsolateral traces in the thoracic and abdominal neuromere.

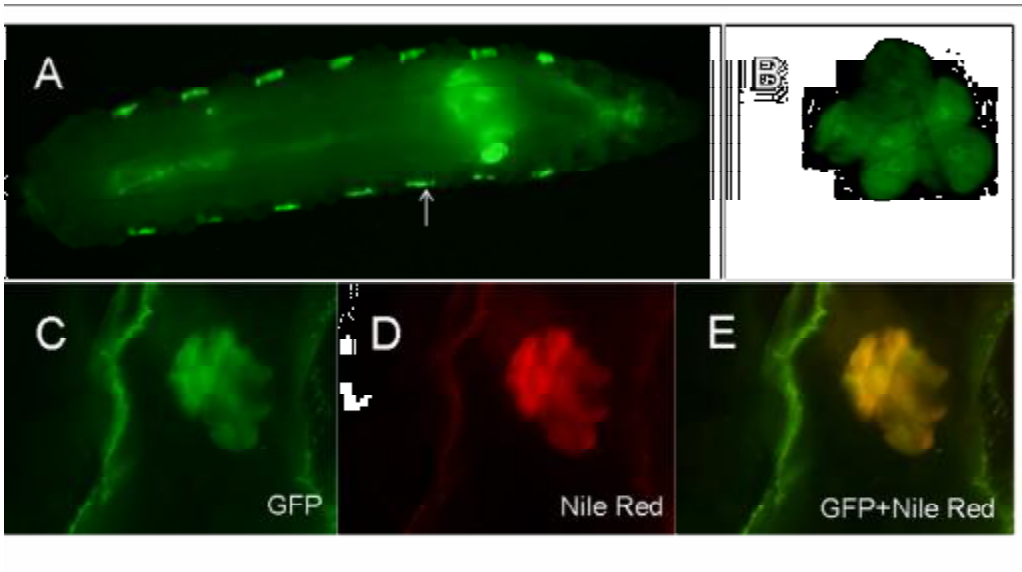

Figure 63: Oenocytes expressing GFP in the *TyrRIII*-GAL4/UAS::GFP larvae.
A, GFP expression in the whole mount 3-rd larval stage; arrow refers to the oenocytes attached to the basal surface of the lateral epidermis each hemisegment. B, optical image using confocal microscope for a oenocytes cluster which consists of about 6 nucleated cells. C-E, oenocytes cluster with GFP expression (C), positively stained with Nile red which stain its intracellular lipid and overlaying of both photos (E).

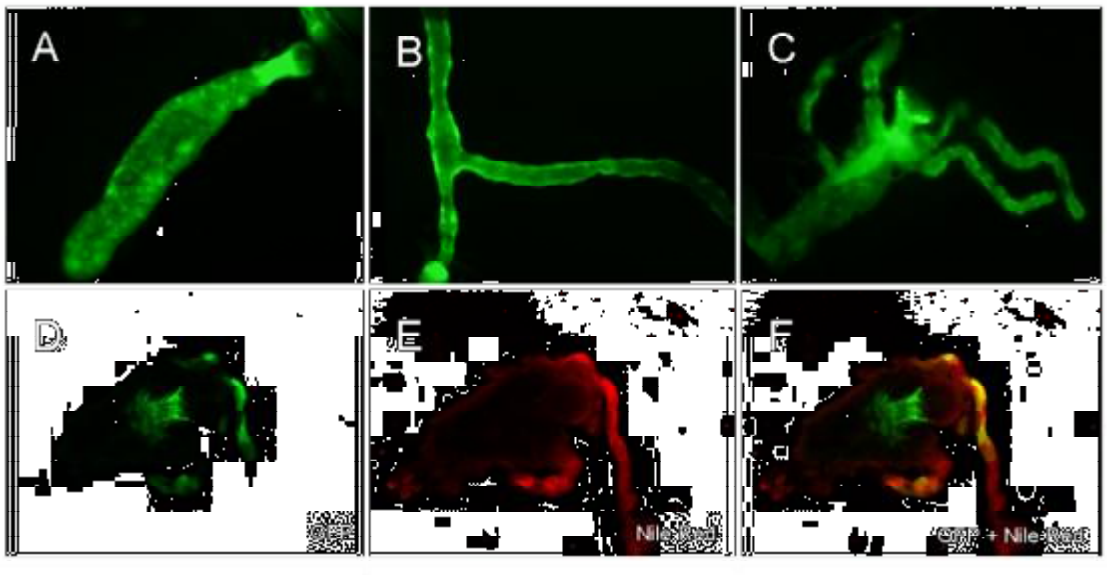

Figure 64: GFP expression pattern in *TyrRIII*-GAL4/UAS::GFP larvae.
GFP could be seen in salivary gland (A), in the malpighian tubule (B), in the foregut especially the proventriculus. D-F, *TyrRIII* expression in the proventriculus; D, GFP expression pattern; E, proventriculus positively with Nile red staining; and F, overlay of GFP and nile red channels.

Adults also show expression in oenocytes (Fig.66)**.** The oenocytes are uninucleated and have dense cytoplasm with accumulative lipid granules. GFP was also observed in the adult salivary glands (Fig.67A) and legs, especially in the articulation areas (Fig. 67B).

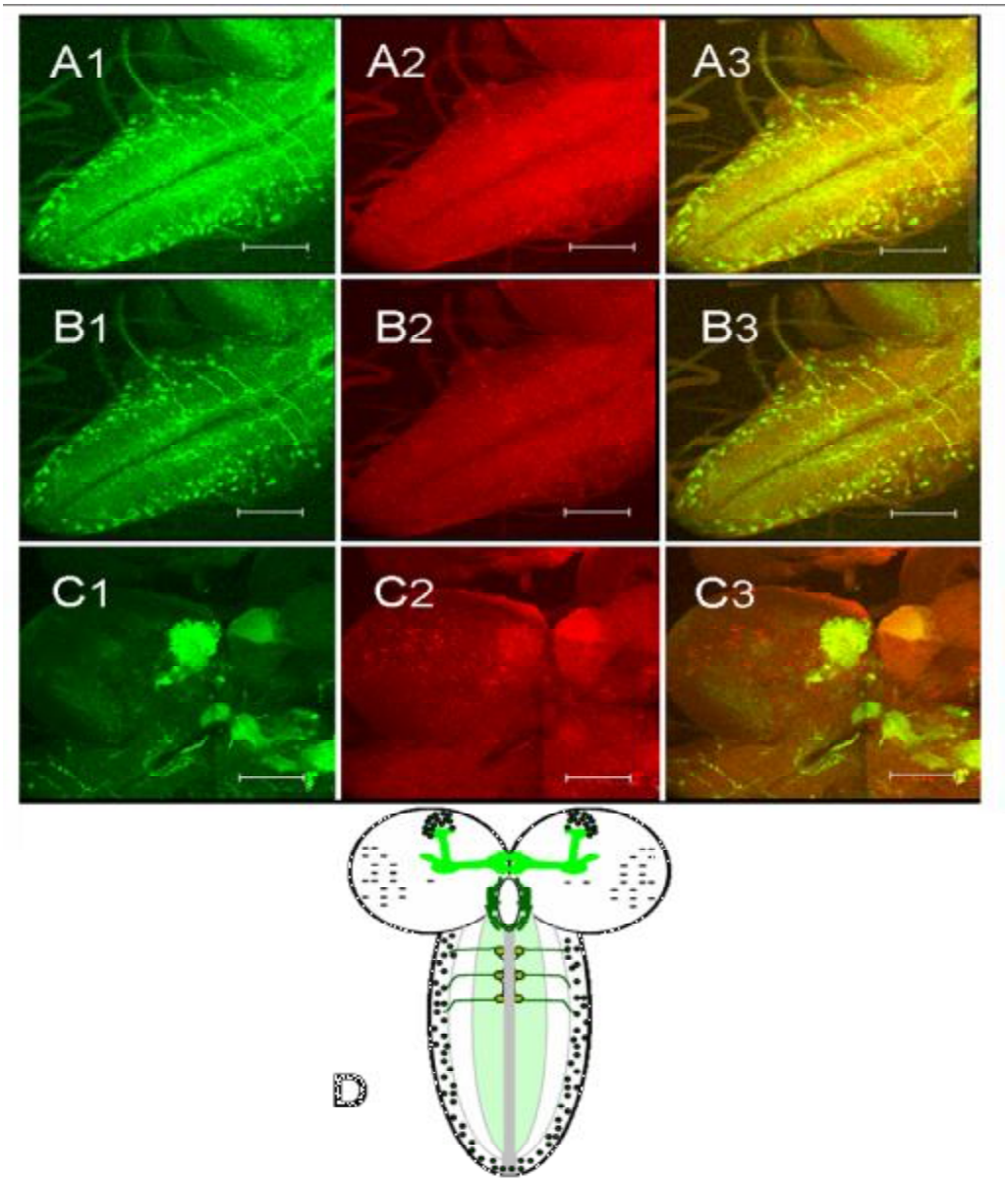

Figure 65: GFP immunoreactivity in the *TyrRIII*-GAL4/UAS::GFP larval CNS.
A1-B3, projection of confocal stacks illustrating the GFP expression pattern in the CNS with maximum intensity (A1-A3) and average intensity (B1-B3). C1-C3, projection of confocal stacks showing the GFP expression pattern in the brain hemisphere. A1 and B1, GFP expression pattern; A2 and B2, dsRed photos as synaptic neuropile were stained by nc82 anti-bruchpilot; A3 and B3, overlay of GFP and dsRed photos; in panels A1 to C3 the larval CNS was tilted about 45° to the right to better visualize the bottom and the upper regions of the CNS. D, schematic drawing of the TyrRIII expression in the larval CNS. Scale bar = 50 µm.

Moderate expression was seen in the adult brain (Fig.68). Mushroom body sub-structures are labelled. Moderately expressed somata were seen in the lateral horn, posterior superior- and posterior medial protocerebrum and in the suboesophageal ganglion. Strong expressed somata are located ventromedially in the antennal lobes. Antennal lobes are moderately innervated by *TyrRIII* positive neurons

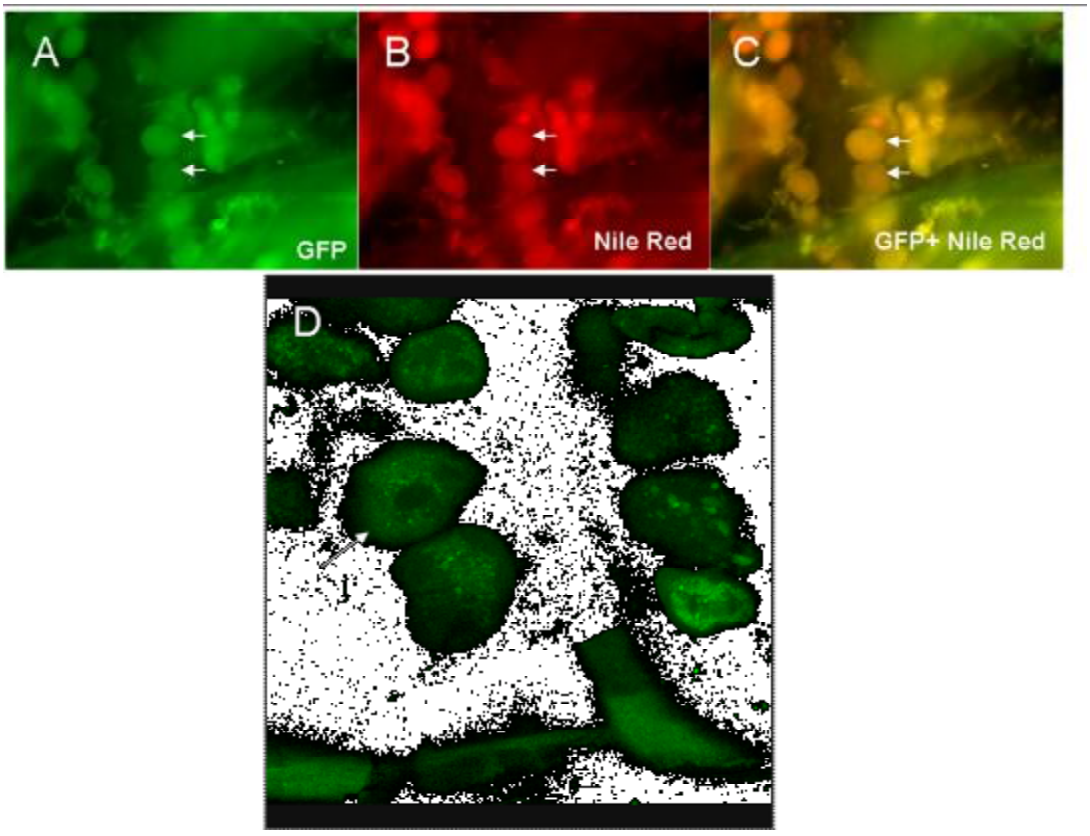

Figure 66: GFP expression pattern in the *TyrRIII*-GAL4/UAS::GFP adult oenocytes
A, GFP expression in the oenocytes which appear as bands of cells near the sternites. B, oenocytes positively stained with Nile red which stain its intracellular lipid. C, overlay of GFP and DsRed photos. D, optical image using confocal microscope illustrating the adult oenocytes. Arrows in panels A-D are referring to the position of the oenocytes.

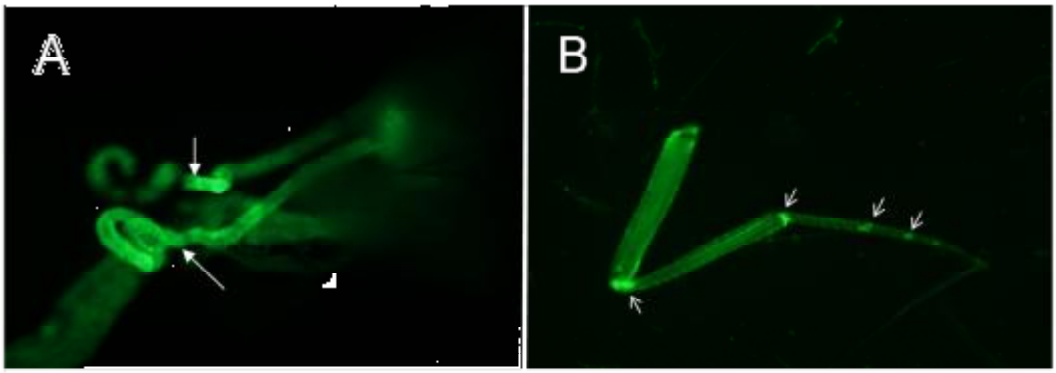

Figure 67: GFP expression pattern in *TyrRIII*-GAL4/UAS::GFP adults.
A, GFP in adult salivary gland. B, adult leg; arrows referring to the GFP in the articulation areas.

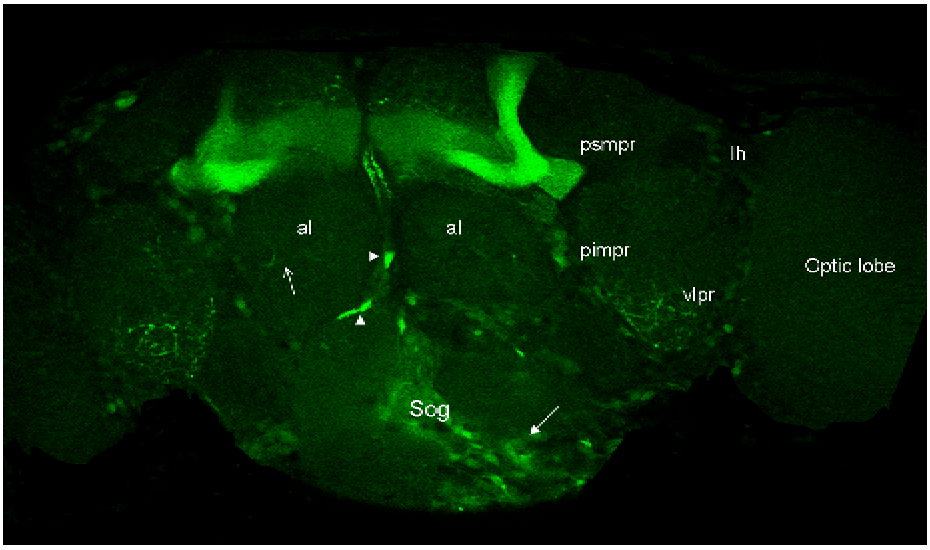

Figure 68: GAL4 immunoreactivity in the Tyr*RIII*-GAL4/UAS::GFP adult CNS.
psmpr, posterior superior protocerebrum; lh, lateral horn; plmpr, posterior lateral protocerebrum; al, antennal lobe; vlpr, ventrolateral protocerebrum; sog, subesophageal ganglion; arrow refers to a neuron innervate the antennal lobe; head arrows refer to somata located ventromedially in the antennal lobes.

3.2. RNAi –based experiments

To evaluate the function of the receptor *Dmel\octß2R* (CG33976), GAL4-UAS binary system was used. By which it is possible to interfere with the gene function practically anywhere and anytime during development. The line *Octß2R*-RNAi-UAS (vdrc stock centre Vienna, Australia) in which the insertion location was on the second chromosome was crossed to (yw; P{tub-GAL4;TM3, sb}) driver line and the line RNAi-Nos-RD was used as control for this experiment. Ten males and five females were used for crossing. The flies were allowed to remain in the same food vial two days. First, the number of eggs was counted every two days and vials were inspected daily and the relevant event and date on which they occur was noted as, the beginning of 1st larval instar, 3rd larval instar wandering, prepupation formation, pupation, eclosion and pupal lethality. Ten males and ten females from the first generation were allowed to cross in new food vial and the number of laid eggs was counted every day. From the previous data, the percentage of hatchability and fecundity were determined. Next, the morphology and locomotor activity of the first generation was examined.

No phenotypic or developmental abnormality could be detected in the first generation. The number of laid eggs in 10 days , number of hatched adults, males and females, the percentage of hatchability and the percentage of first generation fecundity were showed in table(1).

The first line had mean number of laid eggs (238) more than line 2 (125) and the control (200). Line1 had mean number of hatched adult (210) including males (95 ~45.2%) and females (115~ 54%) more than line 2 which had (71) hatched adults, including males (35~

49.2%) and females (36 ~ 50.8 %) and the control which had (158) hatched adults, including (52 ~26 %) males and (106 ~ 54 %) females. Percentage of hatchability was calculated; for line1 (88.2 %); for line2 (56.8 %); and for the control (79 %) and like the other parameters it was lower in line2 than line1. Percentage of fecundity was very low in both line1 and line2; but it was lower in line1 (10.42 %) than line2 (11.1 %) and the control (10.9 %). By following these eggs, no development and hatchability was occurred. As shown in Figure (69), the 10-days old eggs have abnormal egg shell.

Table 1: The main parameters measured for *Octß2R*-dsRNAi×UAS/GAL4-tubp line 1 and 2 compared with NOS-RD as control
including mean number of eggs laid by 10 females in 10 days, mean number of hatched adults, males and females, percentage of hatchability and fecundity.

Parameter	dsRNA Dm*Octß2R* line 1	dsRNA Dm*Octß2R* line 2	RNAi- Nos-rd
Mean no. of laid eggs in 10 days.	238	125	200
Mean no. of hatched adults.	210	71	158
No. of hatched males	95 (45.2 %)	35 (49.2 %)	52 (26 %)
No. of hatched females	115 (54 %)	36 (50.8 %)	106 (54 %)
Percentage of hatchability	88.2 %	56.8 %	79 %
Percentage of fecundity of the 1st generation	10.42 %	11.1 %	10.9 %

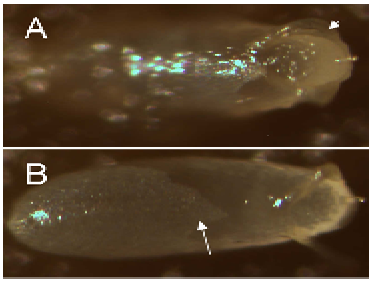

Figure 69: Pattern of eggs laid by the 1st generation *Octß2R*-dsRNAi×UAS/GAL4-tubp.
Arrow sin A and B refers to the abnormal pattern of the egg shell.

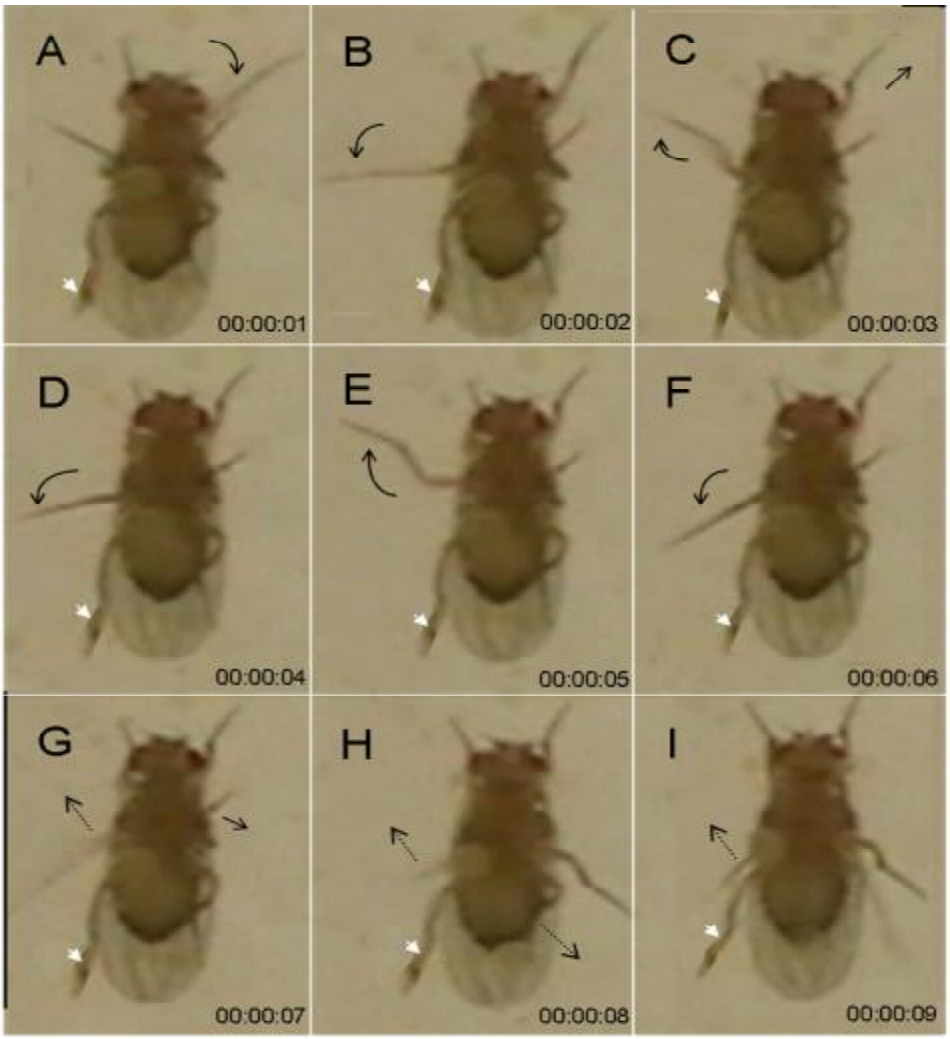

Figure 70: Nine frames of Frame /second snapshots converted video showing the attempt of female *Octß2R*-dsRNAi×UAS/GAL4-tubp.

Adult try to use the left foreleg and followed by many failed attempts to use the right middle leg, in which the insect move the right middle leg back and forth followed by strongly upward movement ; arrows refer to leg movement direction; dashed lines refer to upward directed leg movement.

As showed in Figure (70), adult *Drosophila* try to go up within the new transparent food vial. Adult stage was suffering during movement. To demonstrate this, the locomotor activity of adult flies in a normal food vials was video- taped from the front view; in which Drosophila flies (males, females and virgin females) walked freely in new food vial. All videos were captured at 24°C and Aimer software was used to generate one - second frames. These frames were used to evaluate the adult movement and to determine the movement speed and angle. Adults try to use the left foreleg and followed by many attempts to use the right middle leg, in which the insect move the right middle leg about five times forward-backward and then upward (Fig.70;G-I). This followed by attempts with the left middle leg. However, the adult

remain in the position and there is no change in the direction of the longitudinal body axis. Using ImageJ frame-by-frame analysis, the footprint could be made (Fig.71) which indicated that the adult *Octß2R*.dsRNAi-UAS/GAL4-tubp tried to use the middle leg by back and forth movements followed by the hindleg and also the asymmetrical resting positions of both fore- and middle leg. The movement after 47 sec was with distance ~ 0.7 mm and angle ~ 21.24° to the right direction.

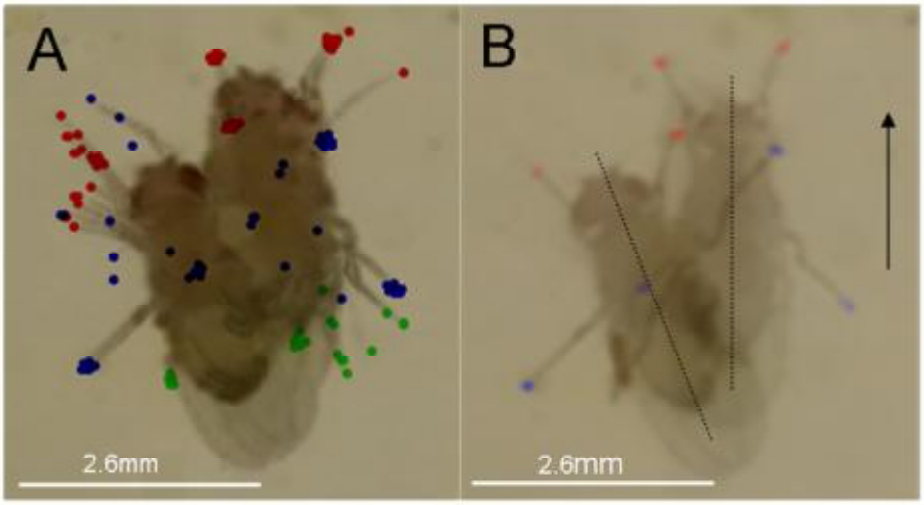

Figure 71: pattern of footprint from a fly obtained by frame by frame analysis for 47 frames (converted from video using Aimer software with frame/sec snapshots) using ImageJ software.
A, maximum projection of stacks image illustrating the footprint indicate the asymmetrical resting positions of legs; the footprint of the forelegs was shown in red colour, of the middle leg in blue colour and of the hind leg in green colour. B, minimum projection of stacks image illustrating footprint; the black dashed line indicate the longitudinal body axis; the black arrow indicate the direction of movement. Scale bar = 2.6mm.

The trails of courtship were video taped and Aimer software was used to convert each video into one/second frames. From these videos it could be seen that there is a strong relationship between the locomotor activity and the courtship (fig.72). First, males tried to tap females with their forelegs. Followed by the love-song (wing vibrations with certain intervals). Next, females slowed down their movement, they remained almost in the same position. Males tried to lick females' genitalia. Female were then run away from males. But males were not able to keep up with their females and then males lose the ability to adjust their position to females (male tried to move the middle leg back and forth many times and keep the forelegs fest to adjust his position and movement toward his female) this led to the incomplete courtship.

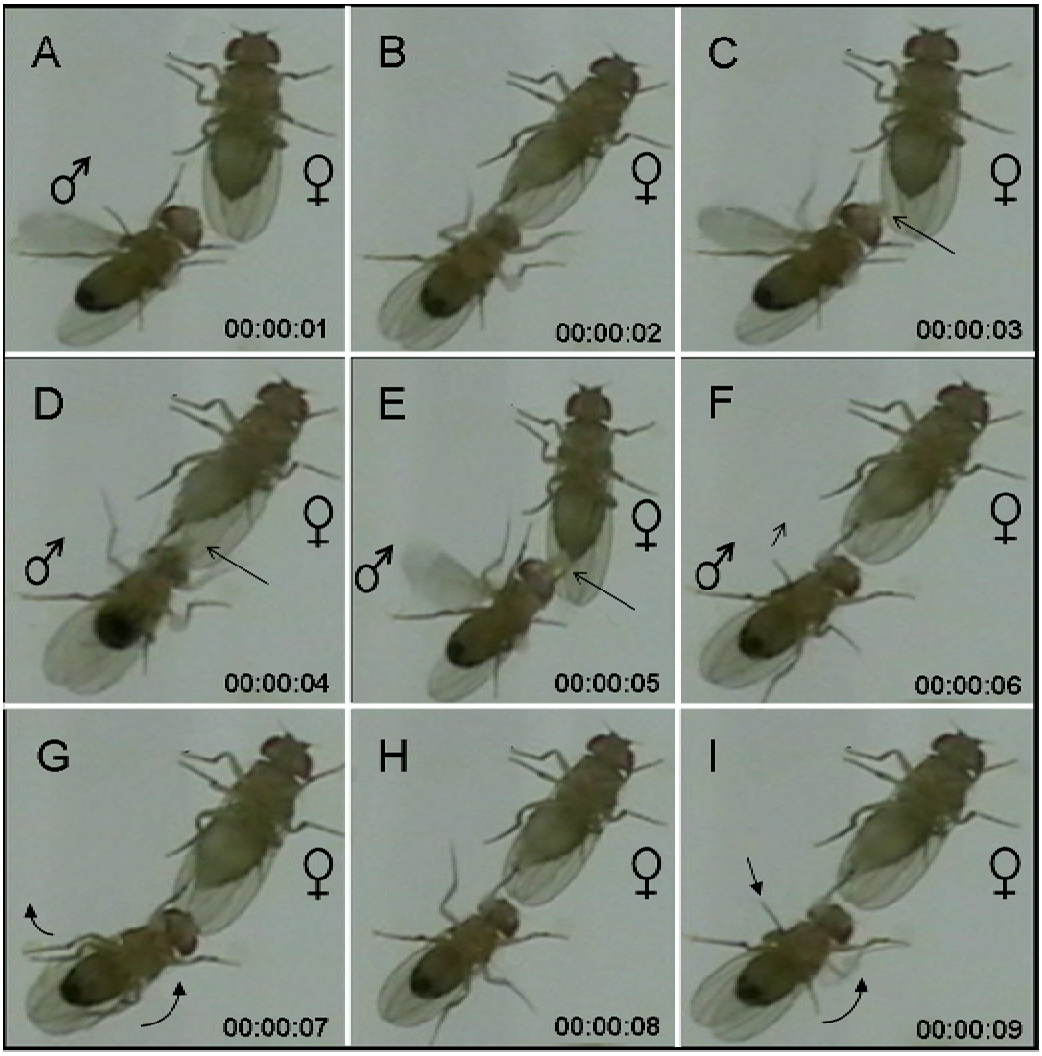

Figure 72: Failure of the first genetration *Octß2R*-dsRNAi×UAS/GAL4-tubp courtship.
A-I, nine snapshots taken snapshot/second using Aimer software. A, male begin love song by vibrating his right wing with certain intervals. B, male tried to tap female with his foreleg to recognize her. C-E, male continued with his love song and tried to lick female genitalia; long arrow refers to the male proboscis. F, female begin run away from male which normally occur in the *Drosophila melanogaster* courtship ; short arrow refers to the trail of male to adjust his position to female but the leg muscles are not strong enough to manage the courtship situation. G-I, male move his middle legs back and forth in a repetitive failed attempts to adjust his body to females but he could not.

3.3. Pharmacological characterization of octopamine receptors using human embryonic kidney cells (HEK 293 cells).

The *Lymnaea stagnalis* OAR was supplied by colleagues (Hiripi *et al.*, 1998). Regarding to *Ocß2R* and *Ocß3R*, the corresponding cDNA was isolated by reverse transcription PCR, which was done using the total RNA. The cDNA was used as template for subsequent PCR reactions using specific sense and anti-sense primers to amplify the full-length gene coding sequence. The full-length coding region of the gene was inserted into the mammalian

expression vector pEAK10CV. Thereafter, transiently transfected HEK-293 cell lines were established to express the *Octß2R* or *Octß3R* genes. HEK 293 cells were cotransfected with the octopamine receptor-coding plasmid pEAK 10CV and the reporter-coding plasmid pCRE-SEAP.

3.3.1. Pharmacology of *Lymnaea OA* receptor

Agonists and antagonists were applied at concentrations ranging from 10^{-3} to 10^{-9} M, resulting in cAMP-inducible, high level SEAP expression. About 12-24h after applying drugs, SEAP was quantified based on the hydrolysis of pNitrophenyl phosphate producing a yellow end product, which was measured spectrophotometrically at 405 nm.

Non-linear regression analysis of the data revealed a sigmosoidal increase in SEAP end product with increasing agonist concentration, which resembles the increase in intracellular cAMP levels. Octopaminergic agonists such as NC5, NC7, demethylchlordimeform and synephrine were able to induce SEAP expression in a dose-dependent manner. NC5 and NC7 have higher affinities than synephrine, which in turn has a higher affinity than demethylchlordimeform (Fig 73,B). The corresponding EC50 values are NC5 4.84×10^{-7} M, NC7 1.52×10^{-7} M, synephrine 4.88×10^{-7} M and demethylchlordimeform 2.74×10^{-7} M. Octopamine has a higher affinity than dopamine, tyramine and serotonin (Fig ,73A). In addition to the effects of octopaminergic agonists on the induction of SEAP expression, I studied the effects of increasing concentrations of octopamine antagonists on the SEAP expression of transfected HEK293 cells challenged with a fixed concentration of octopamine (0.1M) while the concentration of antagonists varied. Seven octopaminergic antagonists: epinastine, phentolamine, chlorpromazine, metoclopramide, yohimbine, rauwolscine, and mianserin were tested, all of them are able to reduce the SEAP expression in a dose-dependent manner. Yohimbine has the highest affinity followed by metoclopramide > phentolamine > rauwolscine > chlorpromazine > mianserin > epinastine.

The EC50 values for biogenic amines and other ligands including octopaminergic agonists and antagonists are summarized in table (2). In general DL-synpherine, NC5, NC6, NC7 and the antagonist Metoclopramide have higher affinity to *Lymnaea* OA receptor than other ligands.

A

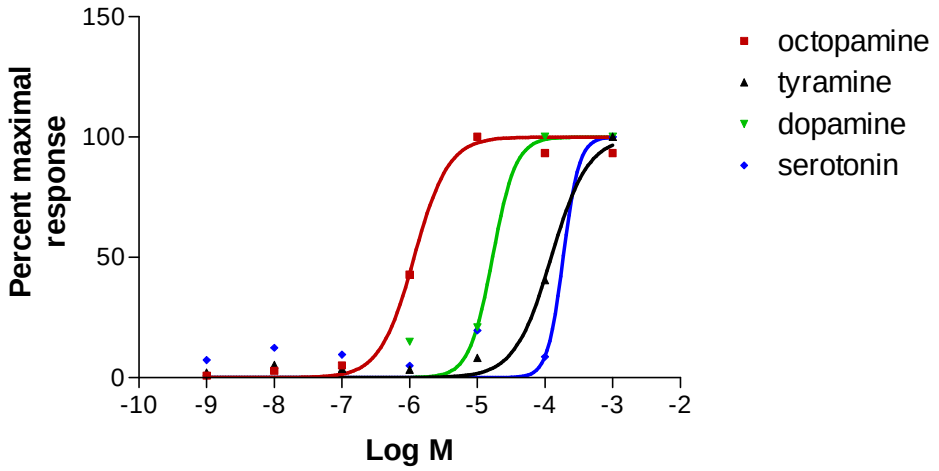

B

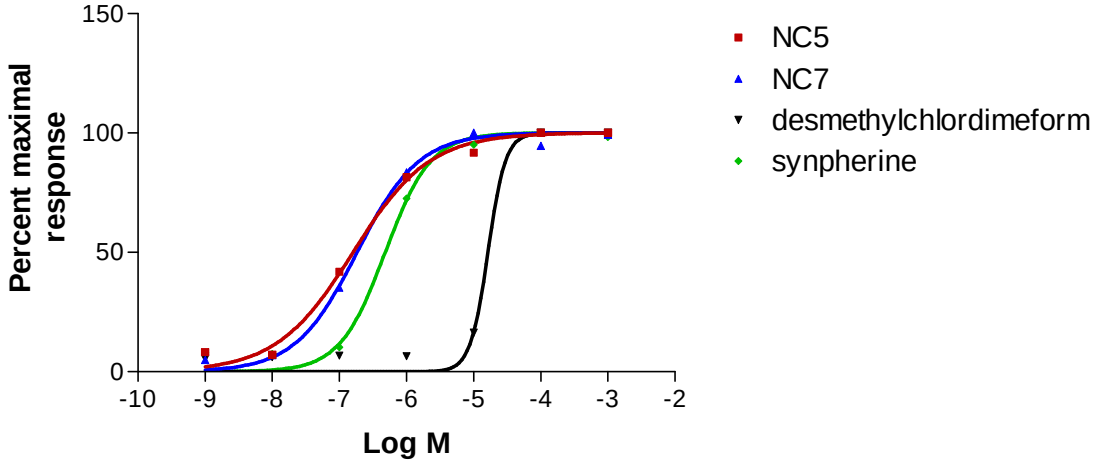

Figure 73: Pharmacological features of *Lymnaea OA* receptor evaluated by SEAP HEK expression system.
After transfection, cells were challenged with increasing concentrations of biogenic amines (A), or octopaminergic agonists (B).

Table 2: Pharmacological properities of *Lymnaea* octopamine receptor OA.

Applied ligand	EC50 value [µM]
Biogenic amines	
Tyramine	12,460
DL-synpherine	4,880
DL-octopamine	3,028
Dopamine	16,840
Serotonin	177,610
Other ligands	
BTS	95,110
Desmethyl	27,400
Naphazoline	4,286
NC4	1,090
NC5	0,484
NC6	0,294
NC7	0,152
NC9	4,710
NC12	2,767
Phentolamine	7,602
Rauwolscine	11,530
Metoclopramide	0,711
Epinostine	40,330
Mainserin	36,260
Yohimbine	0,298
Chlorpromazine	13,970
Amitraz	31,540

3.3.2. Pharmacology of *Drosophila Octß2R*

HEK-293 cells were transfected with a plasmid containing the coding region of the gene under control of the CMV promotor. This plasmid was cotransfected with a reporter plasmid where SEAP is under control of *cre* elements.

Ligands were applied at concentrations ranging from 10^{-3} to 10^{-9} M, resulting in cAMP-inducible, high level SEAP expression. Dopamine, Tyramine and synpherine have higher affinity than octopamine, which in turn has higher affinity than serotonine (Fig.74). The EC50 values were octopamine 1.21×10^{-4} M; Dopamine 1.95×10^{-5} M; Tyramine $4{,}41\times10^{-5}$ M; Serotonin 4.59×10^{-4} M; synephrine 4.88×10^{-5} M. The effects of increasing concentrations of octopamine antagonists on the Octß2R expression of transfected HEK cells was also studied. I tested the same set of antagonists as for the *Lymnaea* OA receptor. Yohimbine has the highest affinity followed by phentolamine > mianserin > rauwolscine > metoclopramide > chlorpromazine > epinastine (table, 3).

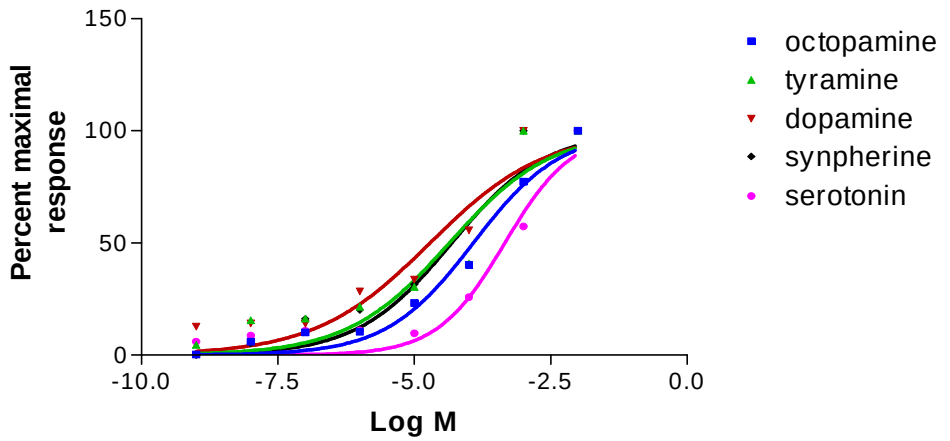

Figure 74: Pharmacological features of *Drosophila Octß2R* receptor evaluated by SEAP HEK 293 expression system.
After transfection , cells were challenged with increasing concentrations of biogenic amines octopamine, tyramine, dopamine, synpherine, or serotonine.

Table 3: Pharmacological properties of *Drosophila Octß2R*.

Applied ligand	**EC50 value [µM]**
Biogenic amines	
Tyramine	44,10
DL-synpherine	48,80
DL-octopamine	121,00
Dopamine	19,50
Serotonine	459,00
Other ligands	
BTS	14,40
Desmethyl	0,283
Naphazoline	0,283
NC3	69,70
NC4	38,80
NC5	91,10
NC6	138,00
NC7	0,441
NC9	4,71
NC12	168,00
Phentolamine	0,273
Rauwolscine	1,290
Metoclopramide	1,320
Epinostine	40,30
Mainserin	0,488
Yohimbine	0,128
Chlopromazine	12,90
Amitraz	171,000

3.3.3. Pharmacology of *Drosophila Octß3R*

HEK-293 cells were transfected with a plasmid containing the coding region of the gene under control of the CMV promotor. This plasmid was cotransfected with a reporter plasmid where SEAP is under control of *cre* elements.

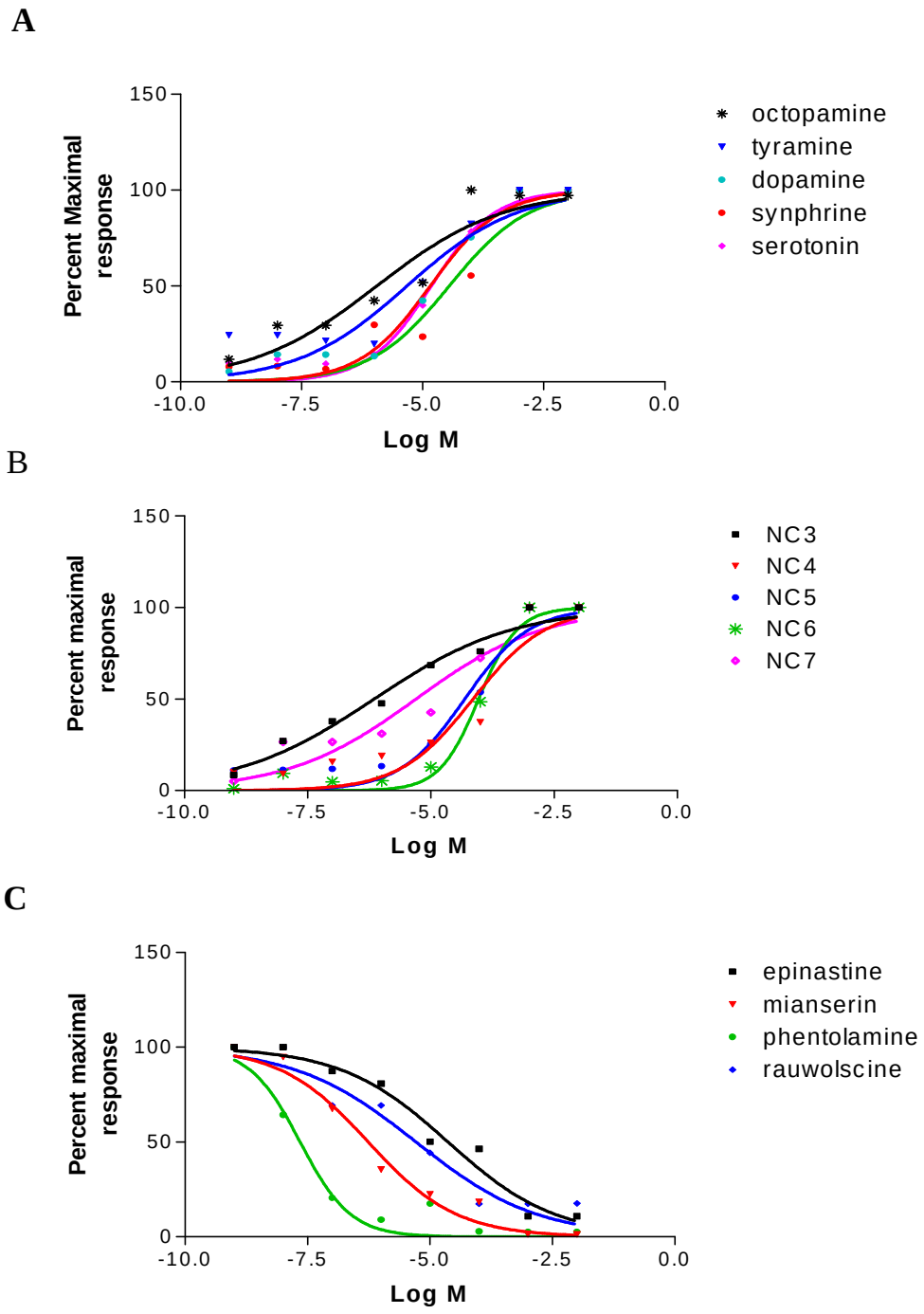

Figure 75: Pharmacological features of *Drosophila Octß3R* evaluated by SEAP HEK expression system.
After transfection , cells were challenged with increasing concentrations of biogenic amines(A), octopaminergic agonists (B) or antagonists (C).

Table 4: Pharmacological properties of *Drosophila Octß3R*.

Applied ligand	EC50 value [µM]
Biogenic amines	
Tyramine	4,71
DL-synpherine	3,55
DL-octopamine	1,13
Dopamine	1,43
Serotonin	1,51
Other ligands	
BTS	4,47
Desmethyl	0,522
Naphazoline	0,079
NC3	0,709
NC4	7,170
NC5	48,80
NC6	93,20
NC7	5,00
NC9	3,02
NC12	19,80
Phentolamine	0,022
Rauwolscine	5,210
Metoclopramide	2,890
Epinostine	23,40
Mainserin	0,551
Yohimbine	1,090
Chlopromazine	0,014
Amitraz	171,000

As known for native octopaminergic receptors, octopamine has a higher affinity than tyramine > serotonin = synephrine > dopamine (Fig 75, A).

Octopaminergic agonists such as NC3, NC4, NC5, NC6 and NC7 were able to induce SEAP expression in a dose-dependent manner. NC3 (EC50 7.09×10^{-7}M) has higher affinity than NC7 (EC50 5.00×10^{-6}M), which in turn has higher affinity than NC4 (EC50 7.17×10^{-5}M) > NC5 (EC50 4.88×10^{-5}M) > NC6 (EC50 9.32×10^{-5}M) (Fig 75, B). The effects of increasing concentrations of octopamine antagonists on the Octß-3R receptor of transfected HEK cells was also studied. Chlorpromazine has the highest affinity followed by phentolamine > mianserin > yohimbine > metoclopramide > rauwolscine > epinastine (Fig.75,C).

4. Discussion

Taking the advantage of genetic methods available for the fruit fly *Drosophila melanogaster*, I tried to characterize the physiological significance of three families of G-protein coupled bioamine receptors, the octopamine, the tyramine and the dopamine receptors. To identify their physiological role, but also to find new targets for insecticides. I tried to elucidate their expression patterns, their pharmacology and their physiological relevance using a set of different approaches. To achieve these goals, I primarily used the GAL4/UAS system for *in vivo* targeting of gene expression in a spatially controlled manner. This system was adapted for use in *Drosophila* by (Brand and Perrimon, 1993a) in which the GAL4, the yeast transcription activator, activates the specific expression of a target gene placed under the control of UAS promotor. This bipartite system is advantageous because each part of the system is maintained in separate parental lines which are viable since no activation is possible if the system is uncoupled. This system was used in my study to analyze the gain-of-function and the loss-of-function of genes coding the biogenic amine receptors as well as their expression pattern using promotor –GAL4 fusion constructs.

4.1. Octopaminergic/tyraminergic receptors:

The biogenic amine octopamine is known as a major neurotransmitter and neuromodulator in the invertebrates (David and Coulon, 1985). It is belived to modulate almost every peripheral organ and most sense organs. The total, four genes for octopamine receptors were identified; namely, *Oamb*, *Octß1R* (OA2), *Octß2R*, and *Octß3R (Maqueira et al., 2005).* Octopamine, together with tyramine, is the invertebrate counterpart of adrenaline/noradrenaline that is very important transmitter/hormone in vertebrates. Tyramine is a monoamine synthesized from the precursor, the amino acid tyrosine by the action of the enzyme, tyrosine decarboxylase (TDC). The tyramine act as a precursor for octopamine synthesise by the action of the enzyme, tyramine-*ß*-hydroxylase (Roeder, 1994, 1999).

Thus, octopaminergic containing cells will contain tyramine as a precursor and therefore both tyramine and octopamine may be released from the same neurons as co-transmitters. On the other hand, some tyramine containing cells do not contain octopamine (Downer *et al.*, 1993; Nagaya *et al.*, 2002).

In this work, I found some new aspects regarding the role of selected octopamine and tyramine receptors. At the beginning of my thesis, there was a fundamental discrepancy between earlier studies with larger insects regarding the physiological significance of octopamine and tyramine and the phenotype of *Drosophila* null mutants. Whereas these

earlier studies reported modulation of almost every organ in insects (Roeder, 1999), the octopamine deficient flies are almost wild type like (Monastirioti *et al.*, 1996). My studies may help to fill this gap in some aspects. Most important may the work dealing with one of the octopamine receptors, namely the *Oct2ßR*. It may give us especially a first indication regarding octopamine and tyramines role in muscle physiology. The *Oct2ß* receptor gene is expressed in the entire muscular system of *Drosophila* larvae including those which are longitudinally and obliquely arranged along the body axis and in transversally arranged muscles orthogonally orientated to the body axis, whereas tyraminergic receptors expressed only in: (1) the segmentally repeated ventral longitudinal muscles which play a major part of the larval musculature used in crawling, (2) lateral longitudinal muscles, and (3) lateral oblique muscles in each body hemisegments from the head to the tail region in addition to the musculature of the tail region which is associated with the anus and the posterior spiracle. In the light of other studies, octopamine and tyramine have opposite effects on muscles, whereas octopamine enhance the contraction of muscles tyramine has the opposite effect (Nagaya *et al.*, 2002) but *Drosophila* larvae require normal octopamine/tyramine function in regulating walking activity (Saraswati *et al.*, 2004; Fox *et al.*, 2006).

In *Drosophila*, flies with a null mutation in the gene encoding the enzyme tyramine *ß*-hydroxylase have reduced octopamine levels and increased tyramine levels (Monastirioti *et al.*, 1996) and they show a slight locomotion defect (Saraswati et al., 2004). This implies that the major role of tyramine is to receive the informations from the sense organs and inhibit the movement accordingly. On the other hand, whole larval body-wall muscles express *Octß2R*. Together, these results suggest that octopamine and tyramine are involved in the initiation and modulation of the coordinated activities involved with crawling in *Drosophila* larvae (Fox *et al.*, 2006), who used mutants defective in transmitter synthesis.

In adults, only two octopamine receptors show expression in muscles, namely the *oct2ß* and the *Oamb* receptors. I could show that these receptors are expressed in a complementary fashion. *Oct2ß* receptors are present in much more skeletal muscles than *Oamb* ones. It appears that the *Oct2ß* receptors are exclusively expressed in those muscles that are relevant for walking. Within the leg, *Oamb* receptors are present in other leg muscles. This broad expression of the *Oct2ß* may be the reason for the deficits I observed in the corresponding RNAi flies. I record muscle weakness of the legs and inability of the insects to go up against the gravity in which adult *Drosophila* attempt many times to move up for ~ 10min without any change in the position. In addition there are no, or only marginal changes in the direction of the longitudinal body axis, which reflects the impact of this gene on the coordination and

consistency of the movement in adult *Drosophila*. More over, during courtship, males were not able to keep up with females because they could not move their legs properly and the males then lost the ability to adjust their position, which leads to the failures in courtship. This may suggest a role of octopamine in *Drosophila* movement and the strong relationship between locomotion and courtship. For this reason, i record zero hatchability in their eggs.

Octopamine is known to initiate or modulate the rhythmic behaviour in other insects, leeches, and earthworms (Hashemzadeh-Gargari and Friesen, 1989; Ramirez and Pearson, 1991; Monastirioti *et al.*, 1995; Roeder, 1999; Mizutani *et al.*, 2002). The role of octopamine in initiation and maintenance of rhythmic behaviour as walking and flying in insects (Sombati and Hoyle, 1984a, b), swimming in crustacean (Mulloney *et al.*, 1987) and chewing in molluscs (Kyriakides and Mccrohan, 1989) was reported. My own experiments have not yield a comparable result at the level of the corresponding receptors. In addition, I see that *TyrR* is strongly expressed in the heart muscles. Heartbeat in *Drosophila*, although myogenic (Dowse *et al.*, 1995; Gu and Singh, 1995), is modulated by neurotransmitters which suggest that tyramine may be involved in such group of neuromodulators. Thus this receptor might be the molecule that transmits the effects of octopamine/tyramine in this organ.

Tyramine receptor 2 was strongly expressed in the central complex (CC), which is located in the center of the supraesophageal ganglia. The CC forms connections to a variety of brain centres. It is a control center for many different behavioural response (motor outputs) and receive visual input (Strauss, 2002). Mutants with CC structural abnormalities are impaired in visual- pattern memory.

In addition to the role in movement control, octopamine and tyramine are thought to play an important role in metabolic control. Octopamine is the hormone of feast, being antagonistic to insulin. Glycogen and triglycerides are the energy reserves in animals including insects. Glucose is stored in a polymeric form, glycogen, that can easily be degraded on demand to be used as a glycolytic fuel (Steele, 1982). Fatty acids are stored as triglycerides in fat body and in oenocytes (Gutierrez *et al.*, 2007) that can be used for energy production through ß-oxidation (Athenstaedt and Daum, 2006). The process of energy mobilization is converting stored glycogen and triglycerides into heamolymph trehalose and diglycerides, respectively. This process is controlled by the neurohormone octopamine which increase the cAMP or Ca^{2+} (Roeder, 2005). Octopamine stimulates the lipid mobilization in several insects (Fields and Woodring, 1991; Orchard *et al.*, 1993; Socha *et al.*, 2008). OA induces the energy mobilization and tyramine induces lipid storage which suggests that octopamine and tyramine

have opposite effect on the lipid content and both generate lipid metabolism program facing the energy demand during larval stage.

Two major hormonal system in the *Drosophila* brain regulate the metabolic state, namely the insulin and the adipokinetic hormones axes (Rulifson *et al.,* 2002). Whereas the insulin producing cells are homologous to the *ß*-cells of the pancreas, the adipokinetic hormone producing cells in the *corpora cardiaca* are homologous to the alpha cells of the pancreas. Thus this interconnected system represents a functional islet of Langerhans within the brain of the fly. A recent genome- wide RNAi screening in adult *Drosophila* with the goal to identify genes affecting the fat content (obese and lean flies) performed by Pospisilik *et al.* (2010) revealed a large number of genes that regulate fat content in they are downregulated. Even if the RNAi is restricted to specific organs, such as the brain, muscle, oenocytes- and /or fat-body, corresponding effects could be seen. Among them, two octopamine/tyramine receptors (*TyrR* and *oa2*) showed reduced body fat content in response to RNAi knockdown.

I observed very strong expression of the *TyrR* gene in the major insulin-producing cells in the Pars intercerebralis located in the median protocerebrum. Within these cells, maximal expression could be seen. In mammals, insulin is a hormone that has effect the metabolism. Insulin causes cells in the liver, muscles and fat tissue to take up glucose from the blood, storing it as a glycogen in the liver and muscles and stop use of fat as a energy source. When insulin is absent or low, glucose is not taken up by body cells and the body begins to use fat a as energy source. In flies, killing these cells induces an obese phenotype. Overexpression of the *TyrR* in these cells should have the same effect, as it is known that this receptor is negatively coupled to activation of adenylate cyclase (Saudou *et al.,* 1990). This would lead to a tyramine induced silencing of insulin secretion, thus showing the same phenotype. Removing the receptor from these cells would have the opposite effect, simply because the inhibitory effect of tyramine on the insulin-producing cells is removed. This is observed in these flies (leanness). Regarding the role of *oa2*, we have currently no idea, because it is coupled to activation of adenylate cyclase. It is possible, that the receptor is also present in the AKH-producing cells that are antagonistic to the insulin producing cells.

Another tyramine receptor might also be part of the metabolic control system of the fly, as it is expressed in the insulin-producing cells but also in the oenocytes, the functional equivalent of the mammalian liver in the fly (Gutierrez *et al.,* 2007). These receptors are the *TyrRIII* receptors. In this study, we reported strong GFP expression in clusters of oenocytes in each abdominal hemisegment of *TyrRIII*-GAL4/UAS::GFP larvae and adults. And these clusters of oenocytes were verified for their lipid storage by using Nile Red staining which stains

intracellular lipids. This may have important implications for the much-hypothesized link between the insulin and storing fat, or in other words, obesity. Flies supposed to have the metabolic regulators parallel to those in mammals; in *Drosophila* the food which not digested and absorbed is stored in the fat body. The fat body acts like the mammalian liver and the white adipose tissue that storing large reserves of glycogen and lipid. The same function is played by a special clusters of cells called oenocytes accumulate lipids during starvation and are proposed to perform hepatocyte-like functions in lipid processing (Gutierrez *et al.*, 2007). A signal than comes to inform the CNS of the energy status of the organism. The CNS regulates the physiological and behavioural outputs to maintain the organism in optimal energetic state. This energy circuit in the flies is similar to that of mammals (Kaun and Heberlein, 2009).

My immunohistochemical studies revealed candidates that may function as autoreceptors. In this study, immunostaining revealed that the larval CNS had profuse tyramine- positive expression (*TyrRII*) in the brain, subesophageal ganglia and thoracico-abdominal ganglia. In the brain, there was a cluster of somata in the ventro-anterior side of each hemisphere and several weakly stained somata in the dorso-anterior side and in the dorsal side. Ventral unpaired median neurons were present in each thoracio-abdominal neuromere. This distribution of somata in the larval brain is typical for octopamine/tyramine producing cells (Nagaya *et al.*, 2002). In addition, I found that *Octß3R* is expressed in unpaired somata that are situated at the ventral mid-line or the dorsal mid-line of the subesophageal ganglion were visualized, these called VUM and DUM neurons in insects (Hoyle, 1975; Hoyle and Barker, 1975; Hoyle *et al.*, 1975; Braünig and Pflüger, 2001). Subesophageal VUM/DUM neurons innervate most parts in the insect brain and a subpopulation of them is octopaminergic (Hoyle, 1975; Hoyle and Barker, 1975; Braünig and Pflüger, 2001). We found that these DUM neuron is bifurcated in the midline to innervate the antennal lobes, rolled up inside and ascend toward median protocerebrum, the same result was obtained in locust *Locusta schistocerca* in which the DUM neurons provide ascending processes to innervate the antennal lobes (Braünig and Burrows, 2004).

One very asthonishing result was that numerous octopaminergic and tyraminergic receptors are expressed within the mushroom body (MB) of the fly. In *Drosophila*, mushroom bodies are critical for olfactory learning and memory (Han *et al.*, 1996; McGuire *et al.*, 2005). The primary olfactory inputs are conveyed from the antennal lobes to the MB and to the lateral horn. Octopaminergic inputs were reported to be important to convey the olfactory informations to the MB. The octopaminergic innervation of the MB are required for

association of odours with sugar in an appetitive (or aversive for dopaminergic receptors such as punishment) conditioning procedure, in which one or two odorants is typically paired with sugar as a reward or electrical shock as a punishing stimulus (Schwaerzel *et al.*, 2003). But it appears that octopaminergic and tyraminergic systems do not have a role in place learning (Sitaraman *et al.*, 2008; Sitaraman *et al.*, 2010). The cAMP/PKA activity within the mushroom body in response to specific neuromodulators is critical for memory formation (McGuire *et al.*, 2005). Not only *Oamb*, but also most other receptors for octopamine and tyramine are present within these cells. Currently, we can't decide if expression of these receptors is restricted to certain subpopulations of cells within this structure or if it is mushroom body wide. This expression pattern can be of great interest for learning physiology, because these receptors have different intracellular signalling pathways.

In *Drosophila* larvae, only two octopamine receptors show expression in tracheal system, namely the *oa2* and the *Oamb* receptors. Whereas *oa*2 expressed especially in the main branches of the tracheal system, *Oamb* is strongly expressed in three levels of the tracheal system; the secondary- and tertiary branches and the blind ending terminal branches (tracheoles), including a lot of visceral branches and transverse connectives forming a dense network. This network is formed by a series of successive branching and fusion events. During this process, specialized tip cells lead the migration of new branches and mediate their interconnection. During the branch fusion process, some tip cells become specialized as "fusion cells" and convert themselves into seamless tubes that span the branch fusion joint. Other tip cells become specialized as "terminal cells" that go on to form branched, blind-ended seamless tubes that ramify extensively on target tissues, and act as the site of gas exchange. The entire organ is made of epithelial cells only, forming a single layer around the central airspace which suggests that octopamine receptors may be involved in the branching and fusion process of the insect tracheal system. The presence of OARs in the tracheal system and subsequent increase in cAMP upon OA binding have been proposed by (Zeng *et al.*, 1996).

In man and mammals adrenergic receptors, which parallels OARs/TARs in invertebrates, are expressed on different cell types in respiratory system including epithelial cells, smooth muscle cells (Svedmyr, 1990; Barnes, 1999; Maris *et al.*, 2006) and mediate various important physiological functions in tracheal epithelium (Folkert and Nijkamp, 1998). In insects, respiratory epithelial cells have important role in defence against airborne pathogens not only through acting as a physical barrier but also through different molecules such as different antimicrobial peptides and lysozymes (Wagner *et al.*, 2008). The same function was

also reported in humans by Giebelen *et al.* (2008) who suggest that endogenous adrenergic receptors are involved in the regulation of respiratory system inflammation induced by bacterial infection and ensuing increase in cAMP in this case which suggest that octopamine and octopamine receptors may be involved in the tracheal innate immunity.

My results reveal that many organs in *Drosophila* larvae which launch an immune response including the barrier epithelia (intestine, salivary gland and malpighian tubules) show OARs and TARs expression. I found that all tyramine receptors and one octopamine receptors namely the *oa2* show expression in gut cells and also I observed strong expression of *TyrRIII* and *oa2* in malpighian tubule. The presence of tyramine in malpighian tubule was reported by Cole *et al.* (2005) that the malpighian tubules contain tyrosine decarboxylase which converts tyrosine into tyramine. Taken together, my results suggest that octopamine and tyramine receptors may be involved in epithelial innate immunity response.

Feeding behaviour in *Drosophila* is neuronally anchored (Melcher *et al.*, 2007). In our results we found that *TyrR* is expressed in the adult *Drosophila* proboscis especially the two labellae and their psuedotrachea, which suggest the role of *TyrR* in the gustatory behaviour. This confirmed the results reported by Pospisilik *et al.* (2010), who suggested that TyrR plays a direct role in nutrient sensing by odorant/gustatory network. In our results, we reported a novel physiological character for *Oamb*, strong expression in the branching pattern of the tracheal system including a lot of visceral branches and transverse connectives in *Oamb*-GAL4/UAS::GFP larvae was seen which were visible through the cuticle of living larvae. In *Drosophila*, three levels of tracheal branching : six primary branches formed first, followed by about 20 secondary branches and hundreds or more terminal branches in each hemisegment. Each of the three levels of tracheal branching appear to involve different cellular mechanisms and different sets of tracheal genes and the development of the tracheal system occurs by a series of branching events and these genes regulates the different steps of branching (Samakovlis *et al.*, 1996). Perhaps *Oamb* is involved in the tracheal branching process.

4.2. Dopaminergic receptors

In both vertebrates and invertebrates, the biogenic amine dopamine is implicated in many functions including locomotion, cognition, and development (Civelli, 1993) Furthermore, misregulation of dopamine signaling is believed to play a role in a number of human disorders including schizophrenia, Parkinson's disease, Tourette's syndrome, and drug addiction. The actions of dopamine are mediated via G protein–coupled receptors (GPCRs). Dopamine

receptors are members of the rhodopsin-like family of GPCRs (Jackson and Westlind-Danielsson, 1994).

Drosophila dopamine receptors belong to three groups: *DopR1* group or *DmDop1*, also known as *dDA1* (Gotzes et al., 1994; Sugamori et al., 1995); *DAMB* or *DopR2* group(Feng et al., 1996; Han et al., 1996) ; and *D2*-like receptor, also called *D2R* (Hearn et al., 2002).

Biosynthesis of dopamine starts from amino acid, tyrosine which converts to dihydroxyphenylalanine (L-DOPA) by the enzyme tyrosine hydroxylase. Dopa decarboxylase enzyme then catalyzes the conversion of L-DOPA to dopamine.

I try in this study to explore the dopamine receptors; *DopR*, *DopR2* localization of each receptor in neuronal and nonneuronal tissues in both larval and adult stages. To achieve this, the GAL4/UAS bipartite system with GFP as a reporter was used.

This study demonstrates distinct expression of *DopR2* and *D2R* in the tracheal system of larvae in the three major parts of the tracheal system; the primary airways, the secondary airways, and the blind ending terminal ones. Enrichment of DA in the trachea was reported earlier (Hsouna et al., 2007). DA pathway mutants show dramatic effects on the stereotyped migratory behaviour of tracheal cells and patterning of the resulting branched structure and those abnormalities could be rescued by DA treatment. Consistently, genes involved in DA biosynthesis also regulate tracheal migration.

In this study, immunohistochemistry with three different primary antisera; anti-GFP, anti-prospero which labelling entroendocrine cells (Campbell et al., 1994) and anti-armadillo which label diploid and polyploid enterocytes that lack prospero (Riggleman et al., 1990) was done to label specifically enterocytes. Most of enteroendocrine cells, which express the transcription factor prospero and also the ß-catenin homologue Armadillo, express also DopR. Entroendocrine, or neuroendocrine, cells secrete peptide hormones to coordinate gastrointestinal functions, such as motility and secretion (Schonhoff et al., 2004).

My study demonstrates a novel expression pattern of the *DopR* in larval and adult CNS except few brain structures which were reported before for *DmDOP1* receptor expression. In larval CNS, the GFP appeared as mesh-like connected bundles where somata are located on almost all neuropile secondary traces including; medial dorsoposterior, lateral dorsoanterior, medial dorsoanterior, lateral dorsoposterior traces which are located dorsally in each hemisphere; centromedial and centroposterior which are located in the centre of the neuropile; basolateral anterior, basolateral ventral and basolateral posterior traces in the base of each brain hemisphere and these somata were connected by secondary small axon traces travelling

radially within the hemisphere. Strongly expressed somata were also seen in the thoracico-abdominal ganglion but also connected by short axons giving the same mesh-like appearance.

In the adult brain, the *DopR* positive clusters were seen almost everywhere in the supra- and subesophageal ganglia as well as in the optic lobes. Mushroom body substructures were reported to express dopaminergic receptors with relatively stronger staining in the mushroom body γ lobe/ heel, according to other studies, this structure implicated in the short- term memory formation (Zars et al., 2000) and less staining was seen in *α/ß* and *α´/ß´* lobes. This fits well with the results reported by Kim et al. (2003) Within the interhemispheric junction, strong GFP expression was seen in the central complex substructures including; the outer margin of the fan-shaped body; some positive *DopR* neurons including somata which innervate the ellipsoid body; noduli and some axonal projections connecting the central complex substructures. Pervious studies suggested the critical role of the central complex in the motor control, olfactory conditioning, courtship and functional tolerance of alcohol (Heisenberg et al., 1985; Strauss and Heisenberg, 1993; Bausenwein et al., 1994; Scholz et al., 2000). Also in adult brain, a dense ramification was seen in the superior and inferior posterior slope surrounding the esophageal foramen. Strong GFP expression was seen in the optic lobe including lobula, lobula plate and inner- and outer medulla. Two large somata were seen in the ventro-medial part of the subesophageal ganglion. *DopR* positive neurons project from posterior inferior lateral protocerebrum into the ventromedial protocerebrum. In addition, *DopR* positive neurons project from posterior inferior lateral protocerebrum towards the midline. Strongly expressing somata are also located in the lateral protocerebrum and in the ventrolateral part of the antennal lobe and antennal nerve. A cluster of strong expressed somata located in the ventrolateral protocerebrum. Positive *DopR* neurons ramified bilaterally in the ventromedial protocerebrum, they have their somata located on the midline of the subesophageal ganglion with mirror symmetry. They can be divided into three neuromeres (mandibular, maxillary, and labial) in the gnathal segment. Therefore, these subclusters are named VMmd, VMmx and VMlb from anterior to posterior. The GFP expression is strong in both VMmx and VMlb but it is moderate in the VMmd cluster. The secondary neurons turn ventrally to descend through the cervical connective. These descending axons terminate in all three thoracic ganglia and abdominal ganglia. The expression within the thoracicoabdominal ganglia was reported by Kim et al. (2003).

This study demonstrates the *D2R* expression pattern in both larval and adult CNS. In the larval CNS, moderate GFP was seen in mushroom body substructures including: *b /b´* lobes, GFP expression pattern in the α/α´ lobes was seen as a cap over the lobes and GFP expression

appears as a cap over the calyx of mushroom body. Somata and projections were seen allover the brain hemisphere. Strongly expressing somata were seen in the thoracicoabdominal ganglia along the midline, they send transverse projections toward the dorsolateral trace and some of their projections come out of the brain to the periphery. These abdominal projections which send projections laterally toward the outer edges of the neuropile and *D2R* longitudinal traces that run parallel on either side of the midline were reported before by Draper et al. (2007).

D2R expression was seen in the larval eye anlagen. The eye anlage remains part of the surface epithelium until later in embryogenesis, giving rise to the cortices of the lamina and the distal medulla (Meinertzhagen, 1993).

In adult CNS, Mushroom body substructures could not be distinguished. *D2R* positive projections appear as a net of fibers observed throughout the hemispheres. These projection were seen before by Draper et al. (2007). In this study, some positive stained projections adjacent to the mushroom body were identified. This huge number of projections appears as a net of fibers observed throughout the hemispheres. This characteristic immunoreactivity was reported also by Draper et al. (2007). This large network of *D2R* neurons may suggest that *D2R* projections serve as neural circuits linking the central complex with the mushroom body and antennal lobe to facilitate the flow of informations

Results in this study demonstrate that *D2R* expression was highly enriched in larval salivary gland, esophagus, pharynx, pharyngeal muscles and muscular stripes of the hindgut but midgut cells did not show detectable *D2R* which conflicts with the results obtained by Draper et al. (2007) who demonstrate the *D2R* in some of the midgut cells but not in the salivary glands, esophagus and proventriculus. A previous study used reverse transcription followed by quantitative PCR to confirm that the *D2R* gene is expressed in larvae, pupae, and adults (Hearn et al., 2002).

4.3. Pharmacology of octopaminergic receptors

Performing pharmacological studies is a prerequisite for a detailed analysis of the corresponding receptors. Tissue culture systems that allow heterologous expression, such as HEK-293 cells are advantageous, because they combine a simple read-out with the occurrence of only a single receptor that has to be analyzed.

In this study, the ability to change intracellular cAMP levels in octopaminergic receptors, *Lymnaea OA*, *DmOcß2R* and *DmOctß3R*, in response to exposure to a wide range of naturally occurring biogenic amines or known synthetic ligands was tested. My results demonstrated

that NC5 and NC7 have higher affinities to *Lymnaea OA* receptor than synpherine, which in turn has a higher affinity than desmethylchlordimeform. The biogenic amines octopamine has a higher affinity than dopamine, tyramine and serotonine. The EC50 values were octopamine 3.03×10^{-6} M; Dopamine 1.68×10^{-5} M; Tyramine $1{,}25\times10^{-5}$ M; Serotonin 1.78×10^{-4} M. *Lymaea* OA receptor was reported to has a 12,6 –fold higher affinity for octopamine compared with tyramine (Gerhardt *et al.*, 1997a; Gerhardt *et al.*, 1997b). Using nervous tissue homogenate from the honey bee *Apis mellifera* and from the desert locust *Schistocerca gregaria* (Degen *et al.*, 2000), it was shown that the difference in affinity for octopamine versus tyramine were 3.8- and 6,5-fold, respectively. NC7 was reported as a highly potent and specific agonist to OA receptors in insects (Nathanson, 1985; Roeder and Gewecke, 1990; Hiripi *et al.*, 1994), and also as a high affinity to *Lymnaea* OA receptors (Hiripi *et al.*, 1998).

In the pharmacological characterization of *Lymnaea* OA receptor antagonists, my study demonstrates that yohimbine has the highest affinity to *Lymnaea* OA receptor followed by metoclopramide > phentolamine > rauwolscine > chloromazine > mianserin > epinostine. Phentolamine was reported by Hiripi *et al.* (1998) that it can completely and reversibly block the OA effect on *Lymnaea* OA receptors at concentrations of 10^{-6}M and it is the most effective substance to inhibit the OA response. The antagonists mianserin and phentolamine were also reported by Hiripi et al. (1998) to have higher affinity to *Lymnaea* OA receptors than chlorpromazine and yohimbine. Parallel to my results, rauwolscine was reported by Hiripi et al. (1998) to have high affinity to *Lymnaea* OA receptors but OA could displace rauwolscine only at high concentration range between 0.1-1.0 μM.

The presence of OA-immunopositive neurons and fibres in *Lymaea* brain was demonstrated (Elekes *et al.*, 1993).

DmOcß2R and *DmOctß3R* are members of functional selective octopamine receptors that are coupled to increase in cAMP levels. They are named *ß*-receptors as they show structural similarities with vertebrate *ß*-adrenergic receptors (Maqueira *et al.*, 2005). The most effective naturally occurring ligands at increasing cAMP levels are octopamine, tyramine and synpherine, this was also demonstrated by Maqueira et al. (2005) but my results demonstrate that the rank order of potency for biogenic amines octopamine and tyramine was different for *octß2R* and *octß3R* receptors (EC50: *Octß2R* tyramine > octopamine, *Octß3R* octopamine > tyramine).

In my results, the rank order of potency for the active synthetic agonists tested was the same for both receptors (EC50s : Naphazoline > octopamine), while Maqueira et al. (2005)

reported that the rank of potency for both agonists was different for these receptors (EC50s : *Octß2R* octopamine > Naphazoline, *Octß3R* Naphazoline > octopamine).

Phentolamine , a classical α-adrenergic antagonists was able to increase the cAMP in the transfected cells, as well as able to block the octopamine mediated increase in cAMP. Phentolamine acts as a partial agonist of this response at the *Octß2R* and *Octß3R*. The efficacy for this response is more in *Ocß2R* > *Octß3R* (Maqueira et al., 2005).

This pharmacological characterization opens the possibility to develop new types of ligands that specifically interact with only one subtype and that might serve as lead structures for the development of new insecticides in the future.

5. Summary

The main goal of this work was to explore the functional relevance of selected receptors for biogenic amines in the fruit fly *Drosophila melanogaster* and to find those candidates that may be suited to function as targets for new types of insecticides. I focussed on the receptors for octopamine (OARs), tyramine (TARs) and dopamine (DARs). Therefore, I mapped the expression of the corresponding receptor genes throughout all developmental stages and in all organs in the fruit fly. For selected receptors, these results were supplemented by pharmacological studies. In addition, RNAi-mediated gene silencing was used to identify phenotypical changes associated with this loss of gene expression.

All DARs show a widespread expression within the central nervous system of the fly and all of them show a particularly strong expression in the mushroom bodies, centres for learning and memory in the insect brain. Regarding the TARs a more complex expression profile became apparent. Most importantly, *TyrR* is the sole OAR/TAR receptor that is present in the heart of the fly. In addition, it shows very high expression in the major insulin-producing cells and in oenocytes of larvae and adults, suggesting that *TyrR* might be relevant for controlling the lipid metabolism of the fly. Amongst the OARs, *oa2* show an almost ubiquitous expression in the nervous system, whereas its expression in non-neuronal tissues is only moderate. Regarding the expression in muscles, *Ocß2R* is present in the entire muscle system of larvae and in walking muscles of adults. In the leg, the pattern of expression is complementary to that of the *Oamb*. *TyrR*, as the most relevant representative of TARs, also show expression in muscles; namely in (1) the segmentally repeated ventral longitudinal muscles which play a major part of larval crawling, (2) lateral longitudinal muscles, and (3) lateral oblique muscles in each body hemisegments from the head to the tail region. I concentrated for the functional studies on the *Ocß2R* receptor and found, using RNAi-mediated gene silencing some very interesting phenotypical changes. I recorded muscle weakness during walking and the inability of adults to go up a vertical surface against the gravity, which caused no problems for wild type flies. More over, during courtship, males were not able to keep up with females, which leads to failures of the entire behaviour. Consequently, these flies are sterile.

Pharmacological features of octopamine receptors were quantified using heterologous expression of the corresponding receptors (OARs) in HEK293 cells. The general pharmacological features of all OARs tested have striking similarities. These similarities could even be observed, if a corresponding receptor of the snail *Lymnaea stagnalis* was

included, indicating a very high conservation of pharmacological features among OARs throughout the invertebrates. Nevertheless, distinct peculiarities of the different OARs from the fly could be observed. This pharmacological characterization opens the possibility to develop new types of ligands that specifically interact with only one subtype and that might serve as lead structures for the development of new insecticides in the future.

Zusammenfassung

Das Hauptziel dieser Arbeit bestand darin, die physiologische Relevanz ausgewählter Rezeptoren für biogene Amine der Fruchtfliege *Drosophila melanogaster* aufzuklären. Basierend auf diesen Arbeiten sollten Rezeptoren identifiziert werden, die als Angriffsort neuer Insektizide dienen könnten. Hierfür habe ich mich auf die Rezeptoren für Octopamin (OARs), Tyramin (TARs) und Dopamin (DARs) konzentriert. Ich habe das Expressionsmuster dieser Rezeptorgene, sowohl bei Larven als auch bei Adulten, detailliert analysiert. Für einige dieser Rezeptoren (OARs) wurden weiterführende pharmakologische Studien durchgeführt. Außerdem wurde die physiologische Bedeutung eines besonders interessanten Rezeptors mittels des RNAi vermittelten *gene silencings* aufgeklärt.

Alle DARs zeigen eine relativ weiträumige Expression im Nervensystem sowohl larvaler als auch adulter Fliegen. Besonders hervorzuheben ist hierbei die besonders starke Expression in den sog. Pilzkörpern, die als Orte der Gedächtnisbildung bei Insekten gelten. Die TARs hingegen zeigen ein etwas komplexeres Expressionsmuster, das geringere Überschneidungen zwischen den vier Mitgliedern dieser Gruppe zeigt. *TyrR* ist der einzige Rezeptor aus der Gruppe der OARs/TARs, der im Herzen der Fliege exprimiert wird. Außerdem wird dieser Rezeptor besonders stark in den Insulin-produzierenden Zellen sowie in den Oenozyten, den funktionalen Äquivalenten der Leber, exprimiert. Das lässt vermuten, dass dieser Rezeptor für die Regulation des Fettstoffwechsels von ganz entscheidender Bedeutung ist. Unter den OARs, weist der *oa2* eine besonders breite Expression im Nervensystem von Larven und Adulten auf. Hingegen ist die Expression dieses Rezeptorgens in nicht-neuronalen Geweben eher schwach. In Bezug auf die Expression in Muskeln sticht insbesondere der *Ocß2R* Rezeptor hervor. Bei Larven kann dieser Rezeptor in allen Muskeln nachgewiesen werden, bei Adulten in der Muskulatur, die für das Gehen verantwortlich ist. Im Bein ist das Expressionsmuster komplementär zu dem des *Oamb*-Gens. *TyrR*, als wichtigster Vertreter der Tyraminrezeptoren kommt auch in einigen Muskeln vor, z.B. in ventralen Longitudinalmuskeln der Larve sowie in einigen, segmental angeordneten Lateralmuskeln. Für die funktionelle Analyse habe ich mich auf den *Ocß2R* Rezeptor konzentriert. Mittels der RNAi-vermittelten *gene silencing* konnte ich zeigen, dass die betroffenen Tiere eine ausgeprägte Muskelschwäche aufwiesen. Adulte haben die Befähigung verloren eine senkrechte Fläche hinaus zu krabbeln, eine Aufgabe, die von Wildtypen ohne Weiteres bewältigt wird. Außerdem zeigten sie Defizite im Paarungsverhalten was offensichtlich auf

der Unfähigkeit des Männchens beruhte, dem Weibchen in der erforderlichen stereotypen Weise zu folgen. Daraus ergab sich eine auffällige Sterilität dieser Fliegen.

Die pharmakologischen Charakteristika einiger Octopaminrezeptoren habe ich mittels heterologer Expression in HEK-Zellen evaluiert. Es zeigte sich, dass die generellen pharmakologischen Eigenschaften der unterschiedlichern OARs größere Gemeinsamkeiten aufweisen. Diese Gemeinsamkeiten waren sogar noch dann deutlich, wenn ein homologer Rezeptor aus der Schnecke *Lymnea stagnalis* in die Untersuchungen miteinbezogen wurde, was darauf hindeutet, dass wesentliche Charakteristika dieser Rezeptoren über die gesamte Gruppe der Wirbellosen hinweg konserviert sind. Trotzdem, konnten ich pharmakologische Unterschiede ausmachen, die zur eindeutigen Unterscheidung dieser Rezeptoren dienen und die letztlich dazu dienen könnten, neuartige Leitstrukturen für die Entwicklung von Insektiziden zu entwickeln.

6. References

Adamo, S. A., Linn, C. E. and Hoy, R. R. (1995). "The Role of Neurohormonal Octopamine During Fight or Flight Behavior in the Field Cricket Gryllus-Bimaculatus." *Journal of Experimental Biology* **198**(8): 1691-1700.

Altner, H., Routil, C. and Loftus, R. (1981). "The Structure of Bimodal Chemoreceptive, Thermoreceptive, and Hygroreceptive Sensilla on the Antenna of Locusta-Migratoria." *Cell and Tissue Research* **215**(2): 289-308.

Athenstaedt, K. and Daum, G. (2006). "The life cycle of neutral lipids: synthesis, storage and degradation." *Cellular and Molecular Life Sciences* **63**(12): 1355-1369.

Barnes, P. J. (1999). "Effect of beta-agonists on inflammatory cells." *Journal of Allergy and Clinical Immunology* **104**(2 Pt 2): S10-7.

Bausenwein, B., Muller, N. R. and Heisenberg, M. (1994). "Behavior-Dependent Activity Labeling in the Central Complex, of Drosophila During Controlled Visual-Stimulation." *Journal of Comparative Neurology* **340**(2): 255-268.

Blenau, W., Balfanz, S. and Baumann, A. (2000). "Amtyr1: Characterization of a gene from honeybee (Apis mellifera) brain encoding a functional tyramine receptor." *Journal of Neurochemistry* **74**(3): 900-908.

Blenau, W. and Baumann, A. (2001). "Molecular and pharmacological properties of insect biogenic amine receptors: lessons from Drosophila melanogaster and Apis mellifera." *Archives of Insect Biochemistry and Physiology* **48**(1): 13-38.

Blumenthal, E. M. (2003). "Regulation of chloride permeability by endogenously produced tyramine in the Drosophila Malpighian tubule." *American Journal of Physiology and Cell Physiology* **284**(3): C718-728.

Brand, A. H. and Perrimon, N. (1993a). "Targeted gene expression as a means of altering cell fates and generating dominant phenotypes." *Development* **118**(2): 401-15.

Brand, A. H. and Perrimon, N. (1993b). "Targeted Gene-Expression as a Means of Altering Cell Fates and Generating Dominant Phenotypes." *Development* **118**(2): 401-415.

Braünig, P. and Burrows, M. (2004). "Projection patterns of posterior dorsal unpaired median neurons of the locust subesophageal ganglion." *Journal of Comparative Neurology* **478**(2): 164-175.

Braünig, P. and Pflüger, H. J. (2001). "The unpaired median neurons of insects." *Advances in Insect Physiology, Vol 28* **28**: 185-266.

Brembs, B., Christiansen, F., Pfluger, H. J. and Duch, C. (2007). "Flight initiation and maintenance deficits in flies with genetically altered biogenic amine levels." *J Neuroscience* **27**(41): 11122-11131.

Campbell, G., Goring, H., Lin, T., Spana, E., Andersson, S., Doe, C. Q. and Tomlinson, A. (1994). "Rk2, a Glial-Specific Homeodomain Protein Required for Embryonic Nerve Card Condensation and Viability in Drosophila." *Development* **120**(10): 2957-2966.

Civelli, O. (1993). "Molecular Characterization of the D2, D3, D4 Dopamine-Receptor Family." *Neuropsychopharmacology* **9**(2): S35-S35.

Civelli, O., Bunzow, J. R. and Grandy, D. K. (1993). "Molecular Diversity of the Dopamine-Receptors." *Annual Review of Pharmacology and Toxicology* **33**: 281-307.

Clapham, D. E. and Neer, E. J. (1997). "G protein beta gamma subunits." *Annual Review of Pharmacology and Toxicology* **37**: 167-203.

Cole, S. H., Carney, G. E., McClung, C. A., Willard, S. S., Taylor, B. J. and Hirsh, J. (2005). "Two functional but noncomplementing Drosophila tyrosine decarboxylase genes." *Journal of Biological Chemistry* **280**(15): 14948-14955.

David, J. C. and Coulon, J. F. (1985). "Octopamine in Invertebrates and Vertebrates - a Review." *Progress in Neurobiology* **24**(2): 141-185.

De Cesare, D., Fimia, G. M. and Sassone-Corsi, P. (1999). "Signaling routes to CREM and CREB: plasticity in transcriptional activation." *Trends in Biochemical Science* **24**(7): 281-5.

De Luca, V., Muglia, P., Jain, U., Basile, V. S., Sokolowski, M. B. and Kennedy, J. L. (2002). "A drosophila model for attention deficit hyperactivity disorder (ADHD): No evidence of association with PRKG1 gene." *Neuromolecular Med* **2**(3): 281-287.

Degen, J., Gewecke, M. and Roeder, T. (2000). "Octopamine receptors in the honey bee and locust nervous system: pharmacological similarities between homologous receptors of distantly related species." *British Journal of Pharmacology* **130**(3): 587-594.

Dietzl, G., Chen, D., Schnorrer, F., Su, K. C., Barinova, Y., Fellner, M., Gasser, B., Kinsey, K., Oppel, S., Scheiblauer, S., Couto, A., Marra, V., Keleman, K. and Dickson, B. J. (2007). "A genome-wide transgenic RNAi library for conditional gene inactivation in Drosophila." *Nature* **448**(7150): 151-156.

Downer, R. G. H., Hiripi, L. and Juhos, S. (1993). "Characterization of the Tyraminergic System in the Central-Nervous-System of the Locust, Locusta-Migratoria-Migratoides." *Neurochemical Research* **18**(12): 1245-1248.

Dowse, H., Ringo, J., Power, J., Johnson, E., Kinney, K. and White, L. (1995). "A congenital heart defect in Drosophila caused by an action-potential mutation." *J Neurogenetics* **10**(3): 153-168.

Draper, I., Kurshan, P. T., McBride, E., Jackson, F. R. and Kopin, A. S. (2007). "Locomotor activity is regulated lay D2-like receptors in Drosophila: An anatomic and functional analysis." *Developmental Neurobiology* **67**(3): 378-393.

Dudai, Y. and Zvi, S. (1984). "High-Affinity [Octopamine-H-3-Binding Sites in Drosophila-Melanogaster - Interaction with Ligands and Relationship to Octopamine Receptors."

Comparative Biochemistry and Physiology C-Pharmacology Toxicology & Endocrinology **77**(1): 145-151.

Duffy, J. B. (2002). "GAL4 system in Drosophila: A fly geneticist's Swiss army knife." *Genesis* **34**(1-2): 1-15.

Elekes, K., Eckert, M. and Rapus, J. (1993). "Small Sets of Putative Interneurons Are Octopamine-Immunoreactive in the Central-Nervous-System of the Pond Snail, Lymnaea-Stagnalis." *Brain Research* **608**(2): 191-197.

Erspamer, V. (1952). "[Active substances of the posterior salivary glands of octopus and the hypobranchial glands of the purpur snail.]." *Arzneimittelforschung* **2**(6): 253-258.

Evans, P. D. and Robb, S. (1993). "Octopamine receptor subtypes and their modes of action." *Neurochemical Research* **18**(8): 869-874.

Feng, G. P., Hannan, F., Reale, V., Hon, Y. Y., Kousky, C. T., Evans, P. D. and Hall, L. M. (1996). "Cloning and functional characterization of a novel dopamine receptor from Drosophila melanogaster." *Journal of Neuroscience* **16**(12): 3925-3933.

Fields, P. E. and Woodring, J. P. (1991). "Octopamine Mobilization of Lipids and Carbohydrates in the House Cricket, Acheta-Domesticus." *Journal of Insect Physiology* **37**(3): 193-199.

Fox, L. E., Soll, D. R. and Wu, C. F. (2006). "Coordination and modulation of locomotion pattern generators in Drosophila larvae: Effects of altered biogenic amine levels by the tyramine beta hydroxlyase mutation." *Journal of Neuroscience* **26**(5): 1486-1498.

Gerhardt, C. C., Bakker, R. A., Piek, G. J., Planta, R. J., Vreugdenhil, E., Leysen, J. E. and vanHeerikhuizen, H. (1997a). "Molecular cloning and pharmacological characterization of a molluscan octopamine receptor." *Molecular Pharmacology* **51**(2): 293-300.

Gerhardt, C. C., Lodder, H. C., Vincent, M., Bakker, R. A., Planta, R. J., Vreugdenhil, E., Kits, K. S. and vanHeerikhuizen, H. (1997b). "Cloning and expression of a complementary DNA encoding a molluscan octopamine receptor that couples to chloride channels in HEK293 cells." *Journal of Biological Chemistry* **272**(10): 6201-6207.

Giebelen, I. A. J., Leendertse, M., Dessing, M. C., Meijers, J. C. M., Levi, M., Draing, C., von Aulock, S. and van der Poll, T. (2008). "Endogenous beta-adrenergic receptors inhibit lipopolysaccharide-induced pulmonary cytokine release and coagulation." *American Journal of Respiratory Cell and Molecular Biology* **39**(3): 373-379.

Gotzes, F., Balfanz, S. and Baumann, A. (1994). "Primary structure and functional characterization of a Drosophila dopamine receptor with high homology to human D1/5 receptors." *Receptors Channels* **2**(2): 131-141.

Gu, G. G. and Singh, S. (1995). "Pharmacological analysis of heartbeat in Drosophila." *Journal of Neurobiology* **28**(3): 269-280.

Gudermann, T., Kalkbrenner, F., Dippel, E., Laugwitz, K. L. and Schultz, G. (1997a). "Specificity and complexity of receptor-G-protein interaction." *Advances in Second Messenger and Phosphoprotein Research* **31**: 253-262.

Gudermann, T., Kalkbrenner, F. and Schultz, G. (1996). "Diversity and selectivity of receptor-G protein interaction." *Annual Review of Pharmacology and Toxicology* **36**: 429-459.

Gudermann, T., Schoneberg, T. and Schultz, G. (1997b). "Functional and structural complexity of signal transduction via G-protein-coupled receptors." *Annual Review of Neuroscience* **20**: 399-427.

Gutierrez, E., Wiggins, D., Fielding, B. and Gould, A. P. (2007). "Specialized hepatocyte-like cells regulate Drosophila lipid metabolism." *Nature* **445**(7125): 275-280.

Hammer, M. (1993). "An Identified Neuron Mediates the Unconditioned Stimulus in Associative Olfactory Learning in Honeybees." *Nature* **366**(6450): 59-63.

Han, K. A., Millar, N. S., Grotewiel, M. S. and Davis, R. L. (1996). "DAMB, a novel dopamine receptor expressed specifically in Drosophila mushroom bodies." *Neuron* **16**(6): 1127-1135.

Hartenstein, V. (1988). "Development of Drosophila Larval Sensory Organs - Spatiotemporal Pattern of Sensory Neurons, Peripheral Axonal Pathways and Sensilla Differentiation." *Development* **102**(4): 869-886.

Hashemzadeh-Gargari, H. and Friesen, W. O. (1989). "Modulation of swimming activity in the medicinal leech by serotonin and octopamine." *Comparative Biochemistry and Physiology- Part C* **94**(1): 295-302.

Hauser, F., Cazzamali, G., Williamson, M., Blenau, W. and Grimmelikhuijzen, C. J. P. (2006). "A review of neurohormone GPCRs present in the fruitfly Drosophila melanogaster and the honey bee Apis mellifera." *Progress in Neurobiology* **80**(1): 1-19.

Hearn, M. G., Ren, Y., McBride, E. W., Reveillaud, I., Beinborn, M. and Kopin, A. S. (2002). "A Drosophila dopamine 2-like receptor: Molecular characterization and identification of multiple alternatively spliced variants." *Proceedings of the National Academy of Science* **99**(22): 14554-14559.

Heisenberg, M., Borst, A., Wagner, S. and Byers, D. (1985). "Drosophila Mushroom Body Mutants Are Deficient in Olfactory Learning." *Journal of Neurogenetics* **2**(1): 1-30.

Hildebrandt, H. and Muller, U. (1995). "Pka Activity in the Antennal Lobe of Honeybees Is Regulated by Chemosensory Stimulation in-Vivo." *Brain Research* **679**(2): 281-288.

Hille, B. (1994). "Modulation of Ion-Channel Function by G-Protein-Coupled Receptors." *Trends in Neurosciences* **17**(12): 531-536.

Hiripi, L., Juhos, S. and Downer, R. G. H. (1994). "Characterization of Tyramine and Octopamine Receptors in the Insect (Locusta-Migratoria Migratorioides) Brain." *Brain Research* **633**(1-2): 119-126.

Hiripi, L., Vehovszky, A., Juhos, S. and Elekes, K. (1998). "An octopaminergic system in the CNS of the snails, Lymnaea stagnalis and Helix pomatia." *Philosophical Transactions of the Royal Society of London Series B-Biological Sciences* **353**(1375): 1621-1629.

Horstmeyer, A., Cramer, H., Sauer, T., MullerEsterl, W. and Schroeder, C. (1996). "Palmitoylation of endothelin receptor A - Differential modulation of signal transduction activity by post-translational modification." *Journal of Biological Chemistry* **271**(34): 20811-20819.

Hoyer, S. C., Eckart, A., Herrel, A., Zars, T., Fischer, S. A., Hardie, S. L. and Heisenberg, M. (2008). "Octopamine in male aggression of Drosophila." *Current Biology* **18**(3): 159-167.

Hoyle, G. (1975). "Evidence that insect dorsal unpaired medican (DUM) neurons are octopaminergic." *Jounal of Experimental Zoology* **193**(3): 425-431.

Hoyle, G. and Barker, D. L. (1975). "Synthesis of octopamine by insect dorsal median unpaired neurons." *Jounal of Experimental Zoology* **193**(3): 433-439.

Hoyle, W. C., Koch, W. F. and Diehl, H. (1975). "An electrode for the coulometric generation of hydrogen ion." *Talanta* **22**(8): 649-53.

Hsouna, A., Lawal, H. O., Izevbaye, L., Hsu, T. and O'Donnell, J. M. (2007). "Drosophila dopamine synthesis pathway genes regulate tracheal morphogenesis." *Developmental Biology* **308**(1): 30-43.

Jackson, D. M. and Westlind-Danielsson, A. (1994). "Dopamine receptors: molecular biology, biochemistry and behavioural aspects." *Pharmacology and Therapeuitics* **64**(2): 291-370.

Jankovic, J. (2008). "Parkinson's disease: clinical features and diagnosis." *Journal of Neurology, Neurosurgery and Psychiatry* **79**(4): 368-376.

Kaun, K. R. and Heberlein, U. (2009). "Too Fat to Fly? New Brain Circuits Regulate Obesity in Drosophila." *Neuron* **63**(3): 279-281.

Kebabian, J. W. and Calne, D. B. (1979). "Multiple receptors for dopamine." *Nature* **277**(5692): 93-96.

Kim, Y. C., Lee, H. G., Seong, C. S. and Han, K. A. (2003). "Expression of a D1 dopamine receptor dDA1/DmDOP1 in the central nervous system of Drosophila melanogaster." *Gene Expression Patterns* **3**(2): 237-245.

Koob, G. F. (1992). "Drugs of Abuse - Anatomy, Pharmacology and Function of Reward Pathways." *Trends in Pharmacological Sciences* **13**(5): 177-184.

Kutsukake, M., Komatsu, A., Yamamoto, D. and Ishiwa-Chigusa, S. (2000). "A tyramine receptor gene mutation causes a defective olfactory behavior in Drosophila melanogaster." *Gene* **245**(1): 31-42.

Kyriakides, M. A. and Mccrohan, C. R. (1989). "Effect of Putative Neuromodulators on Rhythmic Buccal Motor Output in Lymnaea-Stagnalis." *Journal of Neurobiology* **20**(7): 635-650.

Lang, A. E. and Lozano, A. M. (1998a). "Parkinson's disease. First of two parts." *The New Engand Journal of Medicine* **339**(15): 1044-1053.

Lang, A. E. and Lozano, A. M. (1998b). "Parkinson's disease. Second of two parts." *The New England Journal of Medicine* **339**(16): 1130-1143.

Lee, H. G., Seong, C. S., Kim, Y. C., Davis, R. L. and Han, K. A. (2003). "Octopamine receptor OAMB is required for ovulation in Drosophila melanogaster." *Developmental Biology* **264**(1): 179-190.

Long, T. F. and Murdock, L. L. (1983). "Stimulation of blowfly feeding behavior by octopaminergic drugs." *Proceedings of the National Academy of Sciences* **80**(13): 4159-4163.

Maqueira, B., Chatwin, H. and Evans, P. D. (2005). "Identification and characterization of a novel family of Drosophila beta-adrenergic-like octopamine G-protein coupled receptors." *Journal of Neurochemistry* **94**(2): 547-560.

Maris, N. A., Florquin, S., van't Veer, C., de Vos, A. F., Buurman, W., Jansen, H. M. and van der Poll, T. (2006). "Inhalation of beta 2 agonists impairs the clearance of nontypable Haemophilus influenzae from the murine respiratory tract." *Respiratory Research* **7**: 57-67.

McGuire, S. E., Deshazer, M. and Davis, R. L. (2005). "Thirty years of olfactory learning and memory research in Drosophila melanogaster." *Progress in Neurobiology* **76**(5): 328-47.

Meinertzhagen, I. A. (1993). "Sleeping neuroblasts." *Current Biology* **3**(12): 904-6.

Melcher, C., Bader, R. and Pankratz, M. J. (2007). "Amino acids, taste circuits, and feeding behavior in Drosophila: towards understanding the psychology of feeding in flies and man." *Journal of Endocrinology* **192**(3): 467-472.

Mercer, A. R. and Menzel, R. (1982). "The Effects of Biogenic-Amines on Conditioned and Unconditioned Responses to Olfactory Stimuli in the Honeybee Apis-Mellifera." *Journal of Comparative Physiology* **145**(3): 363-368.

Missale, C., Nash, S. R., Robinson, S. W., Jaber, M. and Caron, M. G. (1998). "Dopamine receptors: From structure to function." *Physiological Reviews* **78**(1): 189-225.

Mizutani, K., Ogawa, H., Saito, J. and Oka, K. (2002). "Fictive locomotion induced by octopamine in the earthworm." *Journal of Experimental Biology* **205**(2): 265-271.

Monastirioti, M., Gorczyca, M., Rapus, J., Eckert, M., White, K. and Budnik, V. (1995). "Octopamine immunoreactivity in the fruit fly Drosophila melanogaster." *J Comp Neurol* **356**(2): 275-287.

Monastirioti, M., Linn, C. E. and White, K. (1996). "Characterization of Drosophila tyramine beta-hydroxylase gene and isolation of mutant flies lacking octopamine." *Journal of Neuroscience* **16**(12): 3900-3911.

Mulloney, B., Acevedo, L. D. and Bradbury, A. G. (1987). "Modulation of the crayfish swimmeret rhythm by octopamine and the neuropeptide proctolin." *J Neurophysiology* **58**(3): 584-597.

Nagaya, Y., Kutsukake, M., Chigusa, S. I. and Komatsu, A. (2002). "A trace amine, tyramine, functions as a neuromodulator in Drosophila melanogaster." *Neuroscience Letters* **329**(3): 324-328.

Nathanson, J. A. (1985). "Phenyliminoimidazolidines - Characterization of a Class of Potent Agonists of Octopamine-Sensitive Adenylate-Cyclase and Their Use in Understanding the Pharmacology of Octopamine Receptors." *Molecular Pharmacology* **28**(3): 254-268.

Ohta, H. (2009). "Molecular pharmacology on insect biogenic amines." *Journal of Pesticide Science* **34**(3): 187-189.

Orchard, I., Ramirez, J. M. and Lange, A. B. (1993). "A Multifunctional Role for Octopamine in Locust Flight." *Annual Review of Entomology* **38**: 227-249.

Park, J. H. and Keeley, L. L. (1998). "The effect of biogenic amines and their analogs on carbohydrate metabolism in the fat body of the cockroach Blaberus discoidalis." *General and Comparative Endocrinology* **110**(1): 88-95.

Pophof, B. (2002). "Octopamine enhances moth olfactory responses to pheromones, but not those to general odorants." *Journal of Comparative Physiology a-Neuroethology Sensory Neural and Behavioral Physiology* **188**(8): 659-662.

Pospisilik, J. A., Schramek, D., Schnidar, H., Cronin, S. J. F., Nehme, N. T., Zhang, X. Y., Knauf, C., Cani, P. D., Aumayr, K., Todoric, J., Bayer, M., Haschemi, A., Puviindran, V., Tar, K., Orthofer, M., Neely, G. G., Dietzl, G., Manoukian, A., Funovics, M., Prager, G., Wagner, O., Ferrandon, D., Aberger, F., Hui, C. C., Esterbauer, H. and Penninger, J. M. (2010). "Drosophila Genome-wide Obesity Screen Reveals Hedgehog as a Determinant of Brown versus White Adipose Cell Fate." *Cell* **140**(1): 148-160.

Rachinsky, A. (1994). "Octopamine and Serotonin Influence on Corpora Allata Activity in Honey-Bee (Apis-Mellifera) Larvae." *Journal of Insect Physiology* **40**(7): 549-554.

Ramirez, J. M. and Pearson, K. G. (1991). "Octopamine induces bursting and plateau potentials in insect neurones." *Brain Research* **549**(2): 332-337.

Rauschenbach, I. Y., Chentsova, N. A., Alekseev, A. A., Gruntenko, N. E., Adonyeva, N. V., Karpova, E. K., Komarova, T. N., Vasiliev, V. G. and Bownes, M. (2007). "Dopamine and octopamine regulate 20-hydroxyecdysone level in vivo in Drosophila." *Archives of Insect Biochemistry and Physiology* **65**(2): 95-102.

Rhee, S. G. and Bae, Y. S. (1997). "Regulation of phosphoinositide-specific phospholipase C isozymes." *Journal of Biological Chemistry* **272**(24): 15045-15048.

Riemensperger, T., Voller, T., Stock, P., Buchner, E. and Fiala, A. (2005). "Punishment prediction by dopaminergic neurons in Drosophila." *Current Biology* **15**(21): 1953-1960.

Riggleman, B., Schedl, P. and Wieschaus, E. (1990). "Spatial Expression of the Drosophila Segment Polarity Gene Armadillo Is Posttranscriptionally Regulated by Wingless." *Cell* **63**(3): 549-560.

Roeder, T. (1994). "Biogenic-Amines and Their Receptors in Insects." *Comparative Biochemistry and Physiology C-Pharmacology Toxicology & Endocrinology* **107**(1): 1-12.

Roeder, T. (1999). "Octopamine in invertebrates." *Progress in Neurobiology* **59**(5): 533-561.

Roeder, T. (2005). "Tyramine and octopamine: Ruling behavior and metabolism." *Annual Review of Entomology* **50**: 447-477.

Roeder, T., Degen, J. and Gewecke, M. (1998). "Epinastine, a highly specific antagonist of insect neuronal octopamine receptors." *European Journal of Pharmacology* **349**(2-3): 171-177.

Roeder, T. and Gewecke, M. (1990). "Octopamine Receptors in Locust Nervous-Tissue." *Biochemical Pharmacology* **39**(11): 1793-1797.

Roeder, T. and Nathanson, J. A. (1993). "Characterization of insect neuronal octopamine receptors (OA3 receptors)." *Neurochemical Research* **18**(8): 921-925.

Rubin, G. M. and Spradling, A. C. (1982). "Genetic-Transformation of Drosophila with Transposable Element Vectors." *Science* **218**(4570): 348-353.

Rulifson, E. J., Kim, S. K. and Nusse, R. (2002). "Ablation of insulin-producing neurons in flies: growth and diabetic phenotypes." *Science* **296**(5570): 1118-1120.

Samakovlis, C., Manning, G., Steneberg, P., Hacohen, N., Cantera, R. and Krasnow, M. A. (1996). "Genetic control of epithelial tube fusion during Drosophila tracheal development." *Development* **122**(11): 3531-3536.

Saraswati, S., Fox, L. E., Soll, D. R. and Wu, C. F. (2004). "Tyramine and octopamine have opposite effects on the locomotion of Drosophila larvae." *Journal of Neurobiology* **58**(4): 425-441.

Saudou, F., Amlaiky, N., Plassat, J. L., Borrelli, E. and Hen, R. (1990). "Cloning and Characterization of a Drosophila Tyramine Receptor." *Embo Journal* **9**(11): 3611-3617.

Scavone, C., Mckee, M. and Nathanson, J. A. (1994). "Monoamine Uptake in Insect Synaptosomal Preparations." *Insect Biochemistry and Molecular Biology* **24**(6): 589-597.

Scholz, H., Ramond, J., Singh, C. M. and Heberlein, U. (2000). "Functional ethanol tolerance in Drosophila." *Neuron* **28**(1): 261-271.

Schonhoff, S. E., Giel-Moloney, M. and Leiter, A. B. (2004). "Minireview: Development and differentiation of gut endocrine cells." *Endocrinology* **145**(6): 2639-2644.

Schroll, C., Riemensperger, T., Bucher, D., Ehmer, J., Voller, T., Erbguth, K., Gerber, B., Hendel, T., Nagel, G., Buchner, E. and Fiala, A. (2006). "Light-induced activation of distinct

modulatory neurons triggers appetitive or aversive learning in Drosophila larvae." *Current Biology* **16**(17): 1741-1747.

Schwaerzel, M., Monastirioti, M., Scholz, H., Friggi-Grelin, F., Birman, S. and Heisenberg, M. (2003). "Dopamine and octopamine differentiate between aversive and appetitive olfactory memories in Drosophila." *J Neuroscience* **23**(33): 10495-10502.

Sitaraman, D., Zars, M., Laferriere, H., Chen, Y. C., Sable-Smith, A., Kitamoto, T., Rottinghaus, G. E. and Zars, T. (2008). "Serotonin is necessary for place memory in Drosophila." *Proceedings of the National Academy of Sciences* **105**(14): 5579-5584.

Sitaraman, D., Zars, M. and Zars, T. (2010). "Place memory formation in Drosophila is independent of proper octopamine signaling." *Journal of Comparative Physiology a-Neuroethology Sensory Neural and Behavioral Physiology* **196**(4): 299-305.

Socha, R., Kodrik, D. and Zemek, R. (2008). "Stimulatory effects of bioamines norepinephrine and dopamine on locomotion of Pyrrhocoris apterus (L.): is the adipokinetic hormone involved?" *Comparative Biochemistry and Physiology - Part B: Biochemistry and molecular biologyl* **151**(3): 305-310.

Sombati, S. and Hoyle, G. (1984a). "Central Nervous Sensitization and Dishabituation of Reflex Action in an Insect by the Neuromodulator Octopamine." *Journal of Neurobiology* **15**(6): 455-480.

Sombati, S. and Hoyle, G. (1984b). "Generation of Specific Behaviors in a Locust by Local Release into Neuropil of the Natural Neuromodulator Octopamine." *Journal of Neurobiology* **15**(6): 481-506.

Steele, J. E. (1982). "Glycogen-Phosphorylase in Insects." *Insect Biochemistry* **12**(2): 131-147.

Stevenson, P. A., Hofmann, H. A., Schoch, K. and Schildberger, K. (2000). "The fight and flight responses of crickets depleted of biogenic amines." *Journal of Neurobiology* **43**(2): 107-120.

Strauss, R. (2002). "The central complex and the genetic dissection of locomotor behaviour." *Current Opinion in Neurobiology* **12**(6): 633-638.

Strauss, R. and Heisenberg, M. (1993). "A Higher Control Center of Locomotor Behavior in the Drosophila Brain." *Journal of Neuroscience* **13**(5): 1852-1861.

Sugamori, K. S., Demchyshyn, L. L., Mcconkey, F., Forte, M. A. and Niznik, H. B. (1995). "A Primordial Dopamine D1-Like Adenylyl Cyclase-Linked Receptor from Drosophila-Melanogaster Displaying Poor Affinity for Benzazepines." *Febs Letters* **362**(2): 131-138.

Svedmyr, N. (1990). "The current place of beta 2-agonists in the management of asthma." *Lung* **168 Suppl**: 105-110.

Unoki, S., Matsumoto, Y. and Mizunami, M. (2005). "Participation of octopaminergic reward system and dopaminergic punishment system in insect olfactory learning revealed by pharmacological study." *European Journal of Neuroscience* **22**(6): 1409-1416.

Uzzan, A. and Dudai, Y. (1982). "Aminergic Receptors in Drosophila-Melanogaster - Responsiveness of Adenylate-Cyclase to Putative Neurotransmitters." *Journal of Neurochemistry* **38**(6): 1542-1550.

Vallone, D., Picetti, R. and Borrelli, E. (2000). "Structure and function of dopamine receptors." *Neuroscience and Biobehavioral Reviews* **24**(1): 125-132.

Vergoz, V., Roussel, E., Sandoz, J. C. and Giurfa, M. (2007). "Aversive Learning in Honeybees Revealed by the Olfactory Conditioning of the Sting Extension Reflex." *Plos One* **2**(3): e288; 1-10.

Wagner, C., Isermann, K., Fehrenbach, H. and Roeder, T. (2008). "Molecular architecture of the fruit fly's airway epithelial immune system." *Bmc Genomics* **9**.

Walz, B., Baumann, O., Krach, C., Baumann, A. and Blenau, W. (2006). "The aminergic control of cockroach salivary glands." *Archives of Insect Biochemistry and Physiology* **62**(3): 141-152.

Wise, R. A. (1996). "Neurobiology of addiction." *Current Opinion in Neurobiology* **6**(2): 243-251.

Wise, R. A. and Bozarth, M. A. (1987). "A Psychomotor Stimulant Theory of Addiction." *Psychological Review* **94**(4): 469-492.

Zars, T., Fischer, M., Schulz, R. and Heisenberg, M. (2000). "Localization of a short-term memory in Drosophila." *Science* **288**(5466): 672-675.

Zeng, H., Loughton, B. G. and Jennings, K. R. (1996). "Tissue specific transduction systems for octopamine in the locust (Locusta migratoria)." *Journal of Insect Physiology* **42**(8): 765-769.

Curriculum vitae

Personal data:

Name : Samar Ezzat Ghazy El-kholy

Present Position: Assistant Lecturer in Tanta University, Faculty of Science, Zoology Department. Tanta, Egypt

Date and place of Birth: August 1, 1975. Egypt

Marital status: Married

Home Address: 1 Sad El-Agamy Street – Teret EL-Shiaty, Tanta, Egypt.

Telephone: 002 040 351 4909

Email: samarezzat0@yahoo.com

Education:

1990-1993, High school Diploma, Al-Mahalla High School for girls, Al-Mahalla, El-Gharbiya, Egypt.

1993-1997, Zoology Department, Faculty of Science, Tanta University, Tanta, Egypt.
B. Sc. of Entomology (Grade: Very Good). Main subjects include: Zoology, Entomology, General Botany, General Chemistry, Physics and Mathematics, Biostatistics, Biophysics and Radiology, English Language.

1997-1998, Entomology Department, Faculty of Science, Ain Shams University, Cairo, Egypt.
Post-graduate Diploma of Entomology (Physiology).

Main Subjects included : Molecular Biology, Insect Biochemistry, Population Genetics, Muscular and Nervous Physiology, Endocrinology, Enzymology, Insect Hormones and Pheromones, Biostatistics and Computer Science and English language.

1998-1999, Zoology Department, Faculty of Science, Tanta University, Tanta, Egypt.
Post-graduate Diploma of Entomology (Physiology).

Main Subjects include: Immunology and German language.

1999-2003, Zoology Department, Faculty of Science, Tanta University, Tanta, Egypt.
M. Sc. of Entomology. Thesis on Molecular systematic entitled **"MORPHOLOGIC AND GENETIC CHARACTERIZATION OF THE CULEX PIPIENS COMPLEX (DIPTERA: CULICIDAE) IN GHARBIYA GOVERNORATE, EGYPT "**

2006-2010, zoophysiology Department, Faculty of mathematics and natural science, Kiel university , Germany.
PHD. Of molecular genetics. Thesis on molecular biology entitled **"BIOAMINE RECEPTORS OF THE FRUIT FLY DROSOPHILA MELANOGASTER AS TARGETS FOR INSECTICIDES "**

Academic Position:

- **Zoology Department, Faculty of Science, Tanta University, Tanta, Egypt, December 1997–December 2003**
  Instructor

- **Zoology Department, Faculty of Science, Tanta University, Tanta, Egypt, December 2003 till now**
  Assistant Lecturer

Scholarships:

Doctoral scholarship, Funded by the Ministry of Higher education. Mission sector, Egypt.

Kiel, 2010

Samar Ezzat Ghazy El-Kholy

Acknowledgement

I am heartily thankful to my supervisor, Pro. Dr. Thomas Roeder, for giving me the opportunity to carry out my PhD under his supervision and for his encouragement, guidance and support from the initial to the final level.

I would like to acknowledge the ministry of high education, mission sector of Egypt that provided the necessary financial support for this research.

I like to thank my husband, Wesam for his personal support and great patience at all times.

Lastly, but by no means least, I offer my regards and blessings to all of those who supported me in any respect during the completion of my work.

Samar El-kholy

Affirmation

I hereby affirm that I have completed my doctoral thesis entitled " Bioamine receptors of the fruit fly *Drosophila melanogaster* as targets for insecticides" entirely on my own and unassisted, and that I have specially marked all of the quotes I have used from other authors as well as those passages in my work that are extremely close to the thoughts presented by other authors , and listed the sources in accordance with the regulations I have been given.

Samar Ezzat Ghazy El-kholy

Date _____ Signature _____